



IN THE UNITED STATES PATENT AND TRADEMARK OFFICE

Patent Application No. 10/089,009

Applicant: Goldman et al.

Filed: August 6, 2002

TC/AU: 1646

Examiner: Dong Jiang

Docket No.: 218811 (Client Reference No. E-025-1999/0-US-03)

Customer No.: 45733

Mail Stop Amendment
Commissioner for Patents
P.O. Box 1450
Alexandria, VA 22313-1450

DECLARATION UNDER 37 C.F.R. § 1.132 OF RICHARD BAMFORD, Ph.D.

I, Richard Bamford, Ph.D., hereby declare that:

1. I received my degree of Doctor of Philosophy in Molecular Biology/Immunology in 1998 from the Department of Biological Sciences, The George Washington University, Washington, D.C. I am currently owner and principal investigator of Transponics, a company that offers molecular biology and consulting services, located in Mount Wolf, Pennsylvania. I serve as a consultant to the Department of Health and Human Services, which is the assignee of the subject patent application.

2. I have reviewed Colamonici et al., *J. Immunology*, 145: 155-160 (1990) ("the Colamonici reference"). The Colamonici reference mentions two polypeptides having a molecular weight of 37 kDa and 20 kDa as determined by SDS-PAGE, each of which reportedly associates with the p95-110 subunit of the IL-2 receptor (IL-2R) (see Colamonici reference at, e.g., page 159, second column). I do not believe that it is reasonable to assume that the 37 kDa protein and a protein determined to be 32-34 kDa via SDS-PAGE are the same protein. Likewise, I do not believe that it is reasonable to assume that the 20 kDa protein is equivalent to a protein determined to be 26-28 kDa by SDS-PAGE.

3. The experimental conditions for preparing and running SDS-PAGE can influence how a protein band migrates through a gel. However, when estimating the molecular weights of proteins in the range of 20-40 kDa, discrepancies of 3-8 kDa between proteins is significant. When proteins are run in SDS-PAGE alongside markers, experimental conditions affect both the behavior of the protein sample and the markers within the gel. This allows for relatively accurate estimations of protein molecular weight. I would not expect that proteins having a 10% difference in molecular weights as determined by SDS-PAGE (e.g., a protein of 37 kDa and a protein of 34 kDa) to be the same protein, particularly when the sample proteins have molecular weights in the range of 20-40 kDa.

4. HuT 102 cells and MT-1 cells are human T cell lymphotropic virus (HTLV-1)-infected, cytokine independent, human T-cells used to examine the interleukin-2 receptor (IL-2R) (Eddidin et al., *J. Immunology*, 141: 1206-1210 (1988); Tsudo et al., *PNAS USA*, 84: 5394-5398 (1987)). Kit-225 cells are IL-2 dependent, and were derived from a patient with T-cell chronic lymphocytic leukemia (Hori et al., *Blood*, 70: 1069-1072 (1987)). MLA-144 cells originated from a gibbons ape with a spontaneous lymphosarcoma (see, e.g., Tsudo et al., *PNAS USA*, 83: 9694-9698 (1986)). The MLA-144 cell line is an accepted research tool for studying human IL-2R and proteins associated therewith (see, e.g., the Colamonici reference, *supra*).

5. HuT 102, Kit-225, MT-1, and MLA-144 cells express different combinations of the α , β , and γ subunits of the IL-2R. Both HuT 102 cells and Kit-225 cells express the α , β , and γ subunits of the IL-2R (Damjanovich et al., *PNAS USA*, 94: 13134-13139 (1997)). MT-1 cells express only the IL-2R α subunit (Arima et al., *J. Immunology*, 147: 3396-3401 (1991)). MLA-144 cells express the β and γ subunits of the IL-2R (Tsudo et al., *PNAS USA* 84(15): 5394-5398 (1987)). The Colamonici reference states that a 37 kDa protein was identified in HuT 102 cells, MT-1 cells, and MLA-144 cells during cross-linking experiments using IL-2 (the Colamonici reference at paragraph bridging pages 156-160). In my opinion, the 37 kDa protein found in these cell lines is the same (i.e., the 37 kDa protein identified in HuT 102 cells is the same 37 kDa protein identified in MLA-144 cells) given the experimental conditions under which the proteins were identified and that each protein has the same molecular weight.

6. I have reviewed paragraph 9 of the Declaration under 37 C.F.R. § 1.132 of Thomas Waldmann, M.D., submitted on March 21, 2006, and Exhibit 4 cited in paragraph 9. MLA-144 cells were contacted with the 5F7 antibody in a flow cytometric assay. Exhibit 4 demonstrates that IL-2R associated proteins found on MLA-144 cells, including the 37 kDa


protein described in the Colamonici reference, do not form a complex with the 5F7 antibody. Based on these results, I would not expect the 37 kDa protein of Hut 102 cells identified in Colamonici reference to form a complex with the 5F7 antibody.

7. In addition, I believe that experimental results achieved in Kit-225 cells with respect to IL-2R associated polypeptides are reasonably predictive of results that would be achieved in HuT 102 cells. Both of these cell lines are human CD4 positive mature T-cell leukemia cell lines which express the α , β , and γ chains of the IL-2 receptor and also express the proteins identified by the 5F7 antibody.

8. I hereby declare that all statements made herein of my own knowledge are true, that all statements made on information and belief are believed to be true, that these statements were made with the knowledge that willful false statements and the like so made are punishable by fine or imprisonment, or both, under Section 1001 of Title 18 of the United States Code, and that such willful false statements may jeopardize the validity of the application or any patent issued thereon.

Date: _____

8.15.06


Richard Bamford, Ph.D.

THE IL-2 RECEPTOR α -CHAIN ALTERS THE BINDING OF IL-2 TO THE β -CHAIN¹

NOBUYOSHI ARIMA,* MASANORI KAMIO,* MINORU OKUMA,* GRACE JU,[†] AND
TAKASHI UCHIYAMA^{2*}

From the *First Division of Internal Medicine, Faculty of Medicine, Kyoto University, 54 Shogoin-Kawaramachi, Sakyo, Kyoto 606, Japan; [†]Institute for Virus Research, Kyoto University, 53 Shogoin-Kawaramachi, Sakyo, Kyoto 606, Japan; and the ²Department of Molecular Genetics, Roche Research Center, Hoffman-La Roche Inc., Nutley, NJ 07110

The binding of IL-2 to its high affinity receptor results in the formation of the ternary complex consisting of IL-2, α -chain (p55, Tac) and β -chain (p75). We studied the role of α -chain in IL-2 binding to the high affinity receptor using IL-2 analog Lys20 which was made by the substitution of Lys for Asp²⁰ of wild-type rIL-2. Lys20 bound to MT-1 cells solely expressing α -chain at low affinity, but did not bind to YT-2C2 cells which solely expressed β -chain. However, direct binding of radiolabeled Lys20 to ED515-D cells, an HTLV-I-infected and IL-2-dependent T cell line, revealed both high affinity and low affinity binding although the K_d value of high affinity binding was 50 to 100 times higher than that of the high affinity binding of wild-type rIL-2. High affinity binding of Lys20 was completely blocked by 2R-B mAb recognizing IL-2R β -chain. Anti-Tac mAb recognizing IL-2R α -chain abolished all of the specific Lys20 bindings. In contrast to the replacement of cell bound 2R-B mAb with wild-type rIL-2 at 37°C, the addition of an excess of Lys20 did not cause the detachment of cell-bound radiolabeled or FITC-labeled 2R-B mAb. Consistent with the results of binding studies, Lys20 induced the proliferation of ED515-D cells, but not large granular lymphocyte leukemic cells. The growth of ED-515D cells was completely suppressed by either anti-Tac mAb or 2R-B mAb. These results strongly suggest that coexpression of the IL-2R α - and β -chains alters the binding affinity of Lys20 and that the interaction between IL-2 and the α -chain is a key event in the formation of the IL-2/IL-2R ternary complex.

IL-2 is a polypeptide produced by Ag-activated T lymphocytes, first identified as a growth factor required for the proliferation of activated T lymphocytes. Many other hematopoietic cells, including B lymphocytes (1, 2), thymocytes (3, 4), and monocytes (5), were also reported to respond to IL-2.

IL-2 has two distinct binding proteins (α -chain and β -chain), and three different forms of the IL-2R have been identified in terms of their affinity for IL-2 binding (high, intermediate, and low affinity IL-2R) (6-14). α -Chain (Tac, p55) can be detected with anti-Tac mAb (7, 15) and represents a low affinity IL-2R, if present solely. β -Chain (p70-75) represents an intermediate affinity IL-2R by itself (11-14) and both α - and β -chains form a high affinity IL-2R together (16, 17).

It appears that β -chain, in the absence of α -chain, is the receptor responsible for transmitting an IL-2 signal in some kinds of cells. In particular, LGL³ leukemic cells express only β -chain and respond to IL-2 (18-20), although α -chain expression is then induced by the interaction between IL-2 and β -chain (21). Internalization of IL-2 occurs when ligand is bound to the isolated β -chain, but not when bound to the isolated α -chain (22, 23). Recently, mAb reacting with the human IL-2R β -chain have been developed (24-26) and its cDNA was cloned (27). The deduced amino acid sequence of the β -chain revealed that it included a much larger cytoplasmic domain (286 residues) than that present in the α -chain (13 residues) (8, 9). This intracellular region has been postulated to be involved in signal transduction.

The α -chains are induced by specific Ag or by IL-2 itself and are commonly expressed in excess over the β -chains. But, in contrast to the β -chain, the role of the α -chain has not yet been clarified. It is important to study the role of the α -chain and the mechanism of the formation of IL-2/high affinity receptor complex, as these studies may shed light on other cytokine receptors which consist of two or more distinct binding proteins (28, 29) and may mediate signal transduction by a similar pathway as the IL-2R.

Previously Saito et al. proposed an IL-2 binding model that IL-2 would first bind to the α -chain and that the complex of IL-2/ α -chain would then associate with the β -chain, forming the high affinity ternary complex of IL-2/ α -chain/ β -chain (30-32). The level of α -chain expression was proposed to govern IL-2 responsiveness (33). Recently we showed the evidence supporting their model by using a mAb (2R-B mAb) specific for IL-2R β -chain. At 37°C, IL-2/ α -chain complexes bound to β -chains to form the ternary complex with the displacement of 2R-B mAb (26). On the other hand, some data, for example, reported by Saragovi and Malek (34) suggest that the high affinity

Received for publication May 22, 1991.

Accepted for publication August 14, 1991.

The costs of publication of this article were defrayed in part by the payment of page charges. This article must therefore be hereby marked advertisement in accordance with 18 U.S.C. Section 1734 solely to indicate this fact.

¹ This study was supported in part by Grants-in-Aid from the Ministry of Education, Science and Culture, and by Grants from Special Coordination Funds of Science and Technology Agency of the Japanese Government.

² Address correspondence and reprint requests to: Dr. Takashi Uchiyama, Institute for Virus Research, Kyoto University, 53 Shogoin-Kawaramachi, Sakyo, Kyoto 606, Japan.

³ Abbreviations used in this paper: LGL, large granular lymphocyte; MFI, mean fluorescence intensity.

IL-2R exists as a preformed heterodimer of α - and β -chain, and IL-2 is not required for the association of α - and β -chain. The precise mechanism of the ternary complex formation still remains to be clarified.

In the present study, we analyzed the role of α -chain in the interaction between IL-2 and β -chain by using an IL-2 analog and anti-IL-2R mAb.

MATERIALS AND METHODS

IL-2 and its analog. Human rIL-2 (35,200 U/mg) was a kind gift from Takeda Chemical Industries Co., Osaka, Japan. Human IL-2 analog Lys20 (Lys20) was prepared by means of replacement of Asp20 with Lys in human IL-2 as described (35).

Cells. IL-2-independent cell lines such as YT-2C2 and MT-1 were cultured in growth medium containing RPMI 1640, 10% FCS, 60 μ M tobramycin, and 2 mM L-glutamine. YT-2C2, a subclone of the NK-like cell line YT, was kindly provided by Dr. Teshigawara (Kyoto University). ED515-D (kindly provided by Dr. Maeda, Kyoto University) is an IL-2-dependent leukemic T cell line established from an adult T cell leukemia patient (36). Kit 225 is an IL-2-dependent human chronic T lymphocytic leukemic cell line (37). They were cultured in growth medium supplemented with 0.5 nM rIL-2.

In a proliferative assay, we used LGL leukemic cells from an LGL leukemic patient. Mononuclear cells from the venous blood of the patient were prepared by Ficoll-Conray density gradient centrifugation, and then B cells, monocytes and CD3⁺ cells were depleted on a nylon fiber column (Wako Pure Chemical Industries, Ltd., Osaka, Japan) and plates coated with anti-CD3 mAb. Surface markers of the leukemic cells were determined as CD3⁺ CD20⁺ CD56⁺ Tac(CD25)⁺ 2R-B(IL-2R β)⁺, and more than 90% of the cells in the cell suspension examined were leukemic cells.

Antibodies. 2R-B mAb is a mouse anti-IL-2R β -chain mAb, recognizing the IL-2 binding site of the β -chain. The K_d of 2R-B mAb to the β -chain was shown to be 1.5 nM at 4°C or 37°C (26). L61 is a mouse anti-IL-2 mAb which blocks IL-2 binding to the high affinity receptor (38, 39) (kindly provided by Dr. Ide, Shionogi Research Lab., Osaka, Japan).

Binding assay. Wild-type rIL-2 and Lys20 were radiolabeled with Na¹²⁵I (79 MBq/nmol of iodine, Amersham International, Buckinghamshire, UK) by the chloramine T method. The sp. act. of ¹²⁵I-wild-type rIL-2 and ¹²⁵I-Lys20 was 8,000 cpm/ng and 8,500 cpm/ng, and the bindability of ¹²⁵I-wild-type rIL-2 and ¹²⁵I-Lys20 was 100% and 86%, respectively.

After the incubation in IL-2-free medium for 24 h to remove cell surface-bound IL-2, ED515-D cells were incubated with antibodies (100 μ g/ml) for 40 min, if necessary. Then cells were incubated at 4°C for 90 min with serially diluted ¹²⁵I-wild-type rIL-2 or ¹²⁵I-Lys20 in binding medium containing 10 mg/ml BSA, 1 mg/ml sodium azide, and 25 mM HEPES in RPMI 1640 medium (pH 7.4). In some experiments as indicated, cells were also incubated at 37°C for 60 min. After incubation, cells were centrifuged through a layer of a mixture of 20% olive oil and 80% di-n-butylphthalate, and the radioactivity of the cell pellet was counted by a gamma counter. Nonspecific binding was determined by adding 500-fold excess of unlabeled wild-type rIL-2.

Cross-linking study. Cross-linking studies were performed as described elsewhere (40). Briefly, ED515-D cells were incubated at 37°C for 30 min with 150 pM of ¹²⁵I-wild-type rIL-2 or 500 pM of ¹²⁵I-Lys20 under high affinity binding conditions. Cells were cross-linked with 2 mM disuccinimidyl suberate (Pierce Chemical Co., Rockford, IL) and then solubilized with extraction buffer (10 mM Tris-HCl, pH 7.4, 0.15 M NaCl, 0.5% Nonidet P-40, 2 mM PMSF). Extracts were immunoprecipitated with rabbit anti-human IL-2 polyclonal antibody (kindly provided by Dr. Tsudo, Unitika Chuo Hosp., Kyoto, Japan) and protein A-Sepharose. The resulting immunoprecipitates were analyzed by SDS-PAGE under reducing conditions with a 7.5% polyacrylamide gel.

Internalization study. The rate of ligand internalization was measured as previously described (22) with minor modification. After the incubation in IL-2 free medium for 24 h, ED515-D cells were suspended in RPMI 1640, 25 mM HEPES, pH 7.2, 10 mg/ml BSA, 100 μ M chloroquine, and 500 pM ¹²⁵I-Lys20. After the incubation for 20 min at 0°C, cells were warmed to 37°C without washing. At selected times, a 100- μ l aliquot was pelleted by centrifugation, and the supernatant containing free ¹²⁵I-Lys20 was removed. The cells were resuspended in 200 μ l of 10 mM citrate, pH 3, containing 0.14 M NaCl and 100 μ g/ml BSA. After 15 s at 25°C, the cells were centrifuged through a layer consisting of 20% olive oil and 80% di-n-butylphthalate. The radioactivity in the cell pellet and in the supernatant above the oil layer was measured to determine pH 3-

resistant internalized Lys20 and pH 3-sensitive surface-bound Lys20, respectively. Nonspecific binding was determined by adding a 500-fold excess of unlabeled Lys20.

Proliferative response assay. After the incubation in IL-2 free medium for 48 h, ED515-D cells were cultured at 2×10^4 cells/well in a 96-well flat bottom plate for 8 h with serially diluted wild-type rIL-2 or Lys20 in the presence or the absence of antibodies (100 μ g/ml). LGL leukemic cells were cultured at 1×10^5 cells/well for 72 h. Cells were pulsed with 19 kBq of [³H]TdR (Dupont/NEN Research Product, Boston, MA) for the last 6 h of incubation and harvested on glass fiber filters. The radioactivity was measured by a liquid scintillation counter.

Assay for cell-bound ¹²⁵I-2R-B mAb. ED515-D cells (preincubated in IL-2-free medium) were incubated with a saturating amount of ¹²⁵I-2R-B mAb (30 nM) for 30 min at 37°C. After washing three times, cells were incubated with 10 nM unlabeled wild-type rIL-2 or 10 nM unlabeled Lys20 or none at 37°C. At various times, the cell-associated radioactivity of each aliquot was measured as described for the binding assay.

Flow cytometric analysis of the detachment of the 2R-B mAb. ED515-D cells were incubated with a saturating amount of FITC-conjugated 2R-B mAb (30 nM) for 30 min at 37°C as previously described (26). The wild-type rIL-2 was incubated with L61 mAb at 37°C for 60 min. Without washing, cells were further incubated with various concentrations of Lys20, wild-type rIL-2, or wild-type rIL-2 which had been preincubated with L61 mAb (finally 630 nM). After two washings, live cells were analyzed with a FACScan flow cytometer (Becton Dickinson Immunocytometry System Co., Mountain View, CA). %MFI was calculated as MFI (sample value - negative control value)/MFI (positive control value [without IL-2] - negative control value) \times 100.

RESULTS

IL-2 analog Lys20 cannot bind to the β -chain without the help of the α -chain. We performed ¹²⁵I-radiolabeled Lys20 binding assay by using four different types of cell lines in order to determine to which types of IL-2R Lys20 can bind. MT-1 cells expressed only IL-2R α -chain but no β -chain. YT-2C2 cells solely expressed β -chain.

¹²⁵I-Lys20 could bind to the α -chain of MT-1 cells with an apparent dissociation constant (K_d) of 26 nM, which was comparable to the K_d of wild-type rIL-2 (Table I). However, no binding of ¹²⁵I-Lys20 to YT-2C2 cells was detected even when 80 nM of ¹²⁵I-Lys20 was added to the cells. In contrast, ED515-D cells showed a low affinity binding (K_d = 27 nM) and a higher affinity binding (K_d = 660–850 pM) of ¹²⁵I-Lys20. The K_d value of the higher affinity binding of Lys20 was 50 to 100 times higher than that of the high affinity binding of wild-type rIL-2 (K_d = 9–22 pM). The incubation temperature (4°C or 37°C) of the binding did not affect this higher affinity binding of ¹²⁵I-Lys20. Kit 225 cells which is an IL-2 dependent and HTLV-I-uninfected T cell line also showed both low and higher affinity binding of ¹²⁵I-Lys20.

We next performed ¹²⁵I-Lys20 binding assay in ED515-D cells in the presence of 2R-B mAb which blocks IL-2 binding to the β -chain to see whether the α -chain, the β -chain or both are responsible for the higher affinity binding of Lys20. The higher affinity binding but not the low affinity binding was blocked by 2R-B mAb. In contrast, in the presence of anti-Tac mAb, the Lys20 binding even to the IL-2R β -chain completely disappeared (Fig. 1).

Figure 2 shows the cross-linking studies of ¹²⁵I-labeled wild-type rIL-2 and Lys20 on ED515-D cells. ¹²⁵I-Lys20 cross-linking study revealed two major bands migrating at about 70 and 85 kDa which were also detected in the ¹²⁵I-wild-type rIL-2 cross-linking study and represented the IL-2R α - and β -chains, respectively. Therefore, Lys20 protein is in close proximity to both the α - and β -chains.

Cell-bound Lys20 is internalized. We examined whether cell-bound Lys20 was internalized into ED515-

TABLE I
Binding characteristics of wild-type rIL-2 and its analog, Lys20

Cell	Affinity	Lys20		Wild-type rIL-2	
		K_d (pM)	Sites/cell	K_d (pM)	Sites/cell
MT-1	High	— ^a	—	—	—
	Intermediate	—	—	—	—
	Low	26,000	310,000	11,000	330,000
YT2C2	High	—	—	—	—
	Intermediate	—	—	2,000	50,000
	Low	—	—	—	—
ED515-D (37°C)	High	660	37,000	9	34,000
	Intermediate	—	—	—	—
	Low	27,000	700,000	12,000	490,000
[0°C]	High	850	44,000	22	42,000
	Intermediate	—	—	—	—
	Low	27,000	710,000	13,000	530,000
Kit 225	High	500	10,000	5	9,000
	Intermediate	—	—	—	—
	Low	17,000	310,000	15,000	300,000

^a — = not detected.

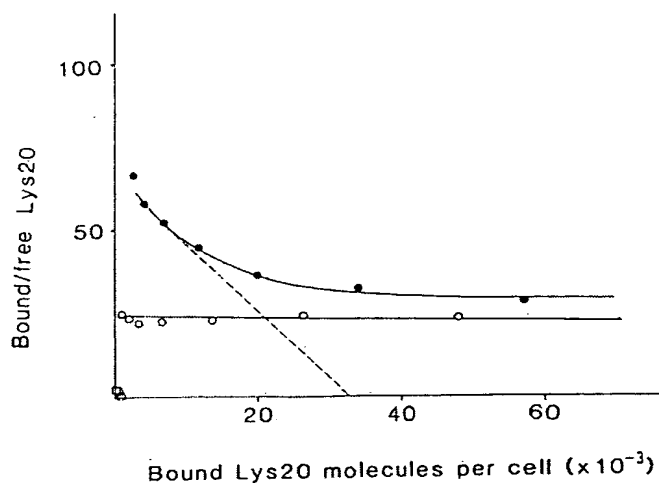


Figure 1. Effect of anti-IL-2R mAb on the high affinity Lys20 binding. Scatchard plot analysis of 125 I-Lys20 binding to ED515-D cells was performed in the presence of 630 nM of 2R-B mAb (○—○), in the presence of 630 nM of anti-Tac mAb (□—□), or none (●—●). The number of high affinity binding sites was 33,000 per cell, and the K_d value was 500 pM.

D cells. Significant internalization of 125 I-Lys20 was detected at various times of cell incubation (Fig. 3), confirming the interaction between Lys20 and the β -chain.

Both α - and β -chain are required for cells to proliferate in response to Lys20. The activity of Lys20 to induce the proliferation of IL-2-dependent cells was studied by the [3 H]TdR incorporation assay and was compared with that of wild-type rIL-2. ED515-D cells proliferated in response to 10 pM Lys20 and 50% of the maximal thymidine incorporation (ED_{50}) was achieved by 40 pM Lys20. Though four times less efficient than wild-type rIL-2, Lys20 could induce the proliferation of ED515-D cells (Fig. 4A). On the other hand, LGL leukemic cells, which expressed only the β -chain, could not respond to Lys20 even at the concentration of 25.6 nM (Fig. 4B). These findings showed that Lys20 could not bind to the β -chain and thus were unable to produce growth of LGL leukemic cells.

Either anti-Tac or 2R-B mAb can completely block the cell proliferation induced by Lys20. Next, we tested the effect of anti-Tac and 2R-B mAbs on the growth of

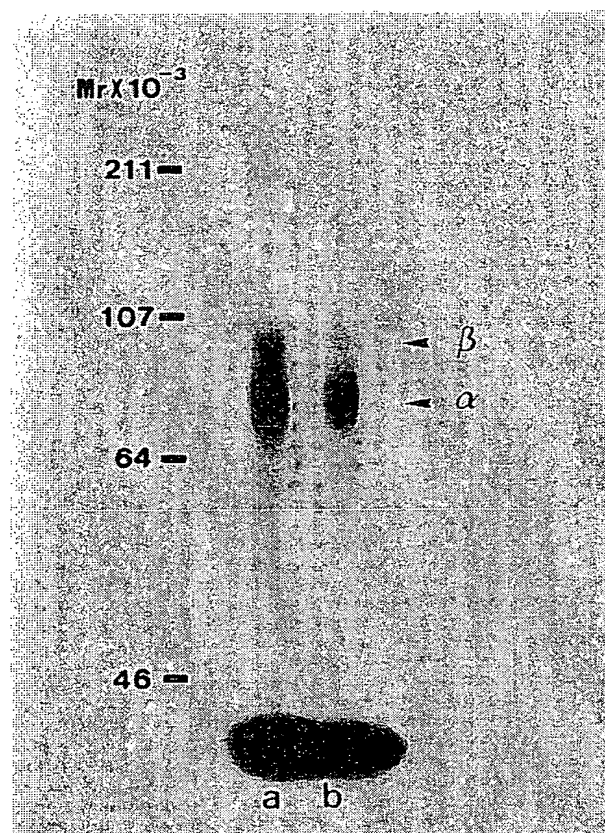


Figure 2. SDS-PAGE analysis of the proteins cross-linked with 125 I-labeled wild-type rIL-2 (lane a) or 125 I-labeled Lys20 (lane b) under the high affinity conditions (150 pM 125 I-wild-type rIL-2; 500 pM 125 I-Lys20) for ED515-D cells. Two arrowheads in order from the top indicate the p70 + IL-2, p55 + IL-2, respectively.

ED515-D cells induced by Lys20. Anti-Tac mAb alone partially suppressed the growth induced by wild-type rIL-2. However, the addition of both anti-Tac and 2R-B mAb markedly suppressed this proliferation (Fig. 5A). 2R-B mAb alone had no effect as reported previously (26). In contrast, the cell growth induced by Lys20 was com-

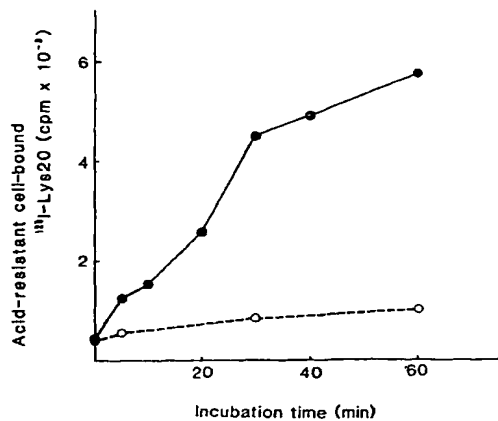


Figure 3. Internalization of ^{125}I -Lys20 into ED515-D cells. At each time, the radioactivity of acid (pH 3) buffer treatment-resistant cell bound ^{125}I -Lys20 in the absence (total internalization) (●—●) or presence of an excess amount of unlabeled Lys20 (nonspecific internalization) (○—○) was measured. The specific internalization of Lys20 is, therefore, the difference between the total and nonspecific internalization.

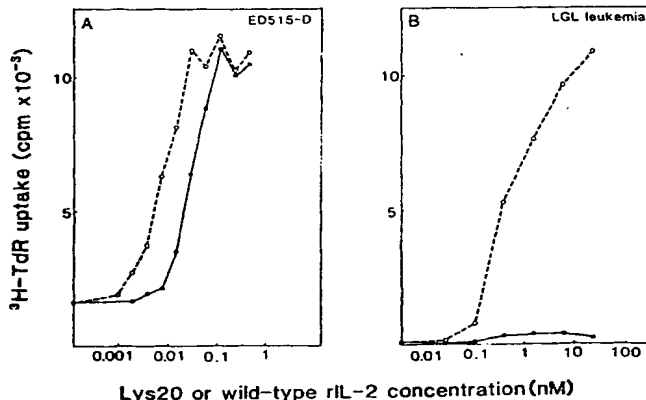


Figure 4. Proliferative response of ED515-D cells (A) and LGL leukemic cells (B) to Lys20 and wild-type rIL-2. Cells were incubated with various concentrations of Lys20 (●—●) or wild-type rIL-2 (○—○).

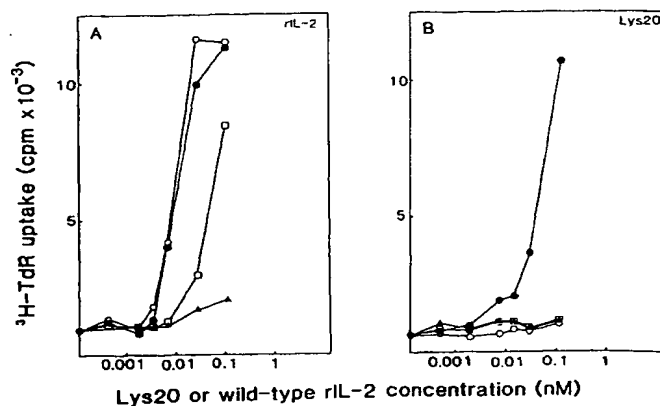


Figure 5. Effect of anti-Tac and 2R-B mAb on wild-type rIL-2- or Lys20-induced proliferation of ED515-D cells. Cells were incubated with various concentrations of wild-type rIL-2 (A) or Lys20 (B) together with no mAb (●—●), 630 nM anti-Tac mAb (□—□), 630 nM 2R-B mAb (○—○), or anti-Tac + 2R-B mAb (▲—▲).

pletely suppressed by 2R-B mAb alone as well as by anti-Tac mAb (Fig. 5B).

Lys20, unlike wild-type rIL-2, cannot produce the

detachment of cell-bound 2R-B mAb at 37°C. 2R-B mAb cannot suppress IL-2-dependent cell growth, because the addition of wild-type rIL-2 produces the detachment and replacement of 2R-B mAb bound to the IL-2R β -chain on cells expressing both IL-2R α - and β -chain at 37°C (26). As we found that 2R-B mAb could suppress Lys20-induced cell growth of ED515-D cells, we examined whether Lys20 produced the detachment of cell-bound 2R-B mAb at 37°C. The addition of 10 nM wild-type rIL-2 rapidly decreased the cell-associated radioactivity of ^{125}I -2R-B mAb on ED515-D cells, but the addition of 10 nM Lys20 did not (Fig. 6A). Figure 6B shows that Lys20 could not induce the detachment of FITC-conjugated 2R-B mAb bound to ED515-D cells, and that wild-type rIL-2 preincubated with L61 mAb, an anti-IL-2 mAb recognizing the high affinity binding site of IL-2, could not induce the detachment of the cell-bound FITC-conjugated 2R-B mAb.

DISCUSSION

In the present study we have presented data strongly suggesting that IL-2R α -chain can facilitate IL-2 interactions with the IL-2R β -chain. It has been postulated that the IL-2/IL-2R α -chain complex forms first, followed by a subsequent interaction with the IL-2R β -chain or an alteration of the binding affinity of the β -chain in cells expressing both α - and β -chains.

The binding assay of ^{125}I -Lys20, an IL-2 analog derivative with a point mutation of Asp²⁰ to Lys, showed a higher affinity binding as well as low affinity binding to ED515-D cells. The number of binding sites and K_d value of the low affinity Lys20 binding were roughly equal to

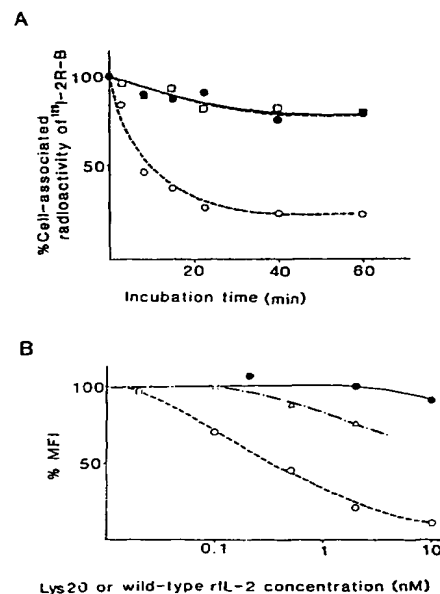


Figure 6. Effect of Lys20 and wild-type rIL-2 on the 2R-B mAb binding to ED515-D cells at 37°C. A. Time dependent decrease of the radioactivity of cell-bound ^{125}I -2R-B mAb. ED515-D cells, pretreated with ^{125}I -2R-B mAb, were incubated with 10 nM of unlabeled Lys20 (●—●), wild-type rIL-2 (○—○) or none (□—□) for various times at 37°C. B. The decrease of the fluorescence intensity of cell-bound FITC-conjugated 2R-B mAb. ED515-D cells, pretreated with FITC-2R-B mAb, were incubated with various concentrations of Lys20 (●—●), wild-type rIL-2 (○—○), or wild-type rIL-2 neutralized by L61 mAb (▲—▲) for 1 h at 37°C, and then examined with a FACScan.

those of low affinity wild-type rIL-2 binding. However, the K_d value of the higher affinity Lys20 binding was about 50 to 100 times higher than that of the standard high affinity binding of wild-type rIL-2.

This higher affinity receptor for Lys20 was considered to consist of an α -chain/ β -chain complex analogous to the high affinity IL-2R because of the following: 1) The number of higher affinity Lys20 binding sites was comparable to that of the high affinity binding sites of wild-type rIL-2; 2) 2R-B mAb, recognizing the IL-2R β -chain, abolished only the higher affinity binding of 125 I-Lys20; 3) affinity cross-linking study of 125 I-Lys20 showed two bands corresponding to α - and β -chains; and 4) Lys20 was rapidly internalized into ED515-D cells presumably via the β -chain as reported for rIL-2.

Our results indicate that Lys20 does not interact with the β -chain without the assistance of the α -chain because 1) cells expressing only β -chains did not have any specific Lys20 binding, and 2) saturating concentrations of anti-Tac mAb (630 nM) completely abolished the specific 125 I-Lys20 binding to ED515-D cells. These data may suggest that the β -chain of a preformed α/β -chain complex have altered binding properties, which are reflected in the higher affinity binding of Lys20 to ED515-D cells. Anti-Tac mAb would abolish the altered binding properties of the β -chain of the preformed α/β -chain complex by preventing association of the two chains by steric effects. An alternative interpretation is that Lys20 binds to the α -chain as the first step and Lys20/ α -chain complex subsequently interacts with β -chain, forming the ternary complex. However, this stepwise model of the Lys20 binding is not necessarily incompatible with the existence of the preformed heterodimer of α - and β -chain. Lys20 binding may induce the conformational change of the α -chain of the preformed heterodimer or Lys20/ α -chain complex may exert a steric effect on the β -chain. To differentiate between these two possibilities, an IL-2 analog that binds only to the β -chain may be useful. The intermediate affinity of the binding of such IL-2 analogs was not significantly affected by the presence of the α -chain in the cells expressing both α - and β -chains (41).

Fung et al. (23) reported that Lys20 neither bound to forskolin-activated YT cells expressing both α - and β -chains nor was internalized into YT cells. We cannot explain clearly the discrepancy between their results and ours. It may be due to the differences of the method used to assay internalization. For example, unbound 125 I-Lys20 was not removed after the initial incubation of cells and ligand in our studies. 125 I-Lys20 may have dissociated during the cell washing or incubation steps in the previous report (23).

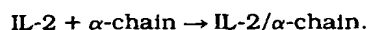
The results of proliferative response assays were consistent with those of binding assays. ED515-D cells expressing both α - and β -chains could proliferate in response to Lys20, whereas LGL leukemic cells solely expressing β -chains could not. In addition, Lys20 also induced the proliferation of Kit 225 cells (data not shown).

We also examined the effect of anti-IL-2R antibodies on the cell growth induced by wild-type rIL-2 or Lys20 to investigate the mechanism of the formation of the IL-2/higher affinity receptor complex. Anti-Tac mAb could not completely block the wild-type rIL-2-induced cell growth of ED515-D cells as reported previously, because wild-

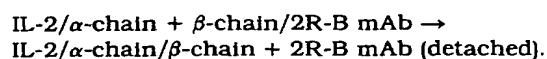
type rIL-2 could bind to the β -chain directly at higher concentrations (42). The addition of anti-Tac mAb could completely block the Lys20-induced cell growth, indicating that Lys20 must bind to the free α -chain.

The addition of 2R-B mAb could not block the cell growth induced by wild-type rIL-2 at all, because the ternary complex of IL-2/ α -chain/ β -chain could be formed at 37°C in spite of the presence of 2R-B mAb as we recently reported (26). The process of the formation of IL-2/ α -chain/ β -chain complex in the presence of 2R-B mAb has been postulated to consist of two steps (26, 30-32).

The first step was:



And the second step was:



In the previous work (26), we could not conclude whether β -chain mainly binds to the IL-2 of the IL-2/ α -chain complex or to its α -chain at the second step of our model. In this study we find the important role of the IL-2 of the IL-2/ α -chain complex to associate with β -chain at the second step. Our results appear to rule out the strict interpretation of the original affinity-conversion model which does not require IL-2 binding to the both chains (30, 31) for the formation of high affinity receptor. As the growth of ED515-D cells induced by Lys20, in contrast to wild-type rIL-2, was completely blocked by the addition of 2R-B mAb, we supposed that the interaction of Lys20/ α -chain and β -chain is not strong enough to replace 2R-B mAb bound to β -chain. This was clearly shown by the following results: 1) the high affinity binding was clearly detectable in the binding assay of ED515-D cells in the presence of 2R-B mAb at 37°C with the use of radiolabeled wild-type rIL-2 but not radiolabeled Lys20 (data not shown); 2) unlike wild-type rIL-2, the detachment of cell bound 2R-B mAb was not detectable after long incubation with high concentrations of Lys20; and 3) L61 mAb recognizing the high affinity binding sites of IL-2, prevented wild-type rIL-2 from detaching 2R-B mAb prebound to β -chains at 37°C.

The data obtained from transfection studies with IL-2R α - and β -chain cDNAs showed that α -chains could not transmit a proliferative signal without β -chains (7, 8, 43). Our observation that 2R-B mAb completely blocked the cell growth induced by Lys20 which binds to α -chain indicates that α -chain by itself cannot transmit the IL-2 signal, at least, in ED515-D cells.

REFERENCES

1. Tsudo, M., T. Uchiyama, and H. Uchino. 1984. Expression of Tac antigen on activated normal human B cells. *J. Exp. Med.* 160:612.
2. Waldmann, T. A., C. K. Goldman, R. J. Robb, J. M. Depper, W. J. Leonard, S. O. Sharrow, K. F. Bongiovanni, S. J. Korsmeyer, and W. C. Greene. 1984. Expression of interleukin 2 receptors on activated human B cells. *J. Exp. Med.* 160:1450.
3. Ceredig, R., J. W. Lowenthal, M. Nabholz, and H. R. MacDonald. 1985. Expression of interleukin-2 receptors as a differentiation marker on intrathymic stem cells. *Nature* 314:98.
4. Raulet, D. H. 1985. Expression and function of interleukin-2 receptors on immature thymocytes. *Nature* 314:101.
5. Malkovsky, M., B. Loveland, M. North, G. L. Asherson, L. Gao, P. Ward, and W. Fiers. 1987. Recombinant interleukin-2 directly augments the cytotoxicity of human monocytes. *Nature* 325:262.
6. Robb, R. J., A. Munck, and K. A. Smith. 1981. T cell growth factor receptors: quantitation, specificity, and biological relevance. *J. Exp.*

- Med. 154:1455.
7. Leonard, W. J., J. M. Depper, T. Uchiyama, K. A. Smith, T. A. Waldmann, and W. C. Greene. 1982. A monoclonal antibody that appears to recognize the receptor for human T-cell growth factor: partial characterization of the receptor. *Nature* 300:267.
8. Nikaido, T., A. Shimizu, N. Ishida, H. Sabe, K. Teshigawara, M. Maeda, T. Uchiyama, J. Yodoi, and T. Honjo. 1984. Molecular cloning of cDNA encoding human interleukin-2 receptor. *Nature* 311:631.
9. Leonard, W. J., J. M. Depper, G. R. Crabtree, S. Rudikoff, J. Pumphrey, R. J. Robb, M. Kronke, P. B. Svetlik, N. J. Peffer, T. A. Waldmann, and W. C. Greene. 1984. Molecular cloning and expression of cDNAs for the human interleukin-2 receptor. *Nature* 311:626.
10. Robb, R. J., W. C. Greene, and C. M. Rusk. 1984. Low and high affinity cellular receptors for Interleukin 2: Implications for the level of Tac antigen. *J. Exp. Med.* 160:1126.
11. Sharon, M., R. D. Klausner, B. R. Cullen, R. Chizzonite, and W. J. Leonard. 1986. Novel interleukin-2 receptor subunit detected by cross-linking under high affinity conditions. *Science* 234:859.
12. Tsudo, M., R. W. Kozak, C. K. Goldman, and T. A. Waldmann. 1986. Demonstration of a non-Tac peptide that binds interleukin 2: a potential participant in a multichain interleukin 2 receptor complex. *Proc. Natl. Acad. Sci. USA* 83:9694.
13. Teshigawara, K., H. Wang, K. Kato, and K. A. Smith. 1987. Interleukin 2 high-affinity receptor expression requires two distinct binding proteins. *J. Exp. Med.* 165:223.
14. Robb, R. J., C. M. Rusk, J. Yodoi, and W. C. Greene. 1987. Interleukin 2 binding molecule distinct from Tac protein: analysis of its role in formation of high-affinity receptors. *Proc. Natl. Acad. Sci. USA* 84:2002.
15. Uchiyama, T., S. Broder, and T. A. Waldmann. 1981. A monoclonal antibody (anti-Tac) reactive with activated and functionally mature human T cells. *J. Immunol.* 126:1393.
16. Tsudo, M., R. W. Kozak, C. K. Goldman, and T. A. Waldmann. 1987. Contribution of a p75 interleukin 2 binding peptide to a high-affinity interleukin 2 receptor complex. *Proc. Natl. Acad. Sci. USA* 84:4215.
17. Lowenthal, J. W., and W. C. Greene. 1987. Contrasting interleukin 2 binding properties of the α (p55) and β (p70) protein subunits of the human high-affinity interleukin 2 receptor. *J. Exp. Med.* 166:1156.
18. Tsudo, M., C. K. Goldman, K. F. Bongiovanni, W. C. Chan, E. F. Winton, M. Yagita, E. A. Grimm, and T. A. Waldmann. 1987. The p75 peptide is the receptor for interleukin 2 expressed on large granular lymphocytes and is responsible for the interleukin 2 activation of these cells. *Proc. Natl. Acad. Sci. USA* 84:5394.
19. Siegel, J. P., M. Sharon, P. L. Smith, and W. J. Leonard. 1987. The IL-2 receptor β -chain (p70): role in mediating signals for LAK, NK, and proliferative activities. *Science* 238:75.
20. Hori, T., T. Uchiyama, R. Onishi, M. Kamio, H. Umadome, S. Tamori, T. Motol, T. Kodaka, and H. Uchino. 1988. Characteristics of the IL-2 receptor expressed on large granular lymphocytes from patients with abnormally expanded large granular lymphocytes: implication of a non-Tac IL-2-binding peptide. *J. Immunol.* 140:4199.
21. Tagawa, S., M. Hatakeyama, M. Shibano, T. Taniguchi, and T. Kitani. 1988. The expression of the p75 subunit of interleukin 2 receptor in Tac negative leukemic cells of two patients with large granular lymphocytic leukemia. *Blood* 71:1161.
22. Robb, R. J., and W. C. Greene. 1987. Internalization of interleukin 2 is mediated by the β -chain of the high-affinity interleukin 2 receptor. *J. Exp. Med.* 165:1201.
23. Fung, M. R., G. Ju, and W. C. Greene. 1988. Co-internalization of the p55 and p70 subunits of the high-affinity human interleukin 2 receptor. *J. Exp. Med.* 168:1923.
24. Tsudo, M., F. Kitamura, and M. Miyasaka. 1989. Characterization of the interleukin 2 receptor β -chain using three distinct monoclonal antibodies. *Proc. Natl. Acad. Sci. USA* 86:1982.
25. Takeshita, T., Y. Goto, K. Tada, K. Nagata, H. Asao, and K. Sugamura. 1989. Monoclonal antibody defining a molecule possibly identical to the p75 subunit of interleukin 2 receptor. *J. Exp. Med.* 169:1323.
26. Kamio, M., T. Uchiyama, N. Arima, K. Itoh, T. Ishikawa, T. Hori, and H. Uchino. 1990. Role of α -chain-IL-2 complex in the formation of the ternary complex of IL-2 and high-affinity IL-2 receptor. *Int. Immunol.* 2:521.
27. Hatakeyama, M., M. Tsudo, S. Minamoto, T. Kono, T. Doi, T. Miyata, M. Miyasaka, and T. Taniguchi. 1989. Interleukin-2 receptor β -chain gene: generation of three receptor forms by cloned human α - and β -chain cDNA's. *Science* 244:551.
28. Itoh, N., S. Yonehara, J. Schreurs, D. M. Gorman, K. Maruyama, A. Ishii, I. Yahara, K. Arai, and A. Miyajima. 1990. Cloning of an interleukin-3 receptor gene: a member of a distinct receptor gene family. *Science* 247:324.
29. Gearing, D. P., J. A. King, N. M. Gough, and N. A. Nicola. 1989. Expression cloning of a receptor for human granulocyte-macrophage colony-stimulating factor. *EMBO J.* 8:3667.
30. Kondo, S., A. Shimizu, Y. Saito, M. Kinoshita, and T. Honjo. 1986. Molecular basis for two different affinity states of the interleukin 2 receptor: affinity conversion model. *Proc. Natl. Acad. Sci. USA* 83:9026.
31. Ogura, T., M. Konishi, N. Suzuki, S. Kondo, H. Sabe, and T. Honjo. 1988. Molecular mechanism for the formation of the high-affinity complex of interleukin 2 and its receptor. *Mol. Biol. Med.* 5:123.
32. Saito, Y., H. Sabe, N. Suzuki, S. Kondo, T. Ogura, A. Shimizu, and T. Honjo. 1988. A larger number of L chains (Tac) enhance the association rate of interleukin 2 to the high affinity site of the interleukin 2 receptor. *J. Exp. Med.* 168:1563.
33. Collins, M. K. L., P. Malde, A. Miyajima, K. Arai, K. A. Smith, and R. C. Mulligan. 1990. Evidence that the level of the p55 component of the interleukin (IL) 2 receptor can control IL2 responsiveness in a murine IL-3-dependent cell. *Eur. J. Immunol.* 20:573.
34. Saragovi, H., and T. R. Malek. 1988. Direct identification of the murine IL-2 receptor p55-p75 heterodimer in the absence of IL-2. *J. Immunol.* 141:476.
35. Collins, L., W. H. Tsien, C. Seals, J. Hakimi, D. Weber, P. Bailon, J. Hoskings, W. C. Greene, V. Toome, and G. Ju. 1988. Identification of specific residues of human interleukin 2 that affect binding to the 70-kDa subunit (p70) of the interleukin 2 receptor. *Proc. Natl. Acad. Sci. USA* 85:7709.
36. Maeda, M., A. Shimizu, K. Ikuta, H. Okamoto, M. Kashiwara, T. Uchiyama, T. Honjo, and J. Yodoi. 1985. Origin of human T-lymphotropic virus I-positive T cell lines in adult T cell leukemia: analysis of T cell receptor gene rearrangement. *J. Exp. Med.* 162:2169.
37. Hori, T., T. Uchiyama, M. Tsudo, H. Umadome, H. Ohno, S. Fukuhara, K. Kita, and H. Uchino. 1987. Establishment of an interleukin 2-dependent human T cell line from a patient with T cell chronic lymphocytic leukemia who is not infected with human T cell leukemia/lymphoma virus. *Blood* 70:1069.
38. Ide, M., K. Kaneda, K. Koizumi, K. Hojo, Y. Murai, K. Sagawa, M. Kono, and K. Sato. 1987. Neutralizing monoclonal antibodies against recombinant human interleukin-2. *J. Immunol. Methods* 101:57.
39. Takemoto, H., Y. Murai, and M. Ide. 1988. Monoclonal antibodies which differentiate high- and low-affinity binding sites of interleukin-2. *FEBS Lett.* 242:53.
40. Tsudo, M., H. Karasuyama, F. Kitamura, Y. Nagasaka, T. Tanaka, and M. Miyasaka. 1989. Reconstitution of a functional IL-2 receptor by the β -chain cDNA: a newly acquired receptor transduces negative signal. *J. Immunol.* 143:4039.
41. Sauve, K., M. Nachman, C. Spence, P. Bailon, E. Campbell, W. H. Tsien, J. A. Kondas, J. Hakimi, and G. Ju. 1991. Localization in human interleukin 2 of the binding site to the α -chain (p55) of the interleukin 2 receptor. *Proc. Natl. Acad. Sci. USA* 88:4636.
42. Wang, H. M., and K. A. Smith. 1987. The interleukin 2 receptor: Functional consequences of its bimolecular structure. *J. Exp. Med.* 166:1055.
43. Greene, W. C., R. J. Robb, P. B. Svetlik, C. M. Rusk, J. M. Depper, and W. J. Leonard. 1985. Stable expression of cDNA encoding the human interleukin 2 receptor in eukaryotic cells. *J. Exp. Med.* 162:363.

Preassembly of interleukin 2 (IL-2) receptor subunits on resting Kit 225 K6 T cells and their modulation by IL-2, IL-7, and IL-15: A fluorescence resonance energy transfer study

(receptor assembly/cytokine binding/cell activation)

SÁNDOR DAMJANOVICH*†, LÁSZLÓ BENE†, JÁNOS MATKÓ†, ABDELKRIM ALILECHE*, CAROLYN K. GOLDMAN*, SUSAN SHARROW‡, AND THOMAS A. WALDMANN*§

*Metabolism Branch and ‡Experimental Immunology Branch, National Cancer Institute, National Institutes of Health, Bethesda, MD 20892; and †Department of Biophysics, University Medical School, Debrecen, H4012-Hungary

Contributed by Thomas A. Waldmann, September 25, 1997

ABSTRACT Assembly and mutual proximities of α , β , and γ_c subunits of the interleukin 2 receptors (IL-2R) in plasma membranes of Kit 225 K6 T lymphoma cells were investigated by fluorescence resonance energy transfer (FRET) using fluorescein isothiocyanate- and Cy3-conjugated monoclonal antibodies (mAbs) that were directed against the IL-2R α , IL-2R β , and γ_c subunits of IL-2R. The cell-surface distribution of subunits was analyzed at the nanometer scale (2–10 nm) by FRET on a cell-by-cell basis. The cells were probed in resting phase and after coculture with saturating concentrations of IL-2, IL-7, and IL-15. FRET data from donor- and acceptor-labeled IL-2R β - α , γ - α , and γ - β pairs demonstrated close proximity of all subunits to each other in the plasma membrane of resting T cells. These mutual proximities do not appear to represent mAb-induced microaggregation, because FRET measurements with Fab fragments of the mAbs gave similar results. The relative proximities were meaningfully modulated by binding of IL-2, IL-7, and IL-15. Based on FRET analysis the topology of the three subunits at the surface of resting cells can be best described by a “triangular model” in the absence of added interleukins. IL-2 strengthens the bridges between the subunits, making the triangle more compact. IL-7 and IL-15 act in the opposite direction by opening the triangle possibly because they associate their private specific α receptors with the β and/or γ_c subunits of the IL-2R complex. These data suggest that IL-2R subunits are already colocalized in resting T cells and do not require cytokine-induced redistribution. This colocalization is significantly modulated by binding of relevant interleukins in a cytokine-specific manner.

Immune responses are regulated by a series of proteins termed cytokines. Cytokines exhibit a high degree of redundancy and pleiotropy controlling a wide range of functions in various cell types. The redundancy is explained in part by the sharing of common receptor subunits among members of the cytokine receptor superfamily. Each cytokine has its own private receptor but may share public receptors with other cytokines. The multisubunit interleukin 2 receptor (IL-2R) includes three elements: the 55-kDa IL-2R α , the 70- to 75-kDa IL-2R β , and the 64-kDa IL-2R γ subunits (1–7). There are three forms of cellular receptors for IL-2 based on their affinity for ligand and receptor subunit utilization: one with a very high affinity (IL-2R $\alpha\beta\gamma$, $K_d 10^{-11}$ M), one with an intermediate affinity (IL-2R $\beta\gamma$, 10^{-9} M), and one with a lower affinity (IL-2R α , 10^{-8} M). IL-2R α is the private subunit employed solely by IL-2

whereas IL-2R β is shared by IL-2 and IL-15, and IL-2R γ (now termed γ_c) is used in common by IL-2, IL-4, IL-7, IL-9, and IL-15 (3–7). Although the physical relationship among the IL-2R subunits on the cell surface has been the subject of extended analyses, certain aspects are still being debated. It is clear that on addition of IL-2 there is heterodimerization of the IL-2R β and γ_c chain cytoplasmic domains that mediate the signal for T cell proliferation (8, 9). Although the existence of the high affinity heterotrimer in the presence of IL-2 is not in question, there are diverse views as to whether the heterotrimer can exist in the absence of IL-2 or whether it requires the presence of this cytokine for its formation. Saito, Kondo and their coworkers, on the basis of kinetic binding studies on human T cells with varying numbers of IL-2R α chains, proposed an “affinity conversion” model for the high affinity IL-2R (10, 11). This model proposes that IL-2R α and IL-2R β subunits normally exist unassociated on the cell surface in the absence of ligand. The first mandatory reaction is proposed to be between IL-2 and IL-2R α and then between this binary complex and IL-2R β . Subsequent studies using anti-IL-2R α or anti-IL-2R β antibodies to inhibit high affinity binding at 4°C and 37°C have been interpreted to support this affinity-conversion model (12, 13). Other studies support the contrasting view that IL-2R α and β exist in preformed complexes. In crosslinking studies performed in the absence of IL-2 there appeared to be a close physical association of IL-2R α and IL-2R β (14, 15). Furthermore, evidence for IL-2R α -IL-2R β heterodimers in the absence of IL-2 was obtained by Scatchard analysis by using cell lines expressing different numbers of IL-2R α chains (16). Finally, we used an IL-2 mutant analog, F42A, that fails to bind to the isolated IL-2R α subunit and an antibody, H1E1, that separates the IL-2R α and β subunits to demonstrate that IL-2R α and β exist as preformed complexes in which the affinity of IL-2R β for IL-2 is altered by the proximity of IL-2R α through mechanisms that do not require the prior binding of IL-2 to IL-2R α (17, 18). Kuziel and coworkers made similar observations (19). Another IL-2 analog, Lys-20, that fails to bind to isolated IL-2R β was used to show that the proximity of IL-2R β affects IL-2 binding by IL-2R α by mechanisms that do not require prior binding to IL-2R β (20).

The relationship of γ_c to the other subunits is less well defined. An interaction between IL-2 and the IL-2R γ chain has been identified (21). Furthermore, in the presence of IL-2,

Abbreviations: Cy3, sulfoindocyanine succinimidyl bifunctional ester; FITC, fluorescein isothiocyanate; FRET, fluorescent resonance energy transfer; IL-2R, interleukin 2 receptor; mAbs, monoclonal antibodies.

§To whom reprint requests should be addressed at: Metabolism Branch/National Cancer Institute, Building 10, Room 4N115, National Institutes of Health, Bethesda, MD 20892-1374. e-mail: tawald@helix.nih.gov.

The publication costs of this article were defrayed in part by page charge payment. This article must therefore be hereby marked “advertisement” in accordance with 18 U.S.C. §1734 solely to indicate this fact.

© 1997 by The National Academy of Sciences 0027-8424/97/9413134-6\$2.00/0 PNAS is available online at <http://www.pnas.org>.

immunoprecipitation using anti-IL-2R β monoclonal antibodies (mAbs) led to the immunoprecipitation of IL-2R β / γ complexes (22). However, in the absence of IL-2, antibodies to IL-2R β did not coprecipitate γ_c , raising the possibility that stable IL-2R β / γ complexes are not preassembled on the cell surface (22). Finally, the effect of the addition of non-IL-2 cytokines (e.g., IL-4, IL-7, IL-9, or IL-15) that bind to IL-2R β or γ_c on the topology of the IL-2R subunits has not been defined. In the present study we used fluorescence resonance energy transfer (FRET) measurements to address these issues. FRET can be successfully applied to determine intra- and intermolecular distances at the 2- to 10-nm level. When an energy donor [usually fluorescein isothiocyanate (FITC)] and an energy acceptor (e.g., Cy3) are closely associated, there is tunneling of energy from the donor to the acceptor so that the emission from the donor is reduced and from the acceptor is increased. In the present work we used FRET measurements to define the assembly and mutual proximity among the three IL-2 receptor subunits in the resting phase and after the addition of saturating concentrations of IL-2, IL-7, and IL-15 that bind to the different IL-2R subunits.

MATERIALS AND METHODS

Cell Culture and Treatment with Cytokines. The Kit 225 K6 cell line (obtained from Takashi Uchiyama, Kyoto, Japan) that was originally derived from a human adult T cell lymphoma (23), was cultured in RPMI 1640 medium supplemented with 10% fetal calf serum, 20 units/ml of recombinant IL-2 and penicillin, and streptomycin. The IL-2 was added on a daily basis. Before the experiments the cells were washed in media without cytokine and were grown for 48–72 hr without further addition of IL-2. These cells were considered as resting control cells. The lymphokine-treated cell samples were supplemented with IL-2 (20 units/ml), IL-7 (20 pM), or IL-15 (20 pM) and cultured at 37°C for 6 hr before harvesting the cells. The cells were then washed out of media and stained at 4°C with the anti-receptor mAbs.

Monoclonal Antibodies. The subunits of the IL-2R complex were targeted by the following antibodies: the α subunit was defined either with anti-Tac (IgG2a) or 7G7/B6 (IgG2a) mAbs. Anti-Tac competes with IL-2 for its binding site whereas 7G7/B6 does not. The MikB1 (IgG2a) and the Mik β 3 (IgG1 κ) are specific for the β subunit, with MikB1 interacting with the cytokine binding site of this subunit. The γ_c subunit was labeled by mAb TUGh4, purchased from PharMingen. The W6/32 (IgG2a) mAb with specificity for the heavy chain of class I HLA A, B, and C molecules and L-368 (IgG1) mAb specific for β 2-microglobulin were kindly provided by F. Brodsky, University of California at San Francisco.

Fab Fragment Preparation. The Fab fragments were prepared from monoclonal antibodies by using a method described earlier by Edidin (24). Briefly, IgG mAbs were dialyzed with PBS (100 mM Na₂HPO₄/150 mM NaCl/1 mM EDTA, pH 8.0) and digested with activated papain at 37°C for 11 min. The enzyme activity was terminated by addition of iodoacetamide. The reaction mixture was passed through a Sephadex G-100 fine column, and the collected Fab fractions were further separated from intact Ig by using a Protein A-Sepharose column.

Conjugation of Monoclonal Antibodies with Fluorescent Dyes. Aliquots of purified whole mAbs or Fab fragments (at least at 1 mg/ml concentration) were conjugated as described previously (25, 26) with fluorescein isothiocyanate (FITC) (Molecular Probes) or sulfoindocyanine succinimidyl bifunctional ester (Amersham). Briefly, the proteins were transferred into a carbonate-bicarbonate buffer at pH 9.4, mixed with 30- to 100-fold molar excess of freshly prepared fluorescence dyes, and incubated for 45–60 min at room temperature. For labeling with Cy3, a kit was used (Amersham). Unreacted

dye molecules were removed by gel filtration through a Sephadex G-25 column. The final antibody concentration and the dye-to-protein ratio were determined spectrophotometrically. In the case of FITC this ratio varied between 1 and 4; for Cy3, it varied between 4 and 8. The fluorescently tagged antibodies retained their biological activity as assessed by competition with identical but unlabeled antibodies.

Labeling of Cells with Monoclonal Antibodies. Freshly harvested cells were washed twice in ice-cold PBS (pH 7.4). The cell pellets were suspended in 100 μ l of PBS (1×10^6 cells per ml) and labeled by incubation with approximately 10 μ g of FITC- or Cy3-conjugated mAbs for 60 min on ice. The excess mAbs over the available binding sites was at least 30-fold during the incubation. To avoid possible aggregation of the antibodies they were air-fuged (at 9×10^4 rpm, for 30 min) before labeling. Staining of cells was checked by fluorescence microscopy after the labeling procedure. Special care was taken to keep the cells at an ice-cold temperature before FRET analysis to prevent unwanted aggregation of cell surface molecules and meaningful receptor internalization. The labeled cells were washed with excess cold PBS and then fixed with 1% formaldehyde. Data obtained with fixed cells did not differ significantly from those of unfixed, viable cells. The number of binding sites on the cell surface was determined from the mean values of flow-cytometric histograms of cells labeled to saturation with FITC-conjugated mAbs. The mean fluorescence intensities were converted to the number of binding sites by calibration with fluorescent microbeads (Quantum 25, Flow Cytometry Standards, San Juan, Puerto Rico). The diameter of the Kit 225 K6 cells was estimated to be 10–13 μ m.

Flow Cytometric Energy Transfer Measurements. The donor (FITC) and acceptor (Cy3) labels were targeted to cell surface molecules by the relevant mAbs. The measurements were carried out in a Becton Dickinson FACStar Plus flow cytometer as described before (27–29), with minor variations in the excitation and emission parameters. Briefly, the cells were excited at 488 and 565 (occasionally 514) nm sequentially, and the respective emission data were collected at 540 and >590 nm. The fluorescence emissions were gated on the forward-angle light scatter signal to avoid artifacts from cell debris. Corrections were made for the direct excitability of the acceptor at the donor's excitation wavelength and the spectral spillover of the donor's and acceptor's fluorescence by using cell samples labeled with only FITC- or, alternatively, Cy3-conjugated mAbs. The necessary signals were collected in list mode and analyzed as described before (27–29). The efficiency of energy transfer (E) is expressed as percentage of the donor's (FITC) excitation energy tunneled to the acceptor (Cy3) molecules. E has an inverse sixth-power dependence on the donor-acceptor separation distance and thus an extremely high sensitivity to changes in distances in the range of 2–10 nm (30), if the orientation factor, accounting for the relative position of the donor's emission and the acceptor's absorption dipoles, can be considered as a statistical average of isotropic random orientations (i.e., 2/3) (31). The energy transfer frequency histograms were calculated from the equations described previously (28). The data analysis was performed by a software program termed FLOWIN (version β 2). The program was written and kindly provided by L. Balkay and M. Emri (Positron Emission Tomography Center, University Medical School of Debrecen, Hungary). The mean values of the calculated energy transfer distribution curves were utilized and tabulated as characteristic energy transfer efficiencies between two epitopes.

Because data have been obtained on a cell-by-cell basis, the means of energy transfer histograms represent averages over the cell population, whereas each data point is an average for a single cell. A computerized normalization procedure was used to correct for the differences in the actual receptor

densities and for the inequalities in the individual dye-to-protein labeling ratios of mAbs. Therefore, a comparison of the energy transfer efficiency data allows a two-dimensional mapping, i.e., a possible projection of mutual proximities onto the plane of the plasma membrane (32, 33).

RESULTS

Distribution of IL-2 Receptor Subunits in the Plasma Membrane of Resting T Cells. A considerable disproportionality was found between the relative cell surface densities of the three IL-2R subunits on Kit 225 K6 T cells as was observed with other activated T cells and T cell lines (1, 2). The α subunit had a 10-fold higher expression level than the β and γ subunits (Table 1). Based on the copy numbers observed and the surface area of these cells, if a random Poissonian distribution of the subunits were present, the occurrence frequency of hetero- and homoassociations of any size was predicted to be negligible. Thus, if there were a random distribution, a lack of FRET would be expected between any pairs of labeled subunits. To determine whether there was nonrandom distribution with colocalization, the mutual proximities of α , β , and γ subunits of the IL-2 receptor complex were characterized by the measure of FRET (mean efficiency: E%) obtained from pair-by-pair measurements between donor- and acceptor-labeled subunits. Because of the larger number of α subunits, the energy transfer was measured for both technical and theoretical reasons (34) from the β or γ subunits toward the α , in a pairwise fashion.

The Kit 225 K6 T cells were cultured in the presence of 20 units per ml of IL-2 administered on a daily basis. Although mAbs 7G7/B6 and Mik β 3 can bind to the α and β subunits, respectively, in the presence of IL-2, other antibodies compete with IL-2 for its binding site (e.g., anti-Tac and Mik β 1). Therefore, before FRET analysis, the added IL-2 was either removed from the cells by acid washing (in 10 mM sodium citrate, 0.14 M NaCl, pH 4.0) or the cells were grown for 48–72 hr without IL-2 addition resulting in internalization and catabolism of the available IL-2 by the cells. These latter cells were considered as “resting” T cells.

The FRET data concurrently obtained for the subunit pairs of β - α , γ - α , and β - γ (Fig. 1 B–D) by using mAbs with different epitope specificities indicated that these subunits must be in close proximity to each other in the plasma membrane of resting T cells (FRET β - α , $25.4 \pm 5.9\%$; γ - α , $20.6 \pm 5.1\%$; and γ - β , $12.4 \pm 5\%$). The FRET efficiencies obtained for these labeled subunit pairs was comparable to the intramolecular FRET efficiency (ca. 15%) measured between the labeled β 2-microglobulin (by L-368 mAb) and heavy chain epitopes (by W6/32 mAb) of class I HLA molecules on Kit 225 K6 and on a number of other cells (33). Because the latter FRET efficiency coincides well with the high-resolution x-ray structure of class I HLA molecule (35), it can also serve as a reference value for any FRET analysis.

Table 1. Relative surface expression of IL-2R α , β and γ subunits on Kit 225 K6 T cells

Subunit		Number of copies ($\times 10^3$)*
IL-2R α	(Tac, p55)	$96 \pm 12^\dagger$
IL-2R β	(p70–75)	11 ± 5
IL-2R γ	(p64)	8 ± 4

*The number of IL-2R subunits per cell was determined from the mean fluorescence intensities of flow cytometric histograms of cells labeled to saturation with fluorescently conjugated mAbs as described in *Materials and Methods*.

† Data represent mean \pm SEM of at least three independent measurements.

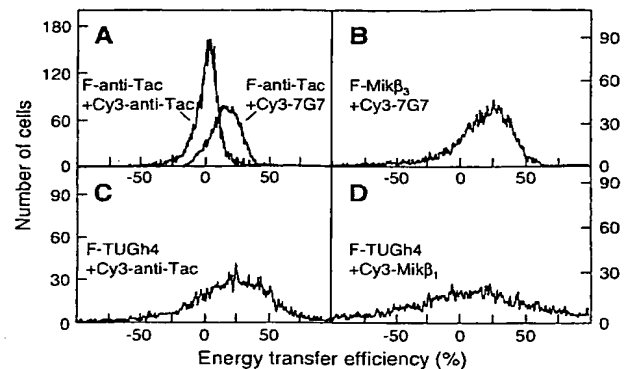


FIG. 1. Representative flow cytometric histograms of energy transfer efficiencies measured between FITC (F)- and Cy3-conjugated mAbs bound to IL-2R α , β , and γ subunits on Kit 225 K6 T cells. Averages and error estimates ($E \pm \Delta E$) of mean values of flow cytometric energy transfer histograms for the indicated donor-acceptor pairs were calculated from data of three to five independent measurements: (A) $1.5 \pm 0.1\%$ for F-anti-Tac + Cy3-anti-Tac, $18.2 \pm 3.5\%$ for F-anti-Tac + Cy3-7G7; (B) $25.4 \pm 5.9\%$ for F-Mik β 3 + Cy3-7G7; (C) $20.6 \pm 5.1\%$ for F-TUGh4 + Cy3-anti-Tac; and (D) $12.4 \pm 5.0\%$ for F-TUGh4 + Cy3-Mik β 1. Displacement from a mean value of 0 indicates energy transfer and nonrandom proximity of the epitopes.

A microaggregation of subunits by bivalent whole IgG antibodies can be excluded as a possible reason for the observed FRET, because application of fluorescent Fab fragments of the mAbs to target the subunits resulted in comparable FRET efficiencies (ranging between 14 and 20%) (data not shown). Because the subunits were labeled and kept on ice before FRET analysis, the possible effects of lateral mobility were also minimized.

There are two plausible interpretations for the high energy transfer efficiencies obtained for the β - α and γ - α subunit pairs. First, the energy transfer observed might reflect the possibility that these subunit pairs are in close proximity to each other within the effective Förster-distance range (ca. 10 nm, in this case). Alternatively, it might mean that both labeled β and γ subunits are surrounded by a large excess of acceptor-labeled α subunits, which would increase the acceptor:donor ratio, favoring a more efficient FRET (34). However, in the latter case, significant homo-transfer of excitation energy would be expected between α subunits labeled with donor- and acceptor-conjugated mAbs directed against the same epitope. This was not observed (Fig. 1A). Furthermore, a significant homo-association of α subunits supporting the second explanation is less likely in the light of recent findings showing a random distribution of gold-labeled IL-2R α polypeptides on mouse T lymphocytes (36) and the lack of a tendency to form aggregates in the case of soluble IL-2R α (37). Therefore, the high FRET efficiencies appear to reflect a close mutual proximity of all the three subunits rather than a high acceptor density. A similarly high FRET efficiency (12%) was found between the β and γ subunits labeled by Cy-Mik β 3 and FITC-TUGh4 mAbs, respectively (Fig. 1D), also supporting the view that the three subunits are in relatively close proximity at the surface of resting T cells, in the absence of IL-2.

IL-2R α Conformation Probed by Intramolecular FRET. The α subunit of IL-2 receptor complex on Kit 225 K6 resting T cells was specifically labeled at two distinct epitopes through the use of two noncompeting mAbs, FITC-anti-Tac and Cy3-7G7/B6, respectively. This analysis yielded results that were similar to those that used intramolecular FRET labels on class I major histocompatibility complex (MHC) molecules and may serve as a “conformational marker” (38) for the α subunit. A mean FRET efficiency of 18% was obtained for this anti-IL-

2R α antibody-pair (Fig. 1A), indicating that the two epitopes located on IL-2R α are well within the critical Förster distance; thus, changes in the *E*% with the two anti-IL-2R α mAbs would be expected to sensitively monitor conformational changes of the IL-2R α molecule.

Modulation of IL-2R Subunit Organization on the T Cell Surface by IL-2, IL-7, and IL-15. The effect of cytokines IL-2, IL-7, and IL-15 on the lateral subunit organization of the IL-2R complex was studied by means of three distinct approaches. The Kit 225 K6 T cells deprived of IL-2 for 72 hr were cultured with these cytokines (for details, see *Materials and Methods*) for 6 hr before harvesting. After staining the cells with mAbs, we examined the effect of the addition of these cytokines on: (i) the accessibility of subunit epitopes to the mAbs applied in FRET analysis, (ii) the intramolecular FRET within IL-2R α (a marker of IL-2R α conformation), and (iii) the FRET efficiencies measured between β - α , γ - α , and β - γ subunit pairs (a measure of subunit proximity).

As shown in Fig. 2, IL-2 addition led to a modulation of the mAb binding (epitope accessibility) to all the three subunits. Here, the mean fluorescence intensities of cells labeled to saturation by mAbs (in the presence of cytokines) were compared with the respective intensities of resting cells without cytokine addition. With all subunits, part of the modulation is probably due to changes in the subunit conformation. The modulation was a bit smaller for the γ chain. IL-7 left the mAb binding to α and β chains unchanged while meaningfully modifying mAb binding to the γ chain to which it binds. IL-15 is a recently recognized cytokine that shares the β and γ subunits with the IL-2R (39). This is consistent with the large mAb-binding modulation observed for the β and a smaller one for the γ chain observed with IL-15 (Fig. 2). The small change in the mAb binding to IL-2R α is possibly due to an indirect cross-modulation of its conformation by IL-15 binding to the IL-2R β and γ chains that normally associate with it.

The conformation of IL-2R α was modulated by all three of the cytokines, as reflected by the changes in intramolecular FRET (Fig. 3). The increased FRET efficiencies indicate a closer proximity of the Tac and 7G7/B6 epitopes, i.e., a more compact conformation of α chains upon addition of IL-2, IL-7, or IL-15 to the T cells.

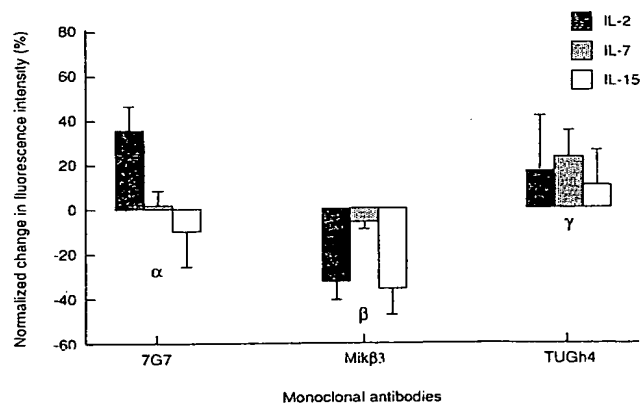


FIG. 2. Effect of IL-2, IL-7, and IL-15 on the accessibility of epitopes to FITC-conjugated mAbs 7G7/B6 (against IL-2R α), Mik β 3 (against IL-2R β), and TUGh4 (against IL-2R γ) added as single agents on Kit 225 K6 wild-type T cells. Interleukins were added to cell cultures 6 hr before harvesting at the following concentrations: IL-2 (solid bars), 20 units/ml; IL-7 (shaded bars) and IL-15 (open bars), both 1 ng/ml (20 pM). The mean values of fluorescence histograms collected on cells treated with the interleukins were expressed as percent change from control values. Bars represent mean \pm SEM of four to six independent measurements.

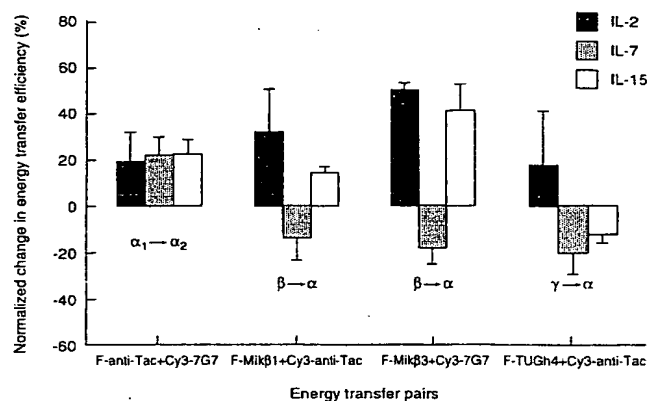


FIG. 3. Effect of IL-2, IL-7, and IL-15 on energy transfer efficiencies measured between FITC (F)- and Cy3-conjugated mAbs specific to the IL-2R α , β , and γ subunits on Kit 225 K6 T cells. The cells were treated with interleukins as described in the legend to Fig. 2 by IL-2 (solid bars), IL-7 (shaded bars), and IL-15 (open bars). The mean values of the fluorescence energy transfer histograms collected from cytokine-treated cells were expressed as percent change from the control values. Bars represent mean \pm SEM of four to six independent measurements. Greek letters with arrows indicate the subunits labeled with the mAbs and the direction of energy transfer. The subscripts 1 and 2 on the letter α designate the two epitopes recognized by mAbs anti-Tac and 7G7, respectively, on the same IL-2R α subunit.

The effects of these cytokines on the mutual proximities of the three IL-2R subunits were tested by FRET measurements on cytokine-pretreated cells (Fig. 3). It should be noted that receptor binding of cytokines also changed the donor:acceptor ratio (influencing FRET efficiency) by modulation of mAb binding in some cases with the exception of the FRET between β and α subunits. In all cases the direction of the changes would not significantly influence the interpretation of FRET data. These FRET data show that IL-2 binding promotes a closer proximity for both β - α and γ - α subunit pairs (the FRET efficiencies increased). This might be a result of conformational changes induced by IL-2 binding that leads to stronger bridges among the subunits in the IL-2R complex or, alternatively, the movement together of IL-2R subunits in the plasma membrane. In contrast, the addition of IL-7 that only binds to γ loosened the interaction of the α subunit with both β and γ chains, as reflected by the reduced FRET efficiencies (Fig. 3). IL-15 increased the proximity between the α and β chains while weakening the interaction between the α and γ chains. This suggests that the binding of IL-15 breaks up (somewhat linearizes) the triangle geometry of the high affinity IL-2R complex, possibly to allow its private specific receptor, IL-15R α , to complex with the IL-2R β / γ subunits (39).

DISCUSSION

In the present study we used fluorescence energy transfer measurements to demonstrate the close proximity of IL-2 receptor subunits in the surface membrane of resting Kit 225 K6 T cells. In contrast to the predictions of the "affinity conversion model," it appears that preassembled subunit pairs (β / γ) or heterotrimers (α / β / γ) form intermediate or high affinity IL-2Rs, respectively, in the absence of added cytokine. These observations are in accord with the IL-2 binding model that postulates the existence of preformed α / β complexes in the plasma membrane (14–20). In the case of the high affinity receptor composed of all of the three IL-2R subunits, a topological two-dimensional projection of subunit organization could be modeled as a triangle (Fig. 4) that is consistent with both the FRET data and the size of the subunits. This triangular model of subunit clustering is very likely in a

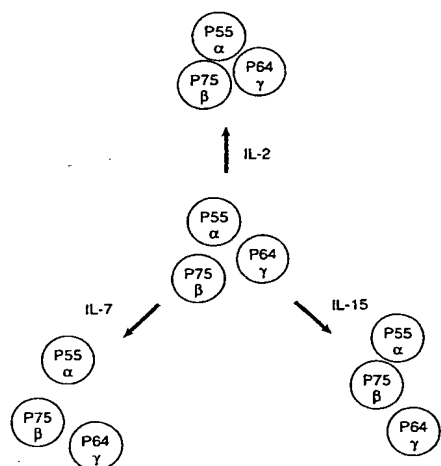


FIG. 4. Schematic representation of lateral organization of the subunits of the IL-2 receptor complex on resting Kit 225 K6 T cells and the complex's modulation by addition of IL-2, IL-7, and IL-15. FRET data suggested that IL-2R α , β , and γ subunits are preassembled, forming heterotrimers on the surface of resting cells (Middle). The proximity between the β and γ subunits was not altered significantly with any of the interleukins. Whereas IL-2 promoted a stronger contact of the α subunit with the β and γ chains (Top), IL-7 loosened it (Bottom Left). IL-15 induced a closer proximity of β and α subunits, whereas the contact between the γ and α subunits became weaker, thereby leading to a somewhat linearized configuration of the IL-2R complex (Bottom Right).

dynamic equilibrium and is in a form that can be modulated by the binding of the ligands IL-2, IL-7, and IL-15 albeit in diverse directions and extents. The addition of the cognate cytokine, IL-2, strengthens the bridges between the IL-2 subunits, making the triangle more compact (Fig. 4). These data indicating a closer association of IL-2R β and γ on IL-2 addition are in accord with previous reports that IL-2R activation leads to heterodimerization of IL-2R β and γ chains, leading to signaling (8, 9). It also is in accord with parallel work that used coprecipitation analysis of IL-2R γ and β to support this tighter assembly of cytokine receptor subunits on IL-2 addition (40, 41). In contrast, the addition of IL-7 and IL-15 acted in the opposite direction by opening the triangle, loosening the contact between the IL-2R α and γ subunits. This may reflect the movement within the cell membrane of the γ subunit so that it becomes associated with the private specific α receptors for IL-7 and IL-15. This suggests that IL-7 and IL-15 and, although not examined in the present study, IL-4 might inhibit the action of IL-2 by diverting γ from the high affinity IL-2R complex. In support of this view, IL-4 has been shown to inhibit the expression of high affinity IL-2Rs on monoclonal human B cells (42). Furthermore, IL-4 manifested an inhibitory action on IL-2-supported human B cell proliferation and differentiation (43).

It is of interest that the addition of IL-7 and IL-15 altered the intramolecular distances of IL-2R α ; that is, the FRET between the 7G7/B6 and Tac epitopes was increased (Fig. 3). Because neither IL-7 nor IL-15 bind to IL-2R α , this suggests that the movement of γ away from IL-2R α mediated by IL-7 and IL-15 addition leads to a change in the conformation of IL-2R α . A similar change in the conformations of IL-2R α and IL-2R β by their proximity was noted previously (17–20).

The present approach, FRET analysis, has been used to demonstrate that intercellular adhesion molecule-1 (ICAM-1) and class I MHC are nonrandomly associated with the IL-2 receptor (32). Such cell surface receptor patterns have also been described for other kinds of receptors. For example, significant subunit clustering in the case of the IL-1 receptor was emphasized by Guo *et al.* (44). Furthermore, two-

dimensional models of receptor distribution have been derived from fluorescence energy transfer data for MHC class I and class II DR and DQ molecules, ICAM-1, the CD20 B cell marker, as well as CD53, CD81, and CD82 "tetraspan" molecules (32, 45–48). In general, these may be critical events involved in effective signal transduction and the cellular adhesion process (49). These studies demonstrate that FRET analysis together with scanning force microscopy and video-tracking techniques may provide new insights into the molecular organization of multisubunit receptor complexes and the rearrangement of this organization upon ligation.

S.D. was a Fulbright Scholar working on the Metabolism Branch, National Cancer Institute with T.A.W. during this work. The work was also supported by Országos Tudományos Kutatási Alap (National Scientific Research Fund) of Hungary (T023873 and T17592) and a special award (AKP-96–316/54).

- Waldmann, T. A. (1989) *Annu. Rev. Biochem.* 58, 875–911.
- Taniguchi, T. & Minami, Y. (1993) *Cell* 73, 5–8.
- Leonard, W. J., Depper, J. M., Uchiyama, T., Smith, K. A., Waldmann, T. A. & Greene, W. C. (1982) *Nature (London)* 300, 267–269.
- Tsuda, M., Kozak, R. W., Goldman, C. K. & Waldmann, T. A. (1986) *Proc. Natl. Acad. Sci. USA* 83, 9694–9698.
- Sharon, M., Klausner, R. D., Cullen, B. R., Chizzonite, R. & Leonard, W. J. (1986) *Science* 234, 859–863.
- Kondo, M., Takeshita, T., Ishii, N., Nakamura, M., Watanabe, S., Arai, K.-I. & Sugamura, K. (1993) *Science* 262, 1874–1877.
- Noguchi, M., Nakamura, Y., Russell, S. M., Ziegler, S. F., Tsang, M., Cao, X. & Leonard, W. J. (1993) *Science* 262, 1877–1880.
- Nakamura, Y., Russell, S. M., Mess, S. A., Friedmann, M., Erdos, M., Francois, C., Jacques, Y., Adelstein, S. & Leonard, W. J. (1994) *Nature (London)* 369, 330–333.
- Nelson, B. H., Lord, J. D. & Greenberg, P. D. (1994) *Nature (London)* 369, 333–336.
- Saito, Y., Ogura, T., Kamio, M., Sabe, H., Uchiyama, T. & Honjo, T. (1990) *Int. Immunol.* 12, 1167–1177.
- Kondo, S., Shimizu, A., Saito, Y., Kinoshita, M. & Honjo, T. (1986) *Proc. Natl. Acad. Sci. USA* 83, 9026–9029.
- Audrain, M., Boeffard, F., Soullillou, J.-P. & Jacques, Y. (1991) *J. Immunol.* 146, 884–892.
- Kamio, M., Uchiyama, T., Arima, N., Itoh, K., Ishikawa, T., Hori, T. & Uchino, H. (1990) *Int. Immunol.* 2, 521–530.
- Saragovi, H. & Malek, T. R. (1988) *J. Immunol.* 141, 476–482.
- Yamaguchi, A., Ide, T., Hatakeyama, M., Doi, T., Kono, T., Uchiyama, T., Kikuchi, K., Taniguchi, T. & Ueda, T. (1989) *Int. Immunol.* 1, 160–168.
- Goldstein, B., Jones, D., Kevekidis, I. G. & Perelson, A. S. (1992) *Int. Immunol.* 4, 23–32.
- Grant, A., Roessler, E., Ju, G., Tsuda, M., Sugamura, K. & Waldmann, T. A. (1991) *Proc. Natl. Acad. Sci. USA* 89, 2165–2169.
- Roessler, E., Grant, A., Ju, G., Tsuda, M., Sugamura, K. & Waldmann, T. A. (1994) *Proc. Natl. Acad. Sci. USA* 91, 3344–3347.
- Kuziel, W. A., Ju, G., Grdina, T. A. & Greene, W. C. (1993) *J. Immunol.* 150, 3357–3365.
- Arima, N., Kamio, M., Okuma, M., Ju, G. & Uchiyama, T. (1991) *J. Immunol.* 147, 3396–3401.
- Boss, S., Leary, T., Sondel, P. & Robb, R. J. (1993) *Proc. Natl. Acad. Sci. USA* 90, 2428–2432.
- Takeshita, T., Ohtani, K., Asao, H., Kumaki, S., Nakamura, M. & Sugamura, K. (1992) *J. Immunol.* 148, 2154–2158.
- Hori, T., Uchiyama, T., Tsuda, M., Umadome, H., Ohno, N., Fukuhara, S., Kita, K. & Uchino, H. (1987) *Blood* 70, 1069–1072.
- Edidin, M. & Wei, T. (1982) *J. Cell Biol.* 95, 458–462.
- Szöllösi, J., Damjanovich, S., Balázs, M., Nagy, P., Trón, L., Fulwyler, M. J. & Brodsky, F. M. (1989) *J. Immunol.* 143, 208–213.
- De Petris, S. (1978) *Methods in Membrane Biology*, ed. Korn, E. D. (Plenum, New York), Vol. 9, pp. 1–201.
- Szöllösi, J., Trón, L., Damjanovich, S., Helliwell, S. H., Arndt-Jovin, D. J. & Jovin, T. M. (1984) *Cytometry* 5, 210–216.
- Trón, L., Szöllösi, J., Damjanovich, S., Helliwell, S. H., Arndt-Jovin, D. J. & Jovin, T. M. (1984) *Biophys. J.* 45, 939–946.

29. Matkó, J., Szöllösi, J., Trón, L. & Damjanovich, S. (1988) *Q. Rev. Biophys.* **21**, 479–544.
30. Stryer, L. (1978) *Annu. Rev. Biochem.* **47**, 819–846.
31. Dale, R. E., Eisinger, J. & Blumberg, W. E. (1979) *Biophys. J.* **26**, 161–194.
32. Damjanovich, S., Gáspár, R. & Pieri, C. (1997) *Q. Rev. Biophys.* **30**, 67–106.
33. Bene, L., Balázs, M., Matkó, J., Möst, J., Dierich, M., Szöllösi, J. & Damjanovich, S. (1994) *Eur. J. Immunol.* **24**, 2115–2123.
34. Fung, B. K. & Stryer, L. (1978) *Biochemistry* **17**, 5241–5248.
35. Silver, M. L., Guo, H.-C., Strominger, J. L. & Wiley, D. C. (1992) *Nature (London)* **360**, 367–369.
36. Breitfeld, O., Kuhlcke, K., Lothar, H., Hohenberg, H., Manweiler, K. & Rutter, G. (1996) *J. Histochem. Cytochem.* **44**, 605–613.
37. Junghans, R. P., Stone, A. L. & Lewis, M. S. (1996) *J. Biol. Chem.* **271**, 10453–10460.
38. Bene, L., Szöllösi, J., Balázs, M., Mátyus, L., Gáspár, R., Ameloot, M., Dale, R. E. & Damjanovich, S. (1997) *Cytometry* **27**, 353–357.
39. Tagaya, Y., Bamford, R. N., DeFilippis, A. P. & Waldmann, T. A. (1996) *Immunity* **4**, 329–336.
40. Voss, S. D., Sondel, P. M. & Robb, R. J. (1992) *J. Exp. Med.* **176**, 531–541.
41. Takeshita, T. K., Ohtani, H., Asao, S., Kumaki, M., Nakamura, M. & Sugamura, K. (1992) *J. Immunol.* **148**, 2154–2158.
42. Karray, S., Dautry-Varsat, A., Tsudo, M., Merle-Beral, H., Debre, P. & Galanaud, P. (1990) *Am. Assoc. Immunol.* **145**, 1152–1158.
43. Jelinek, D. F. & Lipsky, P. E. (1988) *J. Immunol.* **141**, 164–173.
44. Guo, C., Dowers, K. S., Holowka, D. & Baird, B. (1995) *J. Biol. Chem.* **270**, 27562–27568.
45. Szöllösi, J., Damjanovich, S., Goldman, C. K., Fulwyler, M. J., Aszalós, A. A., Goldstein, G., Rao, P., Talle, M. A. & Waldmann, T. A. (1987) *Proc. Natl. Acad. Sci. USA* **84**, 7246–7250.
46. Szöllösi, J., Horejsi, V., Bene, L., Angelisova, P. & Damjanovich, S. (1996) *J. Immunol.* **157**, 2939–2946.
47. Damjanovich, S., Vereb, G., Shaper, A., Jenei, A., Matko, J., Starink, J. P. P., Fox, G., Arndt-Jovin, D. J. & Jovin, T. M. (1995) *Proc. Natl. Acad. Sci. USA* **92**, 1122–1126.
48. Damjanovich, S., Szöllösi, J. & Trón, L. (1992) *Immunol. Today* **13**, A12–A15.
49. Sheets, E. D., Simson, R. & Jacobson, K. (1995) *Curr. Opinion Cell Biol.* **7**, 707–714.

LATERAL DIFFUSION MEASUREMENTS GIVE EVIDENCE FOR ASSOCIATION OF THE Tac PEPTIDE OF THE IL-2 RECEPTOR WITH THE T27 PEPTIDE IN THE PLASMA MEMBRANE OF HUT-102-B2 T CELLS¹

MICHAEL EDIDIN,^{2*} ADORJAN ASZALOS,[†] SANDOR DAMJANOVICH,[†] AND
THOMAS A. WALDMANN[‡]

From the *Department of Biology, The Johns Hopkins University, Baltimore, MD 21218; the †Food and Drug Administration, Washington, D. C. 20204; the ‡Department of Biophysics, Medical University, Debrecen, Hungary; and the §Metabolism Branch, National Cancer Institute, National Institutes of Health, Bethesda, MD 20892

Fluorescence photobleaching recovery measurements show that the FI-IgG-labeled Tac peptide of the IL-2R can diffuse in the plane of the membrane of HUT-102-B2 T lymphocytes, with a mean diffusion coefficient of 2 to $3 \times 10^{-10} \text{ cm}^2\text{s}^{-1}$. Although only a fraction (mean 37%) of the Tac peptides is mobile on any given cell, lateral diffusion of the Tac peptide can be measured in 94% of cells examined. In contrast, the 95-kDa peptide, T27, is 90 to 100% immobilized in cells labeled with OKT27. Immobilization of T27 also affects the lateral diffusion of the Tac peptide, because the Tac peptide is immobile in more than 30% of cells pretreated with OKT27 and then labeled with anti-Tac IgG. The effect is specific for OKT27 to the extent that pretreatment with an anti-HLA mAb does not immobilize the Tac peptide. It appears, then, that Tac and T27 peptide not only are in proximity on HUT-102-B2 lymphocyte membranes but also interact physically in situ.

T lymphocytes stimulated with Ag or mitogen produce IL-2 (1). The hormone exerts its biological effect through specific high affinity receptors expressed on activated but not resting T cells (2, 3). There are at least two classes of IL-2R, differing 1000-fold in their affinities for IL-2. Both high affinity (K_d 10^{-11} M) and low affinity (K_d 10^{-8} M) receptors share the 55-kDa peptide defined by the anti-Tac mAb (3). Antibody blocking (4) and gene cloning (5-7) experiments were used to show that this Tac peptide contains an IL-2-binding site. By using cross-linking methodology and radiolabeled IL-2, we (8) and others (9) have recently identified an additional non-Tac IL-2-binding peptide of 75 kDa. We have proposed a multichain model for the high affinity receptor in which both the 55-kDa Tac and the p75 IL-2-binding peptides are associated in a receptor complex (8).

Recently, we presented evidence supporting an even more complex subunit structure (10). It was suggested

that an additional 95-kDa peptide, T27, is associated with the Tac peptide of the IL-2R on the HUT-102 cell line (10). mAb against T27 variably and inconsistently co-precipitated the p55 Tac peptide, indicating some association between the two. This relationship was investigated in intact cells by labeling each peptide with the appropriate fluorescent mAb and then measuring the average distance between them with a flow cytometric energy transfer technique (10). This technique permits the determination of intermolecular distances at 2- to 10-nm levels on a cell-by-cell basis. The energy transfer data showed proximity of the T27 and Tac peptides, as well as proximity of HLA class I Ag to both T27 and Tac. Appropriate specificity controls showed that the T27 and Tac associations were not fortuitous. The results imply that T27 and Tac peptides are associated on the surface of at least some activated T cells.

In the present study, lateral diffusion measurements were performed to help define the implications of the proximity relationships between the T27 and Tac peptides. The lateral diffusion of cell surface proteins is readily measured by the technique of FPR³ (11, 12). In FPR experiments, the molecules of interest are labeled with a suitable fluorescent label, usually a fluorescent antibody. The fluorescent molecules are bleached in a spot on the cell surface, and the return of fluorescence to this spot is monitored over time. The lateral diffusion coefficient of the labeled molecules may be calculated from the $t_{1/2}$ for recovery of fluorescence. Not all labeled molecules are mobile; the proportion that is mobile is measured in terms of the extent of fluorescence recovery and is defined as the mobile fraction. From 30 to 70% of labeled proteins are found to be mobile in a wide range of cells.

Lateral diffusion is sensitive to the radius of the diffusing species. If molecules are cross-linked or otherwise form complexes on the cell surface, their diffusion is reduced. In extreme cases, diffusion is unmeasurable and the mobile fraction is zero. If T27 and the Tac peptide form a complex, even transiently, then immobilizing one member of the complex ought to affect the lateral diffusion of the other. Here we report measurements of the lateral diffusion of both the Tac and T27 peptides labeled with fluorescent antibodies. We find that T27 itself is

Received for publication January 19, 1988.

Accepted for publication May 13, 1988.

The costs of publication of this article were defrayed in part by the payment of page charges. This article must therefore be hereby marked advertisement in accordance with 18 U.S.C. Section 1734 solely to indicate this fact.

¹ This work was supported by Grants AI-14584 and AI-19814 from the National Institutes of Health to M. E.

² Address all correspondence and reprint requests to Dr. Michael Edidin, Department of Biology, The Johns Hopkins University, Baltimore, MD 21218.

³ Abbreviations used in this paper: FPR, fluorescence photobleaching and recovery; D, diffusion coefficient; R, percent recovery or mobile fraction; HBSS, Hanks' balanced salt solution.

immobilized by mAb against it and that this treatment also immobilizes the Tac peptide on about one-third of all cells so treated. We also find that binding of anti-HLA antibodies affects the lateral diffusion of the Tac peptide, but in a manner quite different from that of anti-T27. These findings extend the results from immunoprecipitation and energy transfer experiments and support the view that not only are the T27 and Tac peptides in proximity, but they interact physically on at least some cells expressing both molecules.

MATERIALS AND METHODS

Cells. HUT-102-B2 is an HTLV-I-associated, Tac-positive, cloned T cell line established from a lymph node of a patient with a cutaneous T cell lymphoma (13).

HUT-102-B2 cells were collected by centrifugation, and pellets of approximately 5×10^4 cells were suspended in antibody, diluted in HBSS. Cells treated with fluorescent mAb were washed three times in HBSS and then checked for the ring stain typical of surface-labeled viable cells. Ring-stained cells were used for FPR measurements. Some cells were incubated in unlabeled (putatively cross-linking) antibodies before addition of a second fluorescent antibody.

Antibodies. Ke-2, an IgG2a mAb reacting with all class I HLA Ag, was the gift of Dr. Roger Kennett (University of Pennsylvania, Philadelphia, PA); OKT27, an IgG2a mAb to the T27 peptide, was a gift of Dr. Gideon Goldstein (Ortho Diagnostic Systems, Inc., Raritan, NJ). The anti-Tac mAb was prepared by one of us (T. A. W.) as previously described (14).

Antibody labeling. mAb were conjugated with FITC by using standard methods. Briefly, a 1 mg/ml solution of antibody was adjusted to pH 9 in carbonate/bicarbonate buffer at room temperature, and FITC (10 μ g) in the same buffer was added. The reaction was allowed to proceed in the dark for 1 hr. Free fluorescein was separated from labeled protein by passing the mixture over Sephadex G-50 (Pharmacia Fine Chemicals, Piscataway, NJ). The labeled protein was dialyzed against isotonic buffer and then centrifuged at $2000 \times g$ immediately before use. Typically, the ratio of dye to protein was 2.

Measurement of lateral diffusion. We used spot photobleaching to measure lateral diffusion of fluorescent antibody-labeled surface molecules. Briefly, an attenuated, focused laser beam was used to define a spot on the surface of a labeled cell. The spot was then bleached for a few milliseconds with the full-strength laser beam. The laser beam was attenuated again, and changes in the fluorescence of the bleached spot with time were then recorded. The time history of recovery of fluorescence in the bleached spot is described by two parameters, the diffusion coefficient, D , and the percentage recovery or mobile fraction, R . The method does not cause detectable damage to membranes (15) and has been used extensively to characterize D in many types of cells (11, 12, 16). Our instrument is computer controlled and utilizes custom-designed hardware and software. It has previously been described in detail (17). With one exception, all measurements were made at a stage temperature of 30°C . In one experiment, mobility of the T27 peptide was measured at 20°C . Repeated measurements of D and R on a single cell varied two-fold in D and at most about 25% in R (29% versus 38%).

RESULTS

The labeled mAb used to visualize the Tac peptide on HUT-102-B2 cells proved suitable for measurements of the lateral diffusion of this Ag. A typical recovery curve for this experiment is shown in Figure 1. The *abscissa* is time in seconds. The *ordinate* shows the fluorescence intensity of the area illuminated by the attenuated laser beam. Values are normalized to the intensity before bleaching, taken as 100%. The *vertical line* indicates the time of bleaching. In this experiment, about 70% of the initial fluorescence is bleached away. The fluorescence in the spot then recovers from 30% of maximum (its level immediately after bleaching) to about 55% of maximum. D values are estimated from such curves in terms of the time required for recovery of fluorescence to half its final level. In the example shown in Figure 1, this value is 2 s.

The percentage of molecules that are free to diffuse, the mobile fraction, or R , is estimated from the asymptote of the fluorescence recovery. In our example, about 36% of the molecules are mobile.

The distribution of diffusion coefficients for the Tac peptide of HUT-102-B2 cells labeled with F1-anti-Tac is shown in Figure 2A, and the distribution of mobile fractions on each cell is shown in Figure 3A. Although the (geometric) mean diffusion coefficient is typical for membrane proteins labeled with antibody, approximately 2 to $3 \times 10^{-10} \text{ cm}^2\text{s}^{-1}$ (Table I), the variation of diffusion coefficients among cells is quite large, covering nearly a 100-fold range. Although many values of D on individual cells are clustered around $1 \times 10^{-10} \text{ cm}^2\text{s}^{-1}$, nearly half are greater than $3 \times 10^{-10} \text{ cm}^2\text{s}^{-1}$. The fraction of mobile Tac molecules also varies widely among cells, between 0 in 6% of the cells (6 of 97) and $\geq 60\%$ in 12% of the cells (12 of 97). However, the distribution of values closely approximates a normal (Gaussian) distribution.

F1-OKT27 labeled cells in a smooth ring, whether labeling at 4°C or at 37°C . T27 molecules so labeled were immobile in 21 of 26 cells examined ($D < \sim 5 \times 10^{-13}$) and were only 10% mobile in the other five cells (Table I). Thus, either T27 occurs in clusters in the surface of HUT-102-B2, or the binding of OKT27 cross-links the T27 peptide, immobilizing it. If T27 complexes preexist in the membrane, then any interactions that they have with Tac peptide are reflected in the diffusion coefficients and mobile fractions measured with F1-anti-Tac (Figs. 2A and 3A). Conversely, if T27 is immobilized as a consequence of the binding of OKT27, then any relationship that it has with Tac peptide may be altered by binding OKT27. To test this, we first treated HUT-102-B2 cells with unlabeled OKT27 and then labeled the Tac peptides of these cells with F1-anti-Tac. A typical experimental curve for these cells is shown in Figure 4. This recovery curve contrasts with that in Figure 1. Although the label is the same (F1-anti-Tac) and the extent of bleaching is the same (70%), the fluorescence in the bleached spot does not increase during the first 30 s after bleaching. The mobile fraction of molecules in this experiment is close to zero.

All of our measurements of Tac peptide lateral diffusion in cells first treated with OKT27 are summarized in Figures 2B and 3B and in Table I. OKT27 treatment slightly affects the average lateral diffusion coefficient of labeled Tac peptide; there are fewer high values of D in treated cells than in control cells. The treatment greatly altered the mobile fraction in two ways. First, cells with $>60\%$ mobile Tac are almost absent from the population. Second, Tac is immobile in 31% (21 of 68) of OKT27-treated cells. This is clearly seen in Figure 3B. The distribution of values is skewed by an excess of values in the range of 0 to 10% recovery (effectively no recovery). Thus, treatment of cells with OKT27, which immobilizes T27, also immobilizes the Tac peptide in many HUT-102-B2 cells and reduces the mobile fraction in many others.

The effect of OKT27 is not a general effect on mobility of surface proteins. The lateral diffusion of class I HLA Ag was not altered when the HUT-102-B2 cells bound OKT27 before being labeled with the anti-HLA class I mAb KE-2 (Table I). Binding anti-Tac to the cells also did not alter the lateral diffusion of HLA Ag (Table I).

Figure 1. A typical recovery curve for a FPR experiment. The ordinate gives fluorescence intensity normalized to that before bleaching. The abscissa is time in seconds. The diffusion coefficient, D , is calculated from the time required for recovery of fluorescence to half its final value, in this case 2 s. From this time and the known area of the laser spot on the cell surface, $D = 6 \times 10^{-10} \text{ cm}^2 \text{ s}^{-1}$ was calculated for labeled Tac peptide. The mobile fraction or R is calculated from the extent of recovery, in this case from 30% of initial fluorescence immediately after bleaching to 55% of initial fluorescence at the asymptote. The maximum possible recovery would have been from 30 to 100% of initial fluorescence. Therefore, R is then calculated as $25/70 \times 100 = 36\%$.

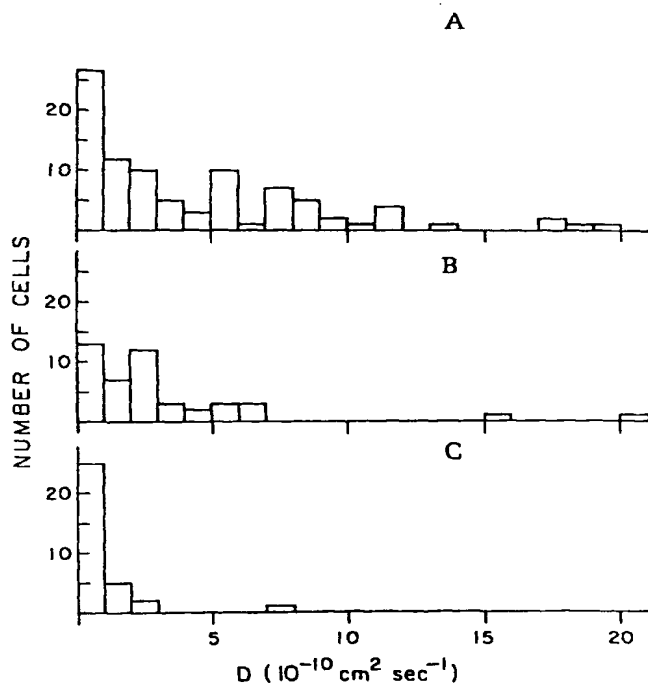
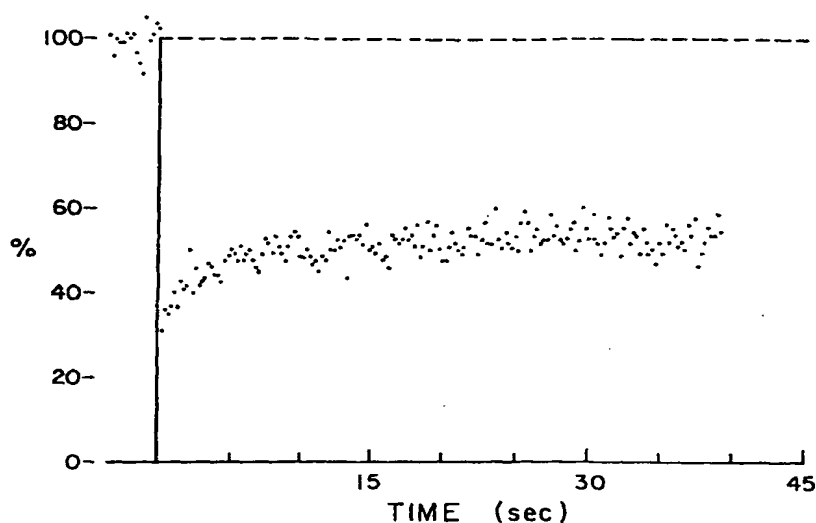


Figure 2. Histogram of D for labeled Tac peptide studied in different cells. The ordinate gives the number of cells for which D had the value indicated on the abscissa. A. Control cells. Values cluster around 2 to $3 \times 10^{-10} \text{ cm}^2 \text{ s}^{-1}$, but there is a long tail of higher values. B. Cells first treated with OKT27. There are few high values of D . C. Cells first treated with the anti-HLA class I mAb KE-2. Only 1 cell of 34 gave $D > 3 \times 10^{-10} \text{ cm}^2 \text{ s}^{-1}$, and most are $D < 1 \times 10^{-10} \text{ cm}^2 \text{ s}^{-1}$. The values are not normally distributed. Hence, geometric means were calculated from the log-normal distribution of values.

Although neither OKT27 nor anti-Tac affects lateral diffusion of HLA Ag, binding of the anti-HLA mAb KE-2 alters the lateral diffusion of Tac peptide. However, the changes due to KE-2 are largely in diffusion coefficient. It can be seen in Figure 2C that all values for D are clustered around $1 \times 10^{-10} \text{ cm}^2 \text{ s}^{-1}$, with only one cell (of 34) showing $D > 3 \times 10^{-10} \text{ cm}^2 \text{ s}^{-1}$. The mobile fraction of Tac peptide in KE-2-treated cells (Fig. 3C) is similar to

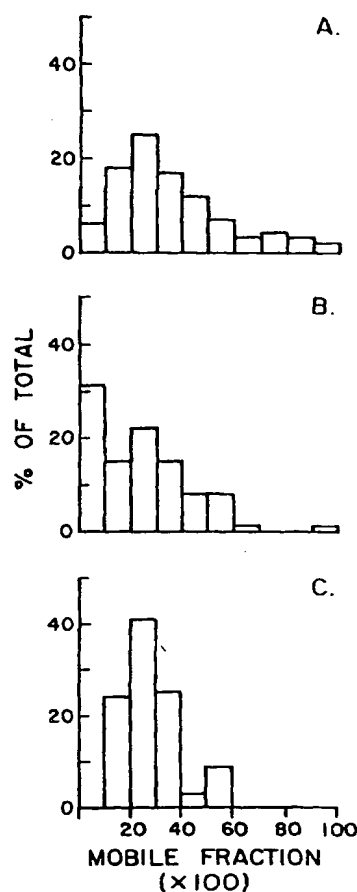


Figure 3. Histogram of R of labeled Tac peptide. A. Control cells. Values form a nearly symmetrical distribution around their mean; cells showing no mobile molecules are rare. B. Cells first treated with OKT27. The distribution of values is skewed low; 31% of the cells had no mobile Tac molecules at all. C. Cells first treated with the anti-HLA mAb KE-2. This is a symmetrical distribution and lacks the tail of high values of R seen in the controls. Data are normalized to 100 cells/group. Actual numbers of measurements are given in Table I.

TABLE I
Lateral mobility of proteins in the membrane of HUT-102 cells

Pretreatment	Fluorescein-labeled Antibody	Diffusion Coefficient ^a	Mobile Fraction (R) ^b	Cells with No Recovery (NR/total)	% NR
None	OKT27		10	21/26	81
None	Anti-Tac	2.6	37	6/97	6
OKT27	Anti-Tac	2.0	33	21/68	31
Anti-HLA	Anti-Tac	0.8 ^c	27	0/34	0
None	Anti-HLA	1.8	31	0/4	0
OKT27	Anti-HLA	1.8	30	0/17	0
Anti-Tac	Anti-HLA	1.9	25	0/9	0

^a Geometric mean diffusion coefficients are in units of $10^{-10} \text{ cm}^2 \text{ s}^{-1}$.

^b SD of R is about 30% for all samples.

^c Significantly different ($p < 0.05$) from control values.

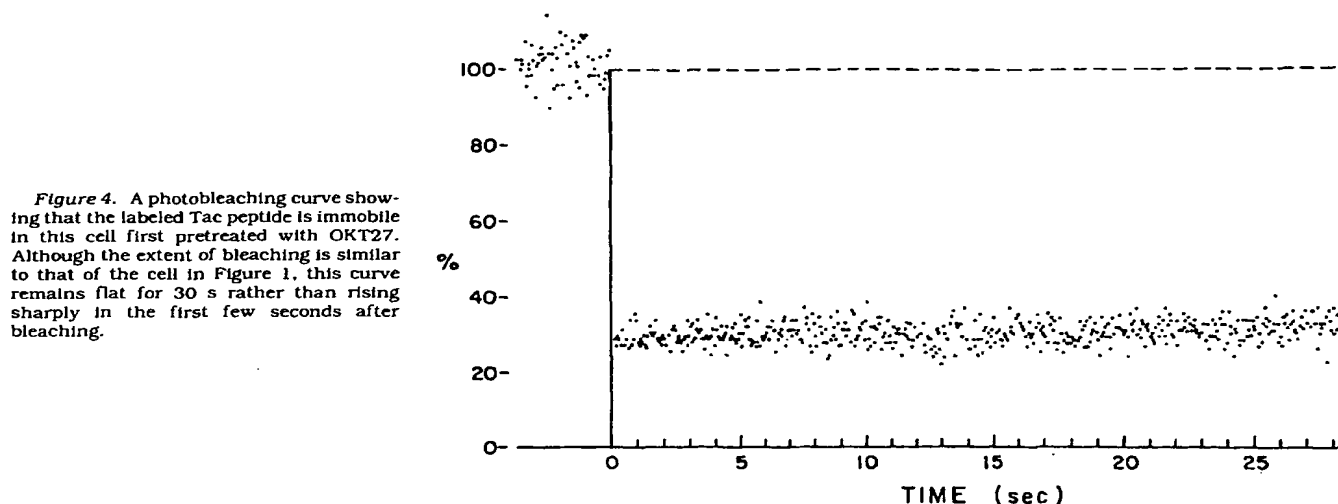


Figure 4. A photobleaching curve showing that the labeled Tac peptide is immobile in this cell first pretreated with OKT27. Although the extent of bleaching is similar to that of the cell in Figure 1, this curve remains flat for 30 s rather than rising sharply in the first few seconds after bleaching.

that in controls, and the values form a normal distribution. In no case were the Tac peptides of KE-2-pretreated cells completely immobilized.

DISCUSSION

Two IL-2-binding peptides, a 55-kDa peptide reactive with the anti-Tac mAb and a 75-kDa non-Tac peptide, have been identified. Cell lines bearing either the p55 Tac or the p75 peptide alone manifested low to intermediate affinity IL-2 whereas cell lines bearing both peptides manifested both high and low affinity receptors. On the basis of these studies, we proposed a multichain model for the high affinity IL-2R in which both the p55 Tac and p75 IL-2-binding peptides are associated in a receptor complex (8). During the examination of the multi-subunit receptor complex, evidence was obtained suggesting a more complex subunit structure that involves peptides in addition to the p55 and the p75 IL-2-binding peptides. Two mAb OKT27 and OKT27b, were produced that react with distinct epitopes of a 95-kDa peptide. The OKT27b antibody inconsistently co-precipitated the 55-kDa peptide as well as the 95-kDa peptide (10). A flow cytometric energy transfer technique was used to demonstrate proximity of the p55 Tac and 95-kDa T27 peptides (10). It was clear from these studies that not all of the T27 peptides identified by OKT27 are associated with the Tac Ag. There were cells that expressed the T27 Ag that were Tac negative; reciprocally, there were cells that expressed the p55 Tac peptide yet

were unreactive with the OKT27 antibody. In addition, the energy transfer between fluorochrome-labeled anti-Tac and rhodamine-labeled OKT27 increased at a decreasing donor-to-acceptor ratio in contrast to the 1:1 stoichiometry observed with two antibodies to different epitopes of the HLA complex.

Although the previous studies suggested proximity of the Tac peptide and the T27 peptide, the nature of their association and its role in the process of lymphocyte activation and differentiation could not be defined. We have now extended the examination of the association of the Tac peptide with the 95-kDa peptide T27 to demonstrate the interaction of the two peptides. Our strategy was based on the finding from fluorescence photobleaching measurements that the T27 peptide labeled with FI-OKT27 does not diffuse in the plane of the membrane. This immobility may be due to cross-linking and aggregation of T27 molecules by OKT27 or to the association of T27 with cytoskeletal proteins when bound to its antibody, so-called "anchorage modulation" (18, 19). Previous fluorescence energy transfer studies (10) indicated that, after the addition of OKT27, cross-linking is the more likely mechanism, since energy transfer is detected between T27 Ag. Whatever the mechanism of the immobilization, we reasoned that, if the Tac peptide and T27 not only are in proximity but make effective physical contacts, then immobilization of T27 ought to alter the lateral diffusion behavior of the Tac peptide.

We measured lateral diffusion of the Tac peptide labeled with FI-anti-Tac IgG in HUT-102 cells that had or

had not been pretreated with OKT27 or other mAb. Three parameters were determined for each group of measurements: the diffusion coefficient (D), the fraction of molecules in the experimentally defined surface area that was free to diffuse (R), and the incidence of cells in which no diffusion could be measured. Treatment of cells with OKT27 affected D to the extent that the subpopulation of cells with $D > 3 \times 10^{-10} \text{ cm}^2\text{s}^{-1}$ was considerably diminished for cells in which lateral diffusion was detectable. More strikingly, it greatly increased the fraction of cells showing no lateral diffusion from 6% in the controls to 31% in OKT27-pretreated cell populations. This effect was specific for T27 and Tac, inasmuch as no parameter of lateral diffusion was affected for the HLA class I Ag of OKT27-pretreated cells.

The total restriction of lateral diffusion in about one-third of all OKT27-treated cells is consistent with the data on energy transfer between T27 and Tac peptides (10). These show that there is a distribution of energy transfer values in a population of HUT-102-B2 cells that ranges from 0 to greater than 20%, implying a similarly wide distribution of relative positions of Tac and T27 on the cell surface. Lateral diffusion of at least some cell surface Ag shows a similarly wide range of values in many cell populations (for example, Reference 20). Thus, we might not expect all cells measured in our photobleaching experiments to show the same effect of OKT27 treatment on lateral diffusion of Tac peptide.

Cross-linking of the HLA Ag of HUT-102-B2 with a mAb, KE-2, also had an effect on the lateral mobility of the Tac peptide. However, unlike OKT27, binding of KE-2 resulted in a two- to three-fold reduction in the D for Tac. Again, this result is reflected in the energy transfer experiments cited, in which a high level of energy transfer, averaging 10%, was found between labeled HLA Ag and Tac peptide (10). In the discussion of those experiments, it was suggested that the association of HLA and Tac peptides was not necessarily specific but, rather, was due to the large number of HLA Ag on the surface, giving an increased probability of random associations. We have since found that, in B cells, cross-linking of HLA Ag by KE-2 plus anti-Ig does not affect any parameter of the diffusion of sIg, although it does not affect the diffusion of other surface molecules thought, on biochemical grounds, to be associated with HLA Ag (J. Reiland and M. Edidin, unpublished observations). Hence, it now appears possible that the association of HLA Ag and Tac peptides is, to some extent, meaningful.

In addition to showing that molecular proximities indicated from energy transfer experiments in fact show molecular interactions between the T27 and Tac peptides, our experiments also indicate a general method for determining associations between molecules at the cell surface. The immobilization of one of a pair of putatively associated molecules by cross-linking ought to affect the lateral diffusion of the other, reducing either D or R .

Extremes of reduction, for example to $D < 1 \times 10^{-12} \text{ cm}^2\text{s}^{-1}$, will be seen as total immobilization of the affected molecules. The application of this general method to the specific case of the IL-2R peptides supports the view that the Tac and T27 peptides not only are in proximity to one another but also physically interact.

REFERENCES

1. Cantrell, D. A., and K. A. Smith. 1984. The interleukin-2 T-cell system: a new cell growth model. *Science* 224:1312.
2. Robb, R. J., W. C. Greene, and C. M. Rusk. 1984. Low and high affinity cellular receptors for interleukin 2. Implications for the level of Tac antigen. *J. Exp. Med.* 160:1126.
3. Waldmann, T. A. 1986. The structure, function and expression of interleukin-2 receptors on normal and malignant lymphocytes. *Science* 232:727.
4. Leonard, W. J., J. M. Deppner, T. Uchiyama, K. A. Smith, T. A. Waldmann, and W. C. Greene. 1982. A monoclonal antibody that appears to recognize the receptor for human T cell growth factor: partial characterization of the receptor. *Nature* 300:267.
5. Leonard, W. J., J. M. Deppner, G. R. Crabtree, S. Rudikoff, J. Pumphrey, R. J. Robb, M. Kronke, P. B. Svetlik, N. J. Peffer, T. A. Waldmann, and W. C. Greene. 1984. Molecular cloning and expression of cDNAs for the human interleukin-2 receptor. *Nature* 311:626.
6. Nikaido, T., A. Shimizu, N. Ishida, H. Sabe, K. Teshigawara, M. Maeda, T. Uchiyama, J. Yodoi, and T. Honjo. Molecular cloning and cDNA encoding human interleukin-2 receptor. *Nature* 311:631.
7. Cosman, D., D. P. Ceretti, A. Larsen, L. Park, C. March, S. Dower, S. Gillis, and D. Urdal. 1984. Cloning, sequence and expression of human interleukin-2 receptor. *Nature* 312:768.
8. Tsudo, M., R. W. Kozak, C. K. Goldman, and T. A. Waldmann. 1986. Demonstration of a non-Tac peptide that binds interleukin 2: a potential participant in a multichain interleukin 2 receptor complex. *Proc. Natl. Acad. Sci. USA* 83:9694.
9. Sharon, M., R. D. Klausner, B. R. Cullen, R. Chizzonite, and W. J. Leonard. 1986. Novel interleukin-2 receptor subunit detected by cross-linking under high-affinity conditions. *Science* 234:859.
10. Szollosi, J., S. Damjanovich, C. K. Goldman, M. J. Fulwyler, A. A. Aszalos, G. Goldstein, P. Rao, M. A. Talle, and T. A. Waldmann. 1987. Flow cytometric resonance energy transfer measurements support the association of a 95-kDa peptide termed T27 with the 55-kDa Tac peptide. *Proc. Natl. Acad. Sci. USA* 84:7246.
11. Jacobson, K., E. Elson, D. Koppel, and W. W. Webb. 1983. International workshop on the application of fluorescence photobleaching techniques to problems in cell biology. *Fed. Proc.* 42:72.
12. Jacobson, K. 1987. Lateral diffusion of proteins in membranes. *Annu. Rev. Physiol.* 49:163.
13. Gazdar, A. F., D. N. Carney, P. A. Bunn, E. K. Russell, E. S. Jaffe, G. P. Schechter, and J. G. Guccione. 1980. Mitogen requirements for the in vitro propagation of cutaneous T-cell lymphomas. *Blood* 55:409.
14. Uchiyama, T., S. Broder, and T. A. Waldmann. 1981. A monoclonal antibody (anti-Tac) reactive with activated and functionally mature human T cells. I. Production of anti-Tac monoclonal antibody and the distribution of Tac (+) cells. *J. Immunol.* 126:1393.
15. Wolf, D. E., M. Edidin, and P. R. Dragsten. 1980. Effect of bleaching light on measurements of lateral diffusion in cell membranes by the fluorescence photobleaching and recovery method. *Proc. Natl. Acad. Sci. USA* 77:2043.
16. McCloskey, M., and M.-M. Poo. 1984. Protein diffusion in cell membranes: some biological implications. *Int. Rev. Cytol.* 87:19.
17. Wolf, D. E., and M. Edidin. 1981. Diffusion and mobility of molecules in surface membranes. In *Techniques in Cellular Physiology*. P. Baker, ed. Elsevier, Amsterdam, p. 1.
18. Schlessinger, J., E. L. Elson, W. W. Webb, I. Yahara, U. Rutishauser, and G. M. Edelman. 1977. Receptor diffusion on cell surfaces modulated by locally bound concanavalin A. *Proc. Natl. Acad. Sci. USA* 74:1110.
19. Woda, B. A., and M. L. McFadden. Ligand-induced association of rat lymphocyte membrane proteins with the detergent-insoluble lymphocyte cytoskeletal matrix. *J. Immunol.* 131:1917.
20. Wier, M. L., and M. Edidin. 1986. Effects of cell density and extracellular matrix on the lateral diffusion of major histocompatibility complex antigens in cultured fibroblasts. *J. Cell Biol.* 103:215.

Establishment of an Interleukin 2-Dependent Human T Cell Line From a Patient With T Cell Chronic Lymphocytic Leukemia Who Is Not Infected With Human T Cell Leukemia/Lymphoma Virus

By Toshiyuki Hori, Takashi Uchiyama, Mitsuru Tsudo, Hiroshi Umadome, Hitoshi Ohno, Shirou Fukuhara, Kenkichi Kita, and Haruto Uchino

We established an interleukin 2 (IL-2)-dependent human T cell line, Kit 225, from a patient with T cell chronic lymphocytic leukemia (T-CLL) with OKT3+, -T4+, -T8- phenotype. Southern blot analysis showed that Kit 225 is not infected with human T cell leukemia/lymphoma virus (HTLV) type I or II, and is probably derived from the major clone in the fresh leukemic cells. Kit 225 cells express a large amount of IL 2 receptors constitutively and their growth is absolutely dependent on IL 2. No other

stimuli, such as lectins or antigens, are required for maintaining the responsiveness to IL 2. As abnormal IL 2 receptor expression was also seen originally in the fresh leukemic cells, the establishment of this cell line with IL 2 suggests that IL 2-mediated T cell proliferation is involved in the leukemogenesis of some cases of HTLV-negative T-CLL.

© 1987 by Grune & Stratton, Inc.

TCELL CHRONIC lymphocytic leukemia (T-CLL) is a heterogeneous disease clinically, morphologically, and immunologically.^{1,5} Although it is believed to be a monoclonal expansion of mature peripheral T cells, the pathophysiology of this disease remains unclear. Our previous study showed that leukemic cells from T-CLL patients with an OKT3+, -T4+, -T8- phenotype express the interleukin 2 (IL 2) receptor without any stimuli and proliferate in response to IL 2.⁶ Because the IL 2/IL 2 receptor system plays an essential role in regulation of T cell growth, it is important to know whether failure of this regulatory mechanism is involved in some T cell malignancies. Recent studies^{7,9} revealed a close association between the abnormal expression of IL 2 receptor and the infection of human T cell leukemia/lymphoma virus type I (HTLV-I),^{10,11} which is believed to be a causative agent of adult T cell leukemia (ATL).¹² The mechanism and role of abnormal expression of IL 2 receptor in HTLV-negative T-CLL has not been well analyzed, however. It appears to be due partly to the lack of appropriate cell lines derived from T-CLL patients. In the present study we established an HTLV-negative and IL 2-dependent T cell line with T4+ phenotype from a T-CLL patient, which was demonstrated to be the same clone as the primary leukemic cells. Using this cell line as a model system, we discuss the implication of IL 2-mediated T cell proliferation in the leukemogenesis of some HTLV-negative T4+ T-CLL cases.

MATERIALS AND METHODS

Patient. A 62-year-old man was admitted on September 26, 1983, because of persistent lymphocytosis, systemic lymph node swelling, and erythroderma. Peripheral blood analysis revealed WBC count of $291 \times 10^9/L$ (leukemic cells 90%), RBC count of $4.81 \times 10^{12}/L$, and platelet count of $3.82 \times 10^{11}/L$. Bone marrow infiltration of 40% pathologic cells was seen. The serologic test was negative for the anti-ATLA antibody.¹² The diagnosis of T-CLL was made on the basis of clinical features, hematologic characteristics, and cell surface phenotypes.⁹

Cell surface marker analysis. Cell surface antigens were detected by indirect immunofluorescence staining and cytofluorometry as described previously.⁶ Monoclonal antibodies OKT3, -T4, -T6, -T8, -T9, -T11 and -Ia were obtained from Ortho Diagnostic Systems (Westwood, MA). Anti-Tac monoclonal antibody (appropriately diluted ascitic fluid) was used as an anti-IL 2 receptor antibody.^{13,14}

Cell separation and culture. The patient's peripheral blood mononuclear cells were separated from heparinized blood by Ficoll-Conray density gradient centrifugation. Separated leukemic cells were then cultivated in RPMI 1640 medium (Nissui Pharmaceutical, Tokyo) supplemented with 10% fetal calf serum (FCS) (GIBCO, Grand Island, NY), 20 $\mu g/mL$ tobramycin, and 20% crude IL 2 (culture supernatant of lectin-stimulated human spleen cells) at 37°C under a humid atmosphere with 5% CO₂. After 3 months, crude IL 2 was replaced by 1 U/mL recombinant human IL 2 generously provided by Takeda Chemical Industries Inc. (Osaka, Japan).

Radiolabeled IL 2 binding assay. Radiolabeled IL 2 binding assay was done as described elsewhere¹⁵ to determine the number of both high-affinity and low-affinity binding sites.

Growth pattern of the cell line cells. To estimate the growth pattern of the cells, 2×10^5 cells in 4 mL culture medium with or without 10 U/mL recombinant human IL 2 were cultured in a set of seven Petri dishes, and the number of viable cells was counted by trypan blue dye exclusion every 24 hours for 7 days.

Southern blot hybridization. For detection of HTLV-I or HTLV-II provirus and abnormalities of IL 2 receptor gene and for analysis of clonal identity of the fresh leukemic cells and the established cell line, Southern blot hybridization was performed as described previously.¹⁶ In brief, high-mol-wt DNA was extracted, digested with restriction endonuclease (*EcoRI*), separated by agarose gel electrophoresis, and transferred onto a nitrocellulose membrane. After being baked, the membrane was hybridized with the nick-translated probes, washed, and autoradiographed. As the probes, *AccI-SmaI* fragment of HTLV-I (kindly provided by Dr T.

From the First Division of Internal Medicine, Faculty of Medicine, Kyoto University, Japan; and the Second Division of Internal Medicine, Faculty of Medicine, Mie University, Japan.

Submitted March 16, 1987; accepted June 5, 1987.

Supported in part by grants from the Ministry of Education, Science and Culture, Japan, the Naito Foundation and from the Mochida Memorial Foundation for Medical and Pharmaceutical Research.

Address reprint requests to Takashi Uchiyama, MD, the First Division of Internal Medicine, Faculty of Medicine, Kyoto University, 54 Shogoin-Kawaramachi, Sakyo-ku, Kyoto, Japan.

The publication costs of this article were defrayed in part by page charge payment. This article must therefore be hereby marked "advertisement" in accordance with 18 U.S.C. §1734 solely to indicate this fact.

© 1987 by Grune & Stratton, Inc.
0006-4971/87/7004-0031\$3.00/0

Table 1. Cell Surface Markers

Source	Positive Cells (%)							
	OKT3	T4	T6	T8	T9	T11	Ia	Tac
Fresh leukemic cells	91	76	0	5	4	99*	84	4
Kit 225	69	96	0	0	63	97	94	96

*Determined on a freshly thawed sample of frozen cells.

Honjo, Kyoto University, Kyoto),¹⁷ LTR of HTLV-II (kindly provided by Dr K. Shimotohno, National Cancer Center, Tokyo), Sau 3A fragment of IL 2 receptor cDNA (Dr T. Honjo),¹⁸ and *Hind*III-*Eco*RI fragment of T cell receptor β chain cDNA (Dr T. Honjo)¹⁷ were used.

Chromosomal analysis. Cells in log phase of IL 2-dependent growth were exposed to 0.05 μ g/mL Colcemid for 1 hour. These cells were suspended in 0.075 mol/L KCl for 20 minutes at 37°C and then fixed with acetic acid/methanol (1:3). They were spread on slides to air-dry, and the chromosomes were stained with trypsin-Giemsa.

RESULTS

Hematologic and immunologic features of the fresh leukemic cells. May-Giemsa staining revealed large leukemic cells with azurophilic granules in abundant cytoplasm. The cell surface phenotype was OKT3+, -T4+, -T8-, as shown in Table 1. Fresh leukemic cells expressed a small amount of IL 2 receptors recognized by anti-Tac monoclonal antibody, and proliferated in response to IL 2 as was seen in normal phytohemagglutinin (PHA)-stimulated T cells (data shown as patient 2 in Fig 3 in the previous report.⁶)

Long-term culture of the leukemic cells with IL 2. Separated leukemic cells soon began to proliferate in the presence of 20% crude IL 2. After 3 months, crude IL 2 was replaced by 1 U/mL recombinant human IL 2, and the cells continued to grow in an IL 2-dependent manner. The established cell line, named Kit 225, has been cultured for >21 months. As shown in Fig 1, Kit 225 cells proliferated exponentially in the presence of IL 2 but died within several days without IL 2.

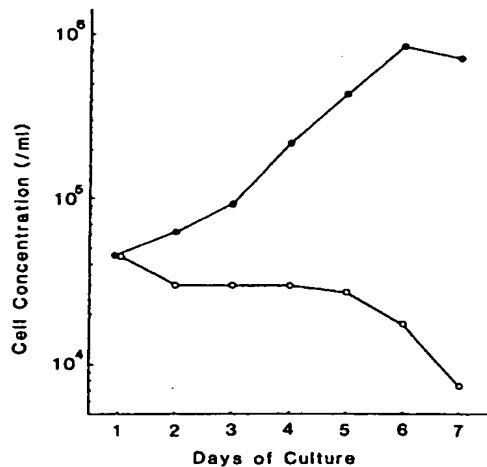


Fig 1. Growth curves of Kit 225 cells. Cells were cultured in medium alone (O) or in the presence of 10 U/mL recombinant human IL 2 (●).

No other stimuli such as antigens or lectins were required for maintaining the responsiveness to IL 2.

Cell surface phenotype and IL 2 receptor expression. Kit 225 had the cell surface phenotype of OKT3+, -T4+, -T8-, which was essentially the same as the fresh leukemic cells (Table 1). However, intense expression of Tac antigen/IL 2 receptor was noted in Kit 225 as compared with the fresh leukemic cells. To determine the number of IL 2 receptors, radiolabeled IL 2 binding assay was performed and Scatchard analysis revealed that Kit 225 cells expressed 3,000 receptors/cell with high affinity (kd 66 pmol/L) and 190,000 receptors/cell with low affinity (kd 7.0 nmol/L) (Fig 2).

Southern blot analysis. High-mol-wt DNA prepared from the fresh leukemic cells and Kit 225 cells was subjected to Southern blot analysis. As shown in Fig 3, Kit 225 cells have no HTLV-I or HTLV-II proviral DNA integration and have a rearrangement pattern of T cell receptor β chain gene identical to that of the fresh leukemic cells, suggesting that Kit 225 was derived from the major clone in the primary leukemic cells. The latter was supported by the results in another restriction enzyme (*Hind*III) digestion (data not shown). Neither gross rearrangement nor amplification of the IL 2 receptor gene was detected in the fresh leukemic cells and Kit 225 cells.

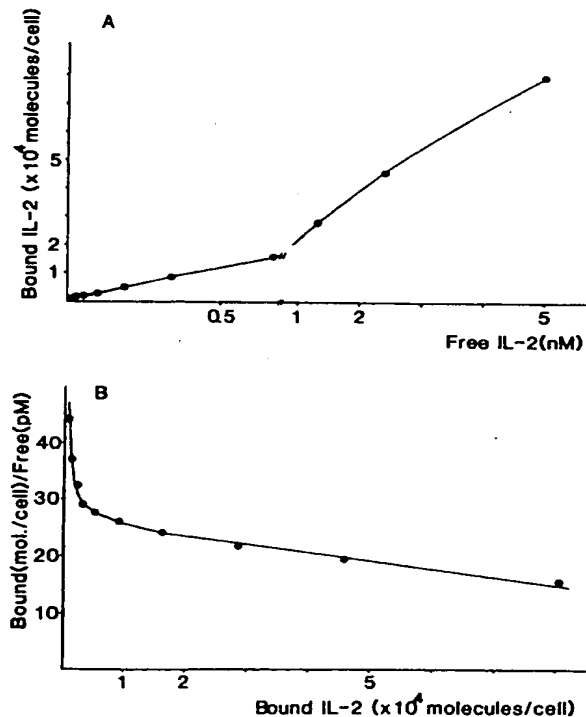


Fig 2. (A) Radiolabeled IL 2 binding to Kit 225 cells. (B) Scatchard plot of the radiolabeled IL 2 binding data shown in A. Estimated numbers of high-affinity and low-affinity IL 2 receptors were 3,000/cell and 190,000/cell, respectively.

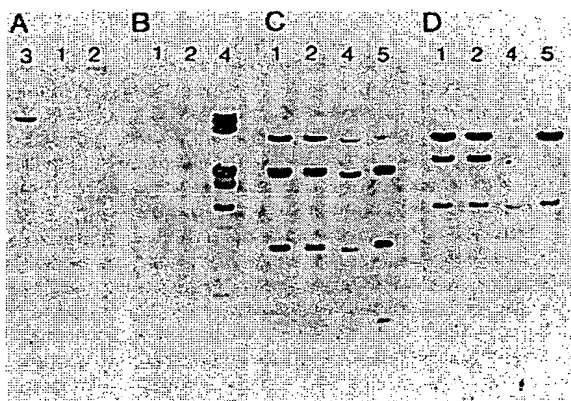


Fig 3. Southern blot analysis of the fresh leukemic cells and Kit 225. High-mol-wt DNA was prepared from the fresh leukemic cells (lane 1), Kit 225 (lane 2), adult T cell leukemia cells (lane 3), Mo, an HTLV-II-infected T cell line (lane 4), and normal human placenta (lane 5). Five micrograms of each DNA sample was digested with restriction enzyme *EcoRI*, separated by agarose gel electrophoresis, and transferred onto a nitrocellulose membrane. After being baked, the membrane was hybridized with the probes of HTLV-I (panel A), HTLV-II (panel B), IL 2 receptor (panel C), and T cell receptor β chain (panel D).

Chromosomal analysis. The karyotype is described in detail (International System for Human Cytogenetic Nomenclature-High Resolution Banding, 1981) as follows: 47, XY, -5, -6, -14, +19, ins inv(1)(pter \rightarrow p36.3::p34.1 \rightarrow p31.2::p36.3 \rightarrow p34.1::p31.2 \rightarrow p22.1::q12 \rightarrow p22.1::q12 \rightarrow qter), inv(3)(pter \rightarrow p26.2::q27.1 \rightarrow p26.2::q27.1 \rightarrow qter), +der(5)t(5;7)(7qter \rightarrow 7q22::5p15.3 \rightarrow cen \rightarrow 5qter), del(6)(pter \rightarrow q21::q23.3 \rightarrow qter), +der(6)t(6;?) (q21;?), +der(14)t(6;14)6q21 \rightarrow 6q23.3::14p12 \rightarrow cen \rightarrow 14qter). No abnormalities were detected in chromosome 10, where the gene that encodes IL 2 receptor is located.¹⁹

DISCUSSION

In the present study, we established an IL 2-dependent human T cell line, Kit 225, from a T-CLL patient with T4+ phenotype. Southern hybridization analysis demonstrated that Kit 225 cells are not infected with HTLV-I or HTLV-II and are probably derived from the major clone in the original leukemic cells.

Some murine IL 2-dependent T cell lines exist.^{20,21} Also, in humans, many IL 2-dependent HTLV-infected T cell lines have been established, some of which are reported to become independent of IL 2 during the passage of culture. Establishment of HTLV negative and IL 2-dependent human T cell lines that require no other stimulation has not been reported however, as far as we know.

The IL 2/IL 2 receptor system is considered to regulate normal T cell proliferation.²² T cells activated by antigens synthesize and release IL 2 as well as express IL 2 receptors on their cell surface membranes, and the binding of IL 2 to its receptors induces the clonal expansion of T cells. The two phenomena, IL 2 production and IL 2 receptor expression, always occur transiently in activated T cells in a normal state, which prevents unlimited growth of T cells. Conversely, it is quite possible that some failure of the IL 2/IL 2 receptor system may cause a neoplastic T cell proliferation.

We previously reported that leukemic cells from most HTLV-negative T-CLL patients with OKT3+, -T4+, -T8- phenotype express IL 2 receptor without any stimuli and proliferate in response to IL 2.⁶ Therefore, they seem to be ready to grow by the paracrine mechanism wherever IL 2 is available, even in vivo environments. In this context, the establishment or immortalization of an IL 2-dependent T cell line, Kit 225, from a T-CLL patient suggests that IL 2-mediated T cell proliferation is involved in the leukemogenesis of some HTLV-negative T-CLL cases with T4+ phenotype. So far, we have succeeded in establishing an IL 2-dependent T cell line from one of eight T-CLL cases we tried. The duration of maintained cell cultures from the remaining seven cases varied from 2 to 16 weeks, which may reflect the heterogeneity of T-CLL in IL 2-dependent growth of leukemic cells.

Recent studies revealed a close association between abnormal expression of the IL 2 receptor and HTLV-I or HTLV-II infection. In such cases, pX region of the virus is speculated to play a key role in augmenting the IL 2 receptor gene expression.⁹ However, the mechanism underlying the abnormal expression of the IL 2 receptor on Kit 225 cells as well as HTLV-negative leukemic cells from T-CLL patients remains to be clarified. Kit 225 is expected to serve as a model system of the abnormal expression of IL 2 receptor that may trigger the development of some HTLV-negative T-CLL cases. Further analyses concerning the mechanism of the unregulated IL 2 receptor expression in Kit 225 will be required, including the search for an unknown virus.

REFERENCES

1. Brouet JC, Flandrin G, Sasportes M, Preud'Homme JL, Seligmann M: Chronic lymphocytic leukaemia of T-cell origin. Immunological and clinical evaluation in eleven patients. *Lancet* 2:890, 1975
2. Nair KG, Han T, Minowada J: T-cell chronic lymphocytic leukemia. Report of a case and review of the literature. *Cancer* 44:1652, 1979
3. Reinherz EL, Nadler LM, Rosenthal DS, Moloney WC, Schlossman SF: T-cell subset characterization of human T-CLL. *Blood* 53:1066, 1979
4. Boumsell L, Bernard A, Reinherz EL, Nadler LM, Ritz J, Coppin H, Richard Y, Dubertret L, Valensi F, Degos L, Lemerle J, Flandrin G, Dausset J, Schlossman SF: Surface antigens on malignant Sezary and T-CLL cells correspond to those of mature T cells. *Blood* 57:526, 1981
5. Pandolfi F, De Rossi G, Semenzato G, Quinti I, Ranucci A, De Sanctis G, Lopez M, Gasparotto G, Aiuti F: Immunologic evaluation of T chronic lymphocytic leukemia cells: Correlations among phenotype, functional activities, and morphology. *Blood* 59:688, 1982
6. Tsudo M, Uchiyama T, Umadome H, Wano Y, Hori T, Tamori S, Uchino H, Kita K, Chiba S, Mitsutani S, Nesumi N:

Expression of interleukin-2 receptor on T cell chronic lymphocytic leukemia cells and their response to interleukin-2. *Blood* 67:316, 1986

7. Uchiyama T, Hori T, Tsudo M, Wano Y, Umadome H, Tamori S, Yodoi J, Maeda M, Sawami H, Uchino H: Interleukin-2 receptor (Tac antigen) expressed on adult T cell leukemia cells. *J Clin Invest* 46:446, 1985

8. Yodoi J, Okada M, Tagaya Y, Teshigawara K, Fukui K, Ishida N, Ikuta K, Maeda M, Honjo T, Osawa H, Diamantstein T, Tateno M, Yoshiki T: Rat lymphoid cell lines producing human T cell leukemia virus II; constitutive expression of rat interleukin-2 receptor. *J Exp Med* 161:924, 1985

9. Inoue J, Seiki M, Taniguchi T, Tsuru S, Yoshida M: Induction of interleukin 2 receptor gene expression by p40^r encoded by human T-cell leukemia virus type I. *EMBO J* 5:2883, 1986

10. Poesz BJ, Ruscetti FW, Gazdar AF, Bunn PA, Minna JD, Gallo RC: Detection and isolation of type-C retrovirus particles from fresh and cultured lymphocytes of a patient with cutaneous T-cell lymphoma. *Proc Natl Acad Sci USA* 77:7415, 1980

11. Hinuma Y, Nagata K, Hanaoka M, Nakai T, Matsumoto T, Kinoshita K, Shirakawa S, Miyoshi I: Adult T cell leukemia: Antigen in an ATL cell line and detection of antibodies to the antigen in human sera. *Proc Natl Acad Sci USA* 78:6476, 1981

12. Uchiyama T, Yodoi J, Sagawa K, Takatsuki K, Uchino H: Adult T cell leukemia: Clinical and hematological features of 16 cases. *Blood* 50:481, 1977

13. Uchiyama T, Broder S, Waldmann TA: A monoclonal antibody (anti-Tac) reactive with activated and functionally mature human T cells. I. Production of anti-Tac monoclonal antibody and distribution of Tac(+) cells. *J Immunol* 126:1393, 1981

14. Leonard WJ, Depper M, Uchiyama T, Smith KA, Waldmann TA, Greene WC: A monoclonal antibody that appears to recognize the receptor for human T-cell growth factor: Partial characterization of the receptor. *Nature (Lond)* 300:267, 1982

15. Hori T, Uchiyama T, Umadome H, Tamori S, Tsudo M, Araki K, Uchino H: Dissociation of interleukin-2-mediated cell proliferation and interleukin-2 receptor upregulation in adult T cell leukemia cells. *Leuk Res* 10:1447, 1986

16. Honjo T, Obata M, Yamawaki-Kataoka Y, Kataoka T, Kawakami T, Takahashi N, Mano Y: Cloning and complete nucleotide sequence of mouse immunoglobulin γ 1 chain gene. *Cell* 18:559, 1979

17. Maeda M, Shimizu A, Ikuta K, Okamoto H, Kashiwara M, Uchiyama T, Honjo T, Yodoi J: Origin of human T-lymphotropic virus I-positive T cell lines in adult T cell leukemia: Analysis of T cell receptor gene rearrangement. *J Exp Med* 162:2169, 1985

18. Nikaido T, Shimizu A, Ishida N, Sabe H, Teshigawara K, Maeda M, Uchiyama T, Yodoi J, Honjo T: Molecular cloning of cDNA encoding human interleukin-2 receptor. *Nature* 311:631, 1984

19. Leonard WJ, Donlon TA, Lebo RV, Greene WC: Localization of the gene encoding the human interleukin-2 receptor on chromosome 10. *Science* 228:1547, 1985

20. Gillis S, Smith KA: Long term culture of tumour-specific cytotoxic T cells. *Nature (Lond)* 268:154, 1977

21. Jones-Villeneuve E, Phillips RA: Potentials for lymphoid differentiation by cells from long-term culture of bone marrow. *Exp Hematol* 8:65, 1980

22. Cantrell DA, Smith KA: The interleukin-2 T-cell system: A new cell growth model. *Science* 224:1312, 1984

Evidence for successive peptide binding and quality control stages during MHC class I assembly

Jonathan W. Lewis and Tim Elliott

Intracellular antigens are continually presented to cytotoxic T lymphocytes by major histocompatibility complex (MHC) class I molecules, which consist of a polymorphic 43 kDa heavy chain and a 12 kDa soluble subunit β 2-microglobulin (β 2m), and which bind an 8–10 amino-acid antigenic peptide. The assembly of this trimolecular complex takes place in the lumen of the endoplasmic reticulum (ER) [1] and almost certainly requires cofactors. Most MHC class I molecules in the ER that have not yet acquired peptide are simultaneously bound to the transporter associated with antigen processing (TAP), to the 48 kDa glycoprotein tapasin and to the lectin-like chaperone calreticulin, in a multicomponent 'loading complex' [2]. Previous studies have shown that a mutant MHC class I molecule T134K (in which Thr134 was changed to Lys) fails to bind to TAP [3]. Here, we show that this point mutation also disrupted, directly or indirectly, the interaction between MHC class I molecules and calreticulin. T134K molecules did not present viral antigens to T cells even though they bound peptide and β 2m normally *in vitro*. They exited the ER rapidly as 'empty' MHC class I complexes, unlike empty wild-type molecules which are retained in the ER and degraded. We show here that, paradoxically, the rapid exit of empty T134K molecules from the ER was dependent on a TAP-derived supply of peptides. This implies that MHC class I assembly is a two-stage process: initial binding of suboptimal peptides is followed by peptide optimisation that depends on temporary ER retention.

Address: Nuffield Department of Clinical Medicine, University of Oxford, John Radcliffe Hospital, Oxford OX3 9DU, UK.

Correspondence: Tim Elliott
E-mail: tim.elliott@ndm.ox.ac.uk

Received: 10 February 1998
Revised: 26 March 1998
Accepted: 17 April 1998

Published: 25 May 1998

Current Biology 1998, 8:717–720
<http://biomednet.com/elecref/0960982200800717>

© Current Biology Ltd ISSN 0960-9822

Results and discussion

In addition to the failure of T134K molecules to interact with the TAP1–TAP2 heterodimer, Figure 1a shows that they did not associate with the ER-resident protein calreticulin either. Both human leukocyte antigens (HLAs)

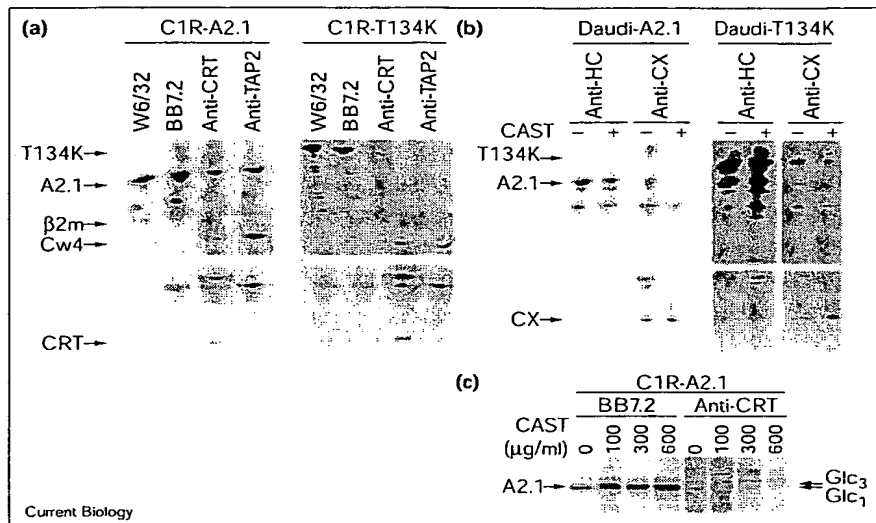
HLA-A*0201 and HLA-Cw4 could be recovered by coimmunoprecipitation with both anti-TAP2 and anti-calreticulin antibodies in digitonin lysates, but no association with T134K was detected. T134K did, however, interact with the ER chaperone calnexin — a protein that is homologous to calreticulin — in the β 2m-negative cell line Daudi (Figure 1b). These experiments demonstrate that whereas calreticulin can discriminate between the wild-type HLA-A*0201 and the T134K mutant, calnexin cannot. The basis for this discrimination is unclear: both calreticulin and calnexin are reported to have very similar, if not identical, substrate specificities and have been shown to bind preferentially to monoglucosylated trimming intermediates of glycoproteins in the ER ([4,5], reviewed in [6,7]). Consistent with this, the interaction between calnexin and HLA-A*0201 or T134K is sensitive to castanospermine, a compound that inhibits the trimming of the immature glycan on the heavy chain by glucosidase I and II (Figure 1b). Figure 1c shows that castanospermine also inhibits the interaction between HLA-A*0201 and calreticulin in a dose-dependent way. Given that Thr134 is at a position distal to the single glycosylation site (Asn86) of human MHC class I molecules, as seen in the three-dimensional structure [8], these results suggest that, in addition to the glycan-dependent aspect of calreticulin binding to MHC class I molecules, other aspects contribute to this interaction.

The failure of T134K to interact with calreticulin could be due to the direct disruption of the calreticulin-binding site on the class I heavy chain, or could be an indirect effect via the disruption of an interaction with TAP, tapasin or some other cofactor. It is possible, for example, that the interaction between MHC class I and calreticulin is dependent on a castanospermine-sensitive interaction with another cofactor such as tapasin. Figure 2 shows that the binding of calreticulin, tapasin and TAP to MHC class I was cooperative. Thus, the amount of HLA-A*0201 recovered from cells with anti-calreticulin antiserum was drastically reduced when either TAP (in T2 cells) or tapasin (in .220 cells) were missing (Figure 2b). To date, it has not been possible to look at the association between TAP, tapasin and HLA-A*0201 in cells that lack calreticulin. It is possible, however, to block the calreticulin–MHC class I interaction with castanospermine. Figure 2c shows that the interaction between HLA-A*0201 and TAP was sensitive to the inhibition of glycan trimming by castanospermine. Like the calreticulin–MHC class I interaction, there was a dose-dependent effect of castanospermine on the TAP–MHC class I interaction (Figure 2d). These experiments indicate

Figure 1

T134K interacts with calnexin (CX) but does not associate with calreticulin (CRT).

(a) Metabolically labelled lysates of C1R cells transfected with HLA-A*0201 (C1R-A2.1) or T134K (C1R-T134K) were immunoprecipitated with monoclonal antibodies W6/32 (anti-HLA-A,B,C) and BB7.2 (anti-HLA-A2) or with anti-calreticulin or anti-TAP2 antisera. The immunoprecipitates were analysed by one-dimensional isoelectric focusing (1D-IEF) to resolve coprecipitating HLA-A*0201 (A2.1) and HLA-Cw4. T134K migrated higher than wild-type HLA-A*0201 in the 1D-IEF gel, due to the addition of positive charge by the threonine-to-lysine mutation. HLA-Cw4 was co-precipitated equally well from lysates of either C1R-A2.1 or C1R-T134K cells, and served as an internal control. (b) β 2m-deficient Daudi cells were infected with recombinant vaccinia virus expressing either HLA-A*0201 or T134K. (Daudi cells were used because calnexin has been shown to bind to free class I heavy chain in the absence of β 2m; the association of HLA-A*0201 and T134K with calnexin is therefore shown best in β 2m-deficient cells.) Infected cells were then split in half; half were not treated and half were treated with 600 μ g/ml castanospermine (CAST) at a concentration known to prevent trimming of precursor triglycosylated N-linked glycans Glc₃ to the monoglucosylated Glc₁ form (this trimming is required for calnexin to bind to class I heavy chains). Metabolically labelled lysates were then immunoprecipitated with either



anti-heavy chain (anti-HC) or anti-calnexin (anti-CX) antisera. The top and bottom of the 1D-IEF gels are shown to save space. (c) The interaction between HLA-A*0201 and calreticulin is carbohydrate dependent. C1R-A2.1 cells were treated with an increasing concentration of castanospermine (0, 100, 300, 600 μ g/ml). Metabolically labelled HLA-A*0201 molecules were then immunoprecipitated with BB7.2 antibody or coimmunoprecipitated with anti-calreticulin antiserum.

The effectiveness of castanospermine was indicated by the change in mobility of HLA-A*0201 in the SDS polyacrylamide gel as the dose of castanospermine increased, corresponding to the inhibition of glucose trimming from the triglycosyl Glc₃ to monoglucosyl Glc₁ core glycan. Note that only the fast mobility Glc₁ is associated with calreticulin. The band migrating just above the Glc₃ heavy chain band in the anti-calreticulin precipitations is most probably tapasin (data not shown).

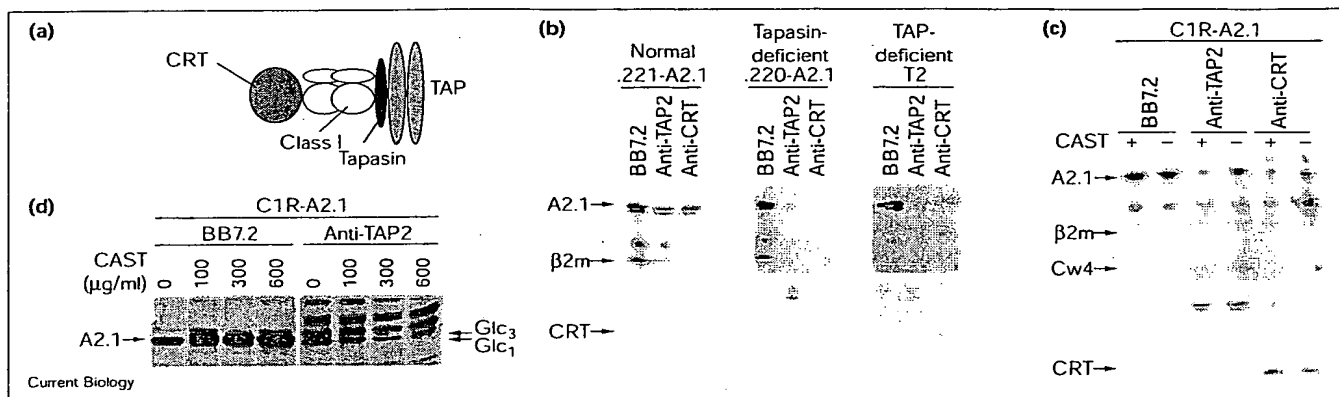
that the failure of T134K to interact with calreticulin could be secondary to its failure to interact with other cofactors in the loading complex. They also show that a stable interaction between class I molecules and each member of this complex is dependent on the presence of the other component members.

T134K molecules are released into the secretory pathway prematurely as peptide-receptive molecules [3]. They escape degradation in the ER — which is the usual fate of peptide-receptive class I molecules synthesised in cells in which the supply of peptides to the ER is limited. If T134K was bypassing the 'peptide loading' step of antigen presentation, we would expect this rapid transport of empty mutant molecules to be insensitive to the presence of a functional TAP.

To test this, we introduced T134K into cell lines that are unable to supply newly synthesised class I molecules with TAP-derived peptides because of an absent or defective TAP complex. In this case, only a TAP-independent peptide pool would exist in the ER. In normal C1R cells,

around 70% of wild-type HLA-A*0201 leaves the ER stably bound to peptides, whereas the remaining 30% of molecules are not stabilised, and as a result remain in the ER to be degraded [3]. In contrast, only a few (14%) T134K molecules leave the ER stably bound to peptides; the majority (70%) exit in a peptide-receptive state, with very few molecules being retained in the ER [3]. The intracellular fate of both T134K and normal HLA-A*0201 expressed in the TAP-defective cell line BM36.1 [9] was then assessed for comparison. Figure 3 shows that in BM36.1 cells, the majority of T134K molecules, like HLA-A*0201, did not exit the ER but were retained as unstable complexes that were sensitive to endoglycosidase H (87% and 61% for T134K and HLA-A*0201, respectively). Only about 10% of T134K molecules and 30% of wild-type HLA-A*0201 molecules exited the ER in BM36.1 cells as stable complexes. Thus, we show for the first time that although a TAP-derived supply of peptides to the ER is necessary to ensure the stable peptide-dependent assembly of MHC class I molecules and the presentation of endogenous antigens to cytotoxic T lymphocytes, it is not sufficient. A supply of TAP-derived peptides is

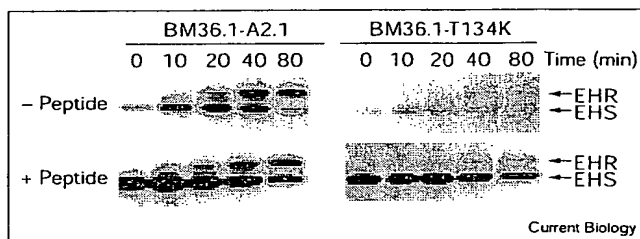
Figure 2



The binding of calreticulin (CRT), tapasin and TAP to HLA-A*0201 (A2.1) is cooperative. (a) A schematic representation of the multicomponent loading complex. Metabolically labelled lysates of (b) normal .221-A2.1 cells, tapasin-deficient .220-A2.1 cells and TAP-deficient T2 cells and of (c) C1R-A2.1 cells (mock-treated or treated with 600 µg/ml castanospermine, CAST) were immunoprecipitated with BB7.2 (anti-HLA-A2) antibody or with anti-TAP2 or anti-calreticulin antisera. The immunoprecipitates were analysed by 1D-IEF to resolve coprecipitating HLA-A*0201 and HLA-Cw4. Note that less HLA-A*0201 associated with calreticulin when cells lacked either

tapasin (.220-A2.1) or TAP (T2). When the interaction between calreticulin and HLA-A*0201 was disrupted with castanospermine (c), less HLA-A*0201 coprecipitated with TAP. (d) Metabolically labelled cell lysates of C1R-A2.1 cells treated with castanospermine at the indicated concentrations were immunoprecipitated with BB7.2 (anti-HLA-A2) antibody or with anti-TAP2 antiserum. Immunoprecipitates were analysed by 10% SDS-PAGE. As the dose of castanospermine increased, the amount of HLA-A*0201 associated with TAP decreased. TAP associated only with the Glc₁ form of HLA-A*0201.

Figure 3



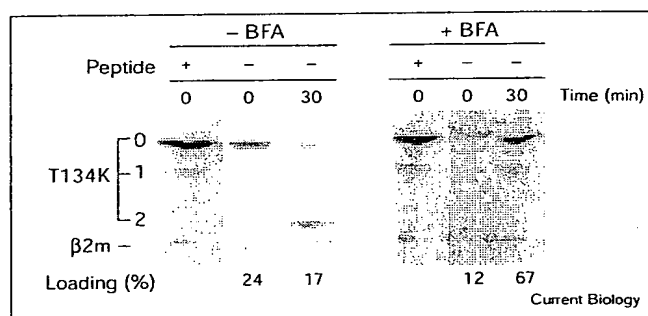
BM36.1 cells were infected with recombinant vaccinia virus expressing either HLA-A*0201 (A2.1) or T134K. Cells were metabolically labelled and chased for the time periods indicated. BB7.2-reactive class I complexes were then recovered from cell lysates after overnight pre-clearing in the absence (- peptide) or presence (+ peptide) of a saturating concentration (20 µM) of stabilising HIV pol peptide. Only heavy-chain bands are shown because human $\beta 2m$ is poorly visualised following a 10 min pulse-label. Intracellular maturation was determined by the sensitivity of class I molecules to endoglycosidase H (EHS) indicates endoglycosidase-H-sensitive; EHR indicates endoglycosidase-H-resistant). The intracellular fate of class I complexes in each cell line could be quantified (see Supplementary material): from each chase, the proportion of stable class I complexes that exited the ER was 32% for HLA-A*0201 and 11% for T134K; the proportion of 'peptide-receptive', unstable complexes that exited was 7% for HLA-A*0201 and 2% for T134K; the proportion of class I molecules that remained in the ER was 61% for HLA-A*0201 and 87% for T134K. When C1R cells were infected with the recombinant vaccinia viruses, both T134K and wild-type HLA-A*0201 exited the ER and became endoglycosidase-H-resistant; this is also the case when T134K and HLA-A*0201 are expressed from transfected genes [3].

clearly essential to allow T134K molecules to escape degradation and to exit the ER. They nevertheless enter the secretory pathway in a peptide-receptive state when assayed *in vitro*. This suggests that the mutation acts to prevent class I molecules from optimising the binding of their peptide ligand, rather than preventing peptide binding per se. It is this failure to optimise the binding of the peptide ligand that leads to the egress of unstable class I molecules from the ER.

The optimisation of peptide loading onto class I complexes may be linked to their retention time in the ER. We have investigated this proposal using the drug brefeldin A (BFA), which promotes the retention of newly synthesised glycoproteins in the ER by reorganising the structure of the ER and Golgi apparatus. Figure 4 shows that when C1R-T134K cells were incubated with BFA for 30 minutes (the approximate half-time for egress of wild-type HLA-A*0201 molecules from the ER, compared with 12 minutes for T134K), the fraction of stable molecules increased dramatically from 17% in the absence of BFA to 67% in its presence. This indicates that ER retention alone may facilitate the assembly of class I molecules with optimal peptides.

Mechanisms by which peptide optimisation could be achieved include peptide exchange, or the enzymatic trimming of suboptimal peptides to a suitable length for class I binding [10,11]. In support of the peptide exchange mechanism, Sijts and Pamer [12] have shown recently that

Figure 4



Retention in the ER promotes intracellular peptide loading of T134K. Cells metabolically labelled for 5 min were incubated in the absence or presence of 10 μ M BFA before they were lysed. The number of sialic acid residues present on the T134K molecules is labeled. T134K that became stably assembled was calculated as a fraction of the total cohort (visualised at $t = 0$ by the addition of stabilising peptide). Note that T134K becomes di-sialylated only in the absence of BFA.

peptide dissociation from class I molecules in the ER is enhanced compared with the cell surface and yet ER-resident class I molecules have a greater capacity to bind new epitopes. This process might be a 'facilitated exchange' process, requiring the assistance of a separate cofactor similar to the role of HLA-DM described for the class II pathway (reviewed in [13]). As for MHC class II, there might be varying degrees of dependency on such a cofactor between alleles in order to bring about effective peptide exchange [14–16].

Materials and methods

Cell lines, antibodies and peptides

The TAP-deficient .174 cells, tapasin-deficient .220 cells, and tapasin-competent .221 cells, as well as .220-A2.1 and .221-A2.1 cells, were the generous gifts of R. DeMars. BM28.7 [9] and TAP-defective BM36.1 cells were a gift from A. Ziegler. T2 cells were a gift from P. Cresswell. C1R cells transfected with HLA-A*0201 (C1R-A2.1) and HLA-A*0201T134K (C1R-T134K) were a gift from J. Frelinger. Monoclonal antibodies used were anti-HLA-A2 (BB7.2 [17]) and anti-HLA-A, anti-HLA-B and anti-HLA-C (W6/32 [18]). Rabbit anti-free-heavy-chain and rabbit anti-TAP2 sera were generated by and were a gift from J.J. Neefjes [3]. Rabbit anti-calnexin was from Affinity Bioreagents. The rabbit antiserum to calnexin was generated by B. Gao to a synthetic peptide corresponding to the 15 carboxy-terminal residues of human calnexin. The HLA-A*0201 binding peptides ILKEPVHGV (HIV pol residues 476–484) and GILGFVFTL (influenza A MP58–66) were synthesised by Research Genetics.

Pulse-chase analysis, immunoprecipitation, coimmunoprecipitation and band analysis

These were performed exactly as described [3]. The fractions of a pulse-labelled cohort of class I molecules which either leave the ER in stable association with peptide, or leave the ER as unstable peptide-receptive complexes, or are retained and degraded in the ER as peptide-receptive complexes were calculated from the integrated optical density (IOD) of endoglycosidase-H-sensitive and endoglycosidase-H-resistant class I heavy chain bands. For details see the Supplementary material.

Viruses

Recombinant vaccinia viruses were made by homologous recombination into the thymidine kinase gene of WR vaccinia as described [11]. For immunoprecipitation experiments, cells were pelleted and infected with recombinant vaccinia at multiplicity of infection (MOI) = 10 for 90 min at 37°C. Cells were then washed once and resuspended in warm medium for 3.5 h prior to metabolic radiolabelling.

Supplementary material

Details of the quantitation of pulse-chase immunoprecipitation are published with this paper on the internet.

References

- Heemels MT, Ploegh H: Generation, translocation, and presentation of MHC class I-restricted peptides. *Annu Rev Biochem* 1995, 64:463–491.
- Sadasivan B, Lehner PJ, Ortmann B, Spies T, Cresswell P: Roles for calreticulin and a novel glycoprotein, tapasin, in the interaction of MHC class I molecules with TAP. *Immunity* 1996, 5:103–114.
- Lewis JW, Neisig A, Neefjes J, Elliott T: Point mutations in the $\alpha 2$ domain of HLA-A2.1 define a functionally relevant interaction with TAP. *Curr Biol* 1996, 6:873–883.
- Rodan AR, Simons JF, Trombetta ES, Helenius A: N-linked oligosaccharides are necessary and sufficient for association of glycosylated forms of bovine RNase with calnexin and calreticulin. *EMBO J* 1996, 15:6921–6930.
- Hebert DN, Foellmer B, Helenius A: Calnexin and calreticulin promote folding, delay oligomerization and suppress degradation of influenza hemagglutinin in microsomes. *EMBO J* 1996, 15:2961–2968.
- Krause KH, Michalak M: Calreticulin. *Cell* 1997, 88:439–443.
- Helenius A, Trombetta ES, Hebert DN, Simons JF: Calnexin, calreticulin and the folding of glycoproteins. *Trends Cell Biol* 1997, 7:193–200.
- Bjorkman PJ, Saper MA, Samraoui B, Bennett WS, Strominger JL, Wiley DC: Structure of the human class I histocompatibility antigen, HLA-A2. *Nature* 1987, 329:506–512.
- Kelly A, Powis SH, Kerr LA, Mockridge I, Elliott T, Bastin J, et al: Assembly and function of the two ABC transporter proteins encoded in the human major histocompatibility complex. *Nature* 1992, 355:641–644.
- Snyder HL, Yewdell JW, Bennink JR: Trimming of antigenic peptides in an early secretory compartment. *J Exp Med* 1994, 180:2389–2394.
- Elliott T, Willis A, Cerundolo V, Townsend A: Processing of major histocompatibility class I-restricted antigens in the endoplasmic reticulum. *J Exp Med* 1995, 181:1481–1491.
- Sijts AJ, Pamer EG: Enhanced intracellular dissociation of major histocompatibility complex class I-associated peptides: a mechanism for optimizing the spectrum of cell surface-presented cytotoxic T lymphocyte epitopes. *J Exp Med* 1997, 185:1403–1411.
- Kropshofer H, Hammerling GJ, Vogt AB: How HLA-DM edits the MHC class II peptide repertoire: survival of the fittest? *Immunol Today* 1997, 18:77–82.
- Kropshofer H, Vogt AB, Moldenhauer G, Hammer J, Blum JS, Hammerling GJ: Editing of the HLA-DR-peptide repertoire by HLA-DM. *EMBO J* 1996, 15:6144–6154.
- Vogt AB, Kropshofer H, Moldenhauer G, Hammerling GJ: Kinetic analysis of peptide loading onto HLA-DR molecules mediated by HLA-DM. *Proc Natl Acad Sci USA* 1996, 93:9724–9729.
- Denzin LK, Cresswell P: HLA-DM induces CLIP dissociation from MHC class II alpha beta dimers and facilitates peptide loading. *Cell* 1995, 82:155–165.
- Parham P, Brodsky FM: Partial purification and some properties of BB7.2. A cytotoxic monoclonal antibody with specificity for HLA-A2 and a variant of HLA-A28. *Hum Immunol* 1981, 3:277–299.
- Parham P, Barnstable CJ, Bodmer WF: Use of a monoclonal antibody (W6/32) in structural studies of HLA-A,B,C, antigens. *J Immunol* 1979, 123:342–349.

Supplementary material

Evidence for successive peptide binding and quality control stages during MHC class I assembly

Jonathan W. Lewis and Tim Elliott

Current Biology 25 May 1998, 8:717–720

The quantitation of pulse-chase immunoprecipitation

Gels were fixed, stained (for SDS polyacrylamide gels), treated with Amplify (Amersham), dried and visualised by autoradiography at -80°C . Bands were quantitated using a MilliGen Bioimage Analyser which expresses band intensities as an integrated optical density (IOD). The fractions of a pulse-labelled cohort of class I molecules which leave the ER in stable association with peptide (A), leave the ER as unstable peptide-receptive complexes (B) or are retained and degraded in the ER as peptide-receptive complexes (C) were calculated from the IOD of endoglycosidase-H-sensitive (EHS) and endoglycosidase-H-resistant (EHR) class I heavy chain bands precipitated by conformation-specific antibodies in the presence or absence of peptide.

$A = (\text{maximum IOD EHR HC without peptide})/T \times 100\%$;

$B = [(\text{maximum IOD EHR HC with peptide}) - (\text{maximum IOD EHR HC without peptide})]/T \times 100\%$;

$C = [(\text{maximum IOD EHS HC with peptide}) - (\text{maximum IOD EHR HC with peptide})]/T \times 100\%$;

where $T = \text{maximum IOD (EHS HC + EHR HC) with peptide}$. All experiments were performed at least twice and the reproducibility was found to be good. Fractions A, B and C varied less than $\pm 20\%$ from day to day and were not affected by minor differences in the total amount of class I heavy chain synthesised following vaccinia delivery of the heavy chain genes. The accuracy of the calculation was checked by ensuring that the fraction C calculated above equalled the difference between fractions A and B.

GPI-microdomains (membrane rafts) and signaling of the multi-chain interleukin-2 receptor in human lymphoma/leukemia T cell lines

János Matkó^{1,5}, Andrea Bodnár², György Vereb¹, László Bene¹, György Vámosi²,
Gergely Szentesi¹, János Szöllősi¹, Rezső Gáspár Jr¹, Václav Horejsi³, Thomas A. Waldmann⁴
and Sándor Damjanovich^{1,2}

¹Department of Biophysics and Cell Biology, ²Cell Biophysics Research Group of the Hungarian Academy of Sciences, University of Debrecen, Health Science Center, Debrecen, Hungary; ³Institute of Molecular Genetics, Academy of Sciences of Czech Republic, Prague, Czech Republic; ⁴Metabolism Branch, National Cancer Institute, National Institutes of Health, Bethesda, MD, USA; ⁵Department of Immunology, Eotvos Lorand University, Budapest, Hungary

Subunits (α , β and γ) of the interleukin-2 receptor complex (IL-2R) are involved in both proliferative and activation-induced cell death (AICD) signaling of T cells. In addition, the signaling β and γ chains are shared by other cytokines (e.g. IL-7, IL-9, IL-15). However, the molecular mechanisms responsible for recruiting/sorting the α chains to the signaling chains at the cell surface are not clear. Here we show, in four cell lines of human adult T cell lymphoma/leukemia origin, that the three IL-2R subunits are compartmented together with HLA glycoproteins and CD48 molecules in the plasma membrane, by means of fluorescence resonance energy transfer (FRET), confocal microscopy and immunobiochemical techniques. In addition to the β and γ_c chains constitutively expressed in detergent-resistant membrane fractions (DRMs) of T cells, IL-2R α (CD25) was also found in DRMs, independently of its ligand-occupation. Association of CD25 with rafts was also confirmed by its colocal-

ization with GM-1 ganglioside. Depletion of membrane cholesterol using methyl- β -cyclodextrin substantially reduced co-clustering of CD25 with CD48 and HLA-DR, as well as the IL-2 stimulated tyrosine-phosphorylation of STATs (signal transducer and activator of transcription). These data indicate a GPI-microdomain (raft)-assisted recruitment of CD25 to the vicinity of the signaling β and γ_c chains. Rafts may promote rapid formation of a high affinity IL-2R complex, even at low levels of IL-2 stimulus, and may also form a platform for the regulation of IL-2 induced signals by GPI-proteins (e.g. CD48). Based on these data, the integrity of these GPI-microdomains seems critical in signal transduction through the IL-2R complex.

Keywords: cytokine receptors; lipid rafts; cell proliferation; T lymphocytes; fluorescence energy transfer.

The multisubunit receptor of interleukin-2 cytokine (IL-2R) is essential in mediating T cell growth/clonal expansion [1] following antigen (or mitogen) stimulation, as well as in the control of activation-induced cell death (AICD) [2]. For IL-2 signaling, hetero-dimerization of the intracellular domains of β and γ_c chains was found critical [3], followed by Jak-assisted tyrosine-phosphorylation of downstream signaling molecules [e.g. signal transducers and activators of transcription (STATs)] [4]. Interestingly, the 'common' γ subunit of IL-2R is shared by a number of other cytokine receptors (e.g. those of IL-4, IL-7, IL-9, IL-15) mediating diverse cellular responses [5,6]. This raises the question: how

are the diverse α chains recruited/sorted to the signaling IL-2R β and γ_c chains? This question is further accentuated by the facts that the diverse α chains, in contrast to the signaling IL-2R β and γ_c chains, do not belong to the hemopoietin receptor superfamily, and their intracellular trafficking is different from that of the β and γ_c chains [7]. It is still not clear whether the assembly of the high affinity IL-2 receptor complex requires ligand occupation of CD25, as do other growth-factor receptors (such as EGF-receptor) [8]. The importance of these questions is also underlined by the recent success of immuno-toxin based cancer therapy targeting the α and β chains of IL-2R [9].

Recent FRET data, in contrast to an earlier 'sequential subunit-organization' (affinity conversion) model [10], suggested a preassembly of the three IL-2R subunits, even in the absence of their relevant cytokine ligands in the plasma membrane of T lymphoma cells. Binding of the physiological ligands (IL-2, IL-7, IL-15) was reported to selectively modulate the mutual molecular proximities/interactions of the IL-2R α , β and γ_c chains [11]. Microscopic (confocal fluorescence and immunogold labeling-based electron microscopy) studies revealed large scale (\approx 4–800 nm) overlapping clusters of CD25 and HLA molecules on T cell lines [12]. These observations all suggest that the above membrane proteins are somewhat compartmentalized in T cell plasma membranes.

Correspondence to J. Matkó, Department of Immunology, Eotvos Lorand University, H-1518, PO Box 120, Budapest, Hungary.
Fax: + 36 1 3812176, Tel.: + 36 1 3812175,
E-mail: Matko@cerberus.elte.hu

Abbreviations: IL, interleukin; AICD, activation-induced cell death; DRMs detergent-resistant membrane fractions; FRET, fluorescence resonance energy transfer; HTLV-I, human T cell lymphotropic virus I; HBSS, Hanks' balanced salt solution; STAT, signal transducer and activator of transcription.

Note: J. Matkó and A. Bodnár contributed equally to this work.
(Received 30 August 2001, revised 14 December 2001, accepted 2 January 2002)

Membrane compartmentation of T cell receptor with its co-receptors (CD4, CD8) and other signaling molecules (src kinases, LAT, etc.) by cholesterol- and glycosphingolipid-rich microdomains (rafts) has already been reported for T cells [13,14]. These lipid rafts were shown to preferentially accumulate GPI-anchored or double-acylated proteins (e.g. src kinase family), while the raft-targeting preference for transmembrane proteins still remains controversial and unclear [14,15], although a few examples of such proteins have been reported to associate with rafts (e.g. a fraction of LAT, CD4 and CD8 in T cells, CD44 in various cell types or influenza virus haemagglutinin in epithelial cells) [14].

Thus, the present study aimed at investigating whether the molecular constituents of the microscopically observed large (μm) scale clusters of CD25 [12] also display proximity (association) at the molecular (nm) scale. CD25 recruitment to the β and γ_c chains at the surface of human leukemia/lymphoma T cell lines was also studied with special attention to its ligand occupation. As lipid rafts (DRMs) can be considered as possible platforms of plasma membrane clustering of IL-2R chains, we investigated the relationship of IL-2R chains to T cell lipid rafts marked by CD48 GPI-anchored protein and the GM-1 ganglioside. Finally, we also investigated the relationship between membrane localization of the IL-2R complex and its signaling activity.

To probe cell surface protein organization, the distance-dependent fluorescence resonance energy transfer (FRET) method [16] was used [17–20], a technique that is very sensitive to molecular localization of membrane proteins on a submicroscopic distance scale of 2–10 nanometers. This is due to the inverse sixth power dependence of FRET efficiency on the actual distance between donor and acceptor dye-labels [19,21,22].

FRET data indicated a molecular level coclustering of the of IL-2R α , β and γ_c chains with the class I HLA, HLA-DR glycoproteins and the GPI-anchored CD48 molecule, similar on all the four distinct human T cell lines. Additional evidence (co-precipitation and co-capping with CD48, detergent-resistance analysis, colocalization with GM-1 lipid raft marker) has also shown supporting association of CD25 to lipid rafts, independent of its ligand occupation. Disintegration of rafts by cholesterol-depletion dispersed supramolecular clusters of CD25 with CD48 and HLA molecules. This compartmentalization may have functional implications, as disintegration of rafts also resulted in a remarkably reduced IL-2 stimulated tyrosine phosphorylation of T cell signaling molecules.

EXPERIMENTAL PROCEDURES

Cell lines and mAbs

The Kit225 K6 cell line is a human T cell with a helper/inducer phenotype and an absolute IL-2 requirement for its growth, while its subclone, Kit225 IG3, is IL-2 independent [23]. The IL-2 independent HUT102B2 cells were derived from a human adult T cell lymphoma associated with the human T cell lymphotropic virus I (HTLV-I) [24]. MT-1 is also an adult T cell leukemia cell line associated with HTLV-1 and is deficient in the signaling IL-2R β and γ subunits [25]. All cell lines were cultured in RPMI-1640 medium supplemented with 10% fetal bovine serum, penicillin and streptomycin [11]. To IL-2 dependent T cells,

20 U·mL⁻¹ of recombinant interleukin-2 was added every 48 h. In some experiments, the cells were washed and then grown in IL-2-free medium for 72 h, and were therefore considered as T cells deprived of IL-2.

The subunits of the IL-2 receptor complex, class I HLA (A,B,C) and HLA-DR proteins were labeled with fluorescent dyes coupled to the following antibodies: IL-2R α was targeted by anti-Tac Ig (IgG2a), while monoclonal anti-(Mik- β 3) Ig (IgG1 κ) and anti-TUGh4 Ig (Pharmingen, San Diego, CA, USA) were used against the IL-2R β and γ_c subunits, respectively. The following monoclonal antibodies were kindly provided by F. Brodsky (UCSF, CA, USA): W6/32 (IgG2a κ), specific for the heavy chain of class I HLA A,B,C molecules; L-368 (IgG1 κ), specific for β 2m; L243 (IgG2a), specific for HLA-DR. The CD48 and the transferrin receptor (CD71) were tagged by MEM-102 (IgG1) and MEM-75 (IgG1), respectively (both from the laboratory of V. Horejsi). Fab fragments were prepared from IgG using a method described previously [19].

Aliquots of purified whole IgGs or Fab fragments were conjugated as described previously [26], with 6-(fluorescein-5-carboxamido) hexanoic acid succinimidyl ester (SFX) or Rhodamine RedTM-X succinimidyl ester (RhRX) (Molecular Probes, Eugene, OR, USA). For labeling with sulfo-indocyanine succinimidyl bifunctional ester (Cy3), a kit was used (Amersham Life Sciences Inc., Arlington Heights, IL, USA). Unreacted dye was removed by gel filtration through a Sephadex G-25 column. The fluorescent antibodies and Fabs retained their affinity according to competition with identical, unlabeled antibodies and Fabs.

Freshly harvested cells were washed twice in ice cold NaCl/P_i (pH 7.4), the cell pellet was suspended in 100 μL of NaCl/P_i (10^6 cells·mL⁻¹) and labeled by incubation with approximately 10 μg of SFX-, RhRX- or Cy3-conjugated Fabs (or mAbs) for 45 min on ice. The excess of mAbs was at least 30-fold above the K_d during the incubation. To avoid possible aggregation of the antibodies or Fab fragments, they were air-fuged (at 110 000 g, for 30 min) before labeling. Special care was taken to keep the cells at ice cold temperature before FRET measurements in order to avoid unwanted induced aggregations of cell surface molecules or significant receptor internalization. Labeled cells were washed with cold NaCl/P_i and then fixed with 1% formaldehyde. Data obtained with fixed cells did not differ significantly from those of unfixed, viable cells.

Measurement of fluorescence resonance energy transfer (FRET)

FRET measurements were carried out in a Becton-Dickinson FACStar Plus flow cytometer as described previously [17,26]. Briefly, cells were excited at 488 nm and 514 nm sequentially, and the respective emission data were collected at 540 and > 590 nm. Cell debris was excluded from the analysis by gating on the forward angle light scatter signal. Signals necessary for cell by cell FRET analysis and for spectral and detection sensitivity corrections were collected in list mode and analyzed as described previously [17,18]. Energy transfer efficiency (E) was expressed as a percentage of the donor (SFX) excitation energy tunneled to the acceptor (RhRX) molecules. The mean values of the calculated energy transfer distribution curves were used and tabulated as characteristic FRET efficiencies between the

two labeled protein epitopes. In the analysis of FRET, the uncertainties related to dye orientation [16] were overcome by using dyes with aliphatic C₆ spacer groups, allowing dynamic averaging of dipole orientations. Thus, the efficiency of FRET depended mostly on the actual donor-acceptor distance and the donor/acceptor ratio. When the two fluorescent labels are confined to two distinct membrane proteins, the dependence of FRET efficiency on the donor/acceptor ratio should also be taken into account [27,28]. In this case, measurements at different donor/acceptor ratios are necessary (as carried out in present experiments) and the normalized FRET efficiencies can be considered as estimates of the minimal fraction of acceptor-proximal donors.

Occasionally FRET was also detected on donor- and double-labeled cells by the microscopic photobleaching (pbFRET) technique [20], using a Zeiss Axiovert 135 fluorescent digital imaging microscope. Here, a minimum of 5000 pixels of digital cell images were analyzed in terms of bleaching kinetics and the efficiency of FRET was calculated from the mean bleaching time-constants of the donor dye measured on donor- and double-labeled cells, respectively [29].

Depletion of plasma membrane cholesterol by methyl- β -cyclodextrin (M β CD)

Freshly harvested T lymphoma cells (2×10^6 per mL) were treated with 7 mM M β CD for 45 min, at 37 °C, in Hanks' balanced salt solution (HBSS). (This treatment removes ≈ 40 –50% of the plasma membrane cholesterol). The efficiency of cholesterol depletion was tested by measuring fluorescence anisotropy of 1,3,5-diphenyl-hexatriene (DPH) lipid probe [30] in control and cyclodextrin-treated cells. For this test, cells were washed with HBSS and loaded with DPH ($0.6 \mu\text{g mL}^{-1}$) for 25 min, at 37 °C.

Isolation of detergent-resistant membrane fractions by sucrose gradient centrifugation

DRMs were isolated by equilibrium density-gradient centrifugation as described previously [31]. Briefly, Kit225 K6 T lymphoma cells were homogenized in ice cold TKM buffer (50 mM Tris/HCl, pH 7.4, 25 mM KCl, 5 mM MgCl₂, 1 mM EGTA) containing 73% (w/v) sucrose and 7 μL of protease inhibitor cocktail (1.5 mg mL^{-1} aprotinin, 1.5 mg mL^{-1} leupeptin, 1.5 mg mL^{-1} pepstatin, 70 mM benzamidin, 14 mM diisopropyl fluorophosphate and 0.7% phenyl-methanesulfonyl fluoride) in a 1-mL suspension of $\approx 10^8$ cells. This homogenate was incubated with 1% Triton X-100 or 15 mM Chaps on ice, for 20 min. Sucrose concentration was adjusted to 40% and the homogenate was placed at the bottom of an SW41 tube (Beckman Instruments, Nyon, Switzerland). It was overlaid with 6 mL of 36% and 3 mL of 5% sucrose in TKM buffer and centrifuged at 250 000 g for 18 h, at 4 °C, in a Centrikon T1180 ultracentrifuge (Kontron Instruments, Milan, Italy). The detergent-resistant, low-density membrane fraction was collected from the 5–36% sucrose interface where it formed a visible band.

Immunoprecipitation and Western-blot analysis

Aliquots of the cell lysate were mixed with antibody-precoated Protein G beads (50 μg mAb per 10 μL beads)

and incubated overnight at 4 °C (10 μL beads was added to a cell lysate equivalent of 10^7 cells). After washing three times in detergent-free buffer, the samples were boiled in nonreducing SDS/PAGE sample buffer and the solubilized proteins were separated from the beads by centrifugation. Proteins precipitated with the applied antibody were analyzed by SDS/PAGE and Western blot techniques. Aliquots of DRMs were boiled in nonreducing SDS/PAGE sample buffer for 10 min. Proteins were separated electrophoretically on a Bio-Rad minigel apparatus (Bio-Rad, Richmond, VA, USA) and were transferred to nitrocellulose membranes (Pharmacia Biotech., San Francisco, CA, USA). Membranes blocked by Tween 20/NaCl/P_i containing low-fat dry milk powder were incubated with primary antibodies for 60 min in Tween 20/NaCl/P_i/1% BSA, washed three times in Tween 20/NaCl/P_i and incubated with horse radish peroxidase-conjugated secondary antibody [rabbit anti-(mouse IgG) Ig, Sigma, Steinheim, Germany] for an additional 1 h. After washing four times in Tween 20/NaCl/P_i and once in NaCl/P_i, the membranes were developed with ECL reagents (Pierce Chemicals, Rockford, IL, USA) and were exposed to an AGFA (Belgium) X-ray film.

Capping experiments

Control and M β CD-treated cells were labeled first either with Alexa488-conjugated anti-CD48 Ig (MEM102) or with RhRX-conjugated anti-CD25 Ig (Tac) on ice for 40 min, then incubated with anti-IgG (whole chain) RAMIG antibody at 37 °C, for 30 min. The cells were then fixed with formaldehyde, blocked with isotype control antibody and stained with the fluorescent antibody against the other protein, on ice. The double-stained cells were analyzed for cocapping by a Zeiss Axiovert 135 TV invert field fluorescence digital imaging microscope.

Detection of IL-2 stimulated tyrosine-phosphorylation of STATs

IL-2 induced tyrosine phosphorylation of STAT3 (and STAT5) was followed by flow cytometry as described previously for STAT1 [32]. Briefly, cells with or without IL-2 treatment were subjected to fixation and permeabilization (Fix & Perm Kit, Caltag Laboratories, Burlingame, CA, USA) and incubated (20 min) with specific rabbit anti-(STAT3/STAT5) Ig or rabbit polyclonal anti-(phospho-STAT3/STAT5) Ig (New England Biolabs, Inc., Beverly, MA, USA). These antibodies detect nonphosphorylated and phosphorylated Tyr moieties on STAT3/STAT5, respectively, without appreciable cross-reaction with other Tyr-phosphorylated STATs. After washing, cells were incubated with a second, FITC-conjugated anti-(rabbit IgG) Ig (DAKO/Frank Diagnostica, Hungary) for 30 min. After a final wash step, cells were resuspended in NaCl/P_i for flow cytometry.

RESULTS

IL-2R α , β , and γ_c chains exhibit nanometer scale supramolecular clusters with HLA glycoproteins and CD48 at the surface of T lymphoma/leukemia cells

For accurate proximity analysis by FRET, the expression levels of the three IL-2R subunits and the other mapped

proteins have been estimated on the four T cell lines by flow cytometry. The IL-2R α and γ_c chains were found constitutively expressed in several (6–10) thousands of copies in all cell lines, except in MT-1, which is deficient in α and γ chains. CD25 was expressed at a level eightfold to 14-fold higher than that of the α and γ chains on all the four T cell types ($\geq 10^5$ per cell), characteristic of leukemic or activated T cells. HLA-DR was abundant on all cell lines ($\geq 5 \times 10^5$ copies per cell). Surface density of class I HLA was low on MT-1 cells ($\approx 3 \times 10^4$ per cell), while very high ($\geq 10^6$ per cell) on the other three cell lines. Interestingly, class I HLA level detected by a conformation-specific mAb interacting with the $\alpha 1/\alpha 2$ domains of the heavy chain, W6/32, was approximately twice as high on T cells deprived of IL-2 than on cells growing in the presence of IL-2. This difference was not observed if L368 mAb against the $\beta 2$ -microglobulin light chain of class I HLA was used for detection (data not shown).

Then we analyzed plasma membrane topography of IL-2R subunits and HLA molecules by both flow cytometric [17–19] and microscopic photobleaching FRET (pbFRET) [20] techniques. Both FRET methods indicated a significant degree of molecular vicinity between CD25 and class I HLA molecules on all cells, regardless of the expression level of β and γ_c chains or class I HLA (see MT-1 cells; Fig. 1B). It is noteworthy that FRET between CD25 and the light chain ($\beta 2$ -microglobulin) of class I HLA was consistently weaker than the FRET between CD25 and the HLA heavy chain marked by anti-W6/32 Ig (data not shown). In addition to this, the signaling IL-2R β and γ_c chains in these cells also displayed molecular colocalization with class I HLA. Furthermore, all the three IL-2R chains showed similar locality to the HLA-DR molecules (Fig. 1B). The HLA glycoproteins (class I HLA and HLA-DR) also exhibited a high degree of homo- and hetero-association on all the four T cell lines (independent of class I HLA expression level), as assessed by FRET data (not shown). Significant FRET ($E \geq 12\%$) was measured also between CD25 and CD48 on these cell lines, while no FRET was detectable between CD48 and TrfR (CD71) (Table 1). Although microscopy failed to detect significant colocalization of CD25 with TrfR on large (μm) scale [12], FRET data ($E \approx 13\%$) suggest their partial colocalization on molecular (nanometer) scale, at the surface of these T cells.

The above molecular locality patterns could be observed in T cells of different growth phases and appeared similarly in Kit225K6 T cells growing in the presence of IL-2 or deprived of IL-2, alike. This strongly suggests that compartmentalization of the above proteins is an inherent (possibly microdomain-organization linked) property of the plasma membrane characteristic of these human leukemia/lymphoma T cell lines and it is not triggered by cytokine binding.

Association of IL-2R chains with GPI-microdomains (rafts) on T cell surfaces: evidence from detergent resistance, cocapping/coprecipitation with CD48 and colocalization with GM-1 ganglioside

Association of a protein with membrane rafts is usually defined biochemically by its presence in low density membrane fractions resistant to cold nonionic detergents [31,33]. Therefore, we investigated here whether the CD25 clusters mentioned previously are promoted by their

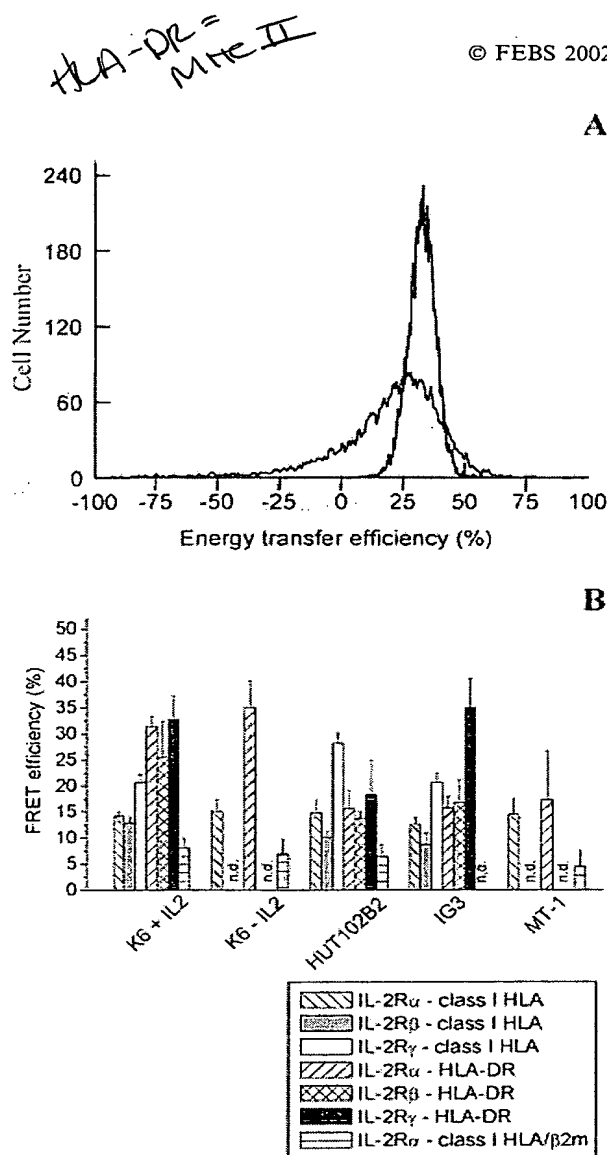


Fig. 1. FRET between IL-2R subunits and HLA glycoproteins in T leukemia and lymphoma cell lines. (A) Representative FRET efficiency (E , %) histograms measured on T lymphoma/leukemia cell lines, on cell-by-cell basis, using flow cytometry. The cell-independent intramolecular FRET between light and heavy chains of class I HLA (used as 'internal standard') (right, narrow distribution) and FRET between IL-2R α and HLA-DR (left, broad distribution) are shown. (B) FRET efficiency data monitoring molecular associations of the IL-2R complex in four different human leukemia/lymphoma T cell lines. Bars represent mean FRET efficiencies \pm SEM ($n \geq 3$) between different pairs of protein epitopes (see legend), on the T cells indicated below the bars. n.d., not determined.

association with DRMs, lipid rafts. Using immunoblotting, CD25 was detected in a significant amount in a low-density, detergent-resistant membrane fraction (DRM) of Kit225 K6 T cells after solubilization with nonionic detergents Triton X-100 (or Chaps, not shown) and the subsequent sucrose gradient centrifugation. The GPI-anchored CD48, as well as the signaling β and γ_c chains were also consistently detected in the same DRM (Fig. 2).

Table 1. FRET between raft and nonraft proteins: effect of cholesterol depletion by M β CD.

Cell Sample	Donor/epitope	Acceptor/epitope	FRET efficiency <i>E</i> (% \pm SEM)
Kit225K6	CD48	CD25	12.6 \pm 1.9
Kit225K6 + M β CD	CD48	CD25	2.3 \pm 1.5
Kit225K6	CD25	HLA-DR	31.2 \pm 0.9
Kit225K6 + M β CD	CD25	HLA-DR	16.3 \pm 1.1
Kit225K6	CD25	CD71	13.6 \pm 2.2
Kit225K6 + M β CD	CD25	CD71	14.1 \pm 2.6
Kit225K6	CD48	CD71	2.1 \pm 0.8
Kit225K6 + M β CD	CD48	CD71	1.9 \pm 1.1

In order to see whether localization of CD25 in DRM depends on its ligand occupation, detergent-resistance analysis was simultaneously performed with the same T cells deprived of IL-2 (unoccupied IL-2R). CD25 and CD48 were similarly colocalized in DRMs of such cells, in a comparable amount, albeit a little less CD25 was found here in DRMs (Fig. 2). Thus, association of CD25 with

detergent-resistant membrane fractions (DRMs) was defined by both Triton X-100 and Chaps detergents, and found approximately independent of the ligand (IL-2) occupation level of receptors on T cells.

Analysis of the whole sucrose gradient sedimentation profile led to some further conclusions. The transferrin receptor (CD71), believed to be a membrane protein excluded from lipid rafts [34,35], was not detectable in the 'light' DRM fractions of the cells, but localized in a higher density, soluble fraction of the sucrose gradient. This soluble fraction also contained CD25, in a comparable amount to that localized in DRMs. Much less CD48 was found in this fraction than in DRMs, according to the expectations (Fig. 2). This finding indicates that a substantial fraction of cell surface CD25 is associated with GPI microdomains, while the rest (approximately half of the cell surface CD25) is located in soluble membrane fractions, and thought to be distributed either randomly or associated with other membrane microdomains (e.g. those accumulating TrfR) at the surface of the T cell lines investigated.

Supporting the detergent-resistance data, CD25 and CD48 also exhibited a detectable, although weak, immuno-coprecipitation and cocapping in the plasma membrane of Kit225 K6 T cells (Fig. 3A,B). Additionally, confocal

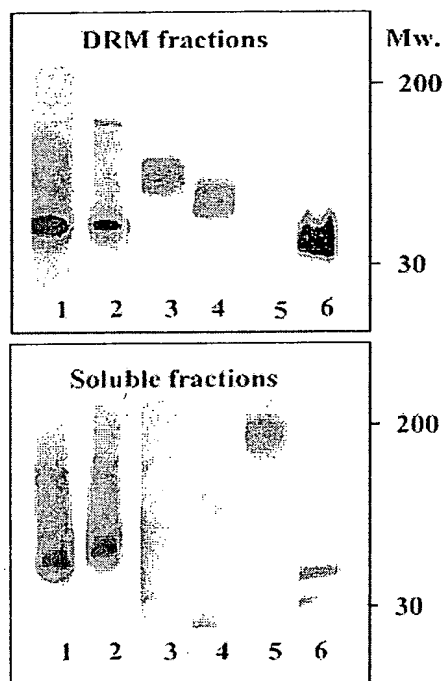


Fig. 2. Detergent resistance analysis of CD25, CD122 (IL-2R β), CD132 (IL-2R γ), CD48 and CD71 (TrfR) in the plasma membrane of the human leukemia T cell line (Kit 225K6). Upper panel: Western blots of DRMs (obtained by Triton X-100 solubilization) from cells growing with or without (lane 2) IL-2 were developed by anti-CD25 Ig (anti-Tac Ig) (lane 1,2), M1K β 1 [anti-(IL-2R β) Ig] (lane 3), TUGH4 [anti-(IL-2R γ) Ig] (lane 4), anti-CD71 Ig (MEM-75) (lane 5) and anti-CD48 Ig (MEM-102) (lane 6). Lower panel: Western blot detection of CD25 in soluble membrane fractions of cells growing in the presence (lane 1) or absence (lane 2) of IL-2. The other four lanes were developed with antibodies corresponding to the samples shown in the appropriate upper lanes.

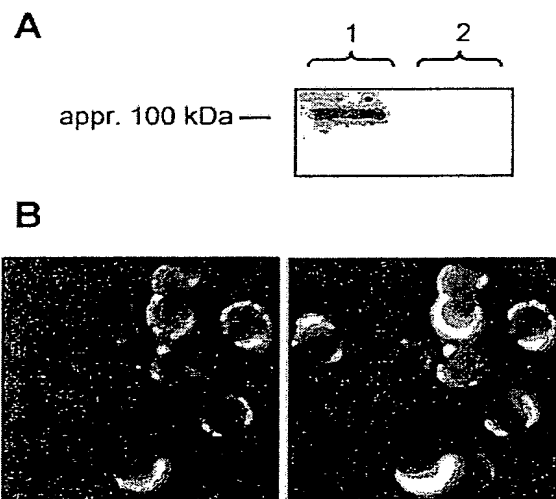


Fig. 3. Association of IL-2R α (CD25) with lipid raft component CD48: evidence from coprecipitation and cocapping. Interaction of CD48 and CD25 in the plasma membrane of Kit225 K6 cells as revealed by immuno-coprecipitation. CD25 content of the cell lysate was immuno-precipitated by anti-Tac Ig. CD48 coprecipitated with CD25 was detected as described in Experimental procedures. Western-blot (nonreduced) was developed by MEM-102 (anti-CD48) Ig (lane 1) and an isotype-matched irrelevant mouse antibody (control) (lane 2). (B) Co-capping of CD25 and CD48 on Kit225 K6 cells. Details of the capping experiment is described in the Experimental procedures. Lane 1, black and white image of the green (Alexa488-anti-CD48 Ig) fluorescence of cells after capping. Lane 2, black and white image of the red (RhRX-anti-Tac Ig) fluorescence of the same cells. (Green fluorescence was detected using a 483 \pm 15 nm excitation filter, a 500-nm dichroic mirror and a 518 \pm 28 nm emission filter, while the red fluorescence was detected by a 548 \pm 10 nm excitation filter, a 578-nm dichroic mirror and a 584-nm LP emission filter.)

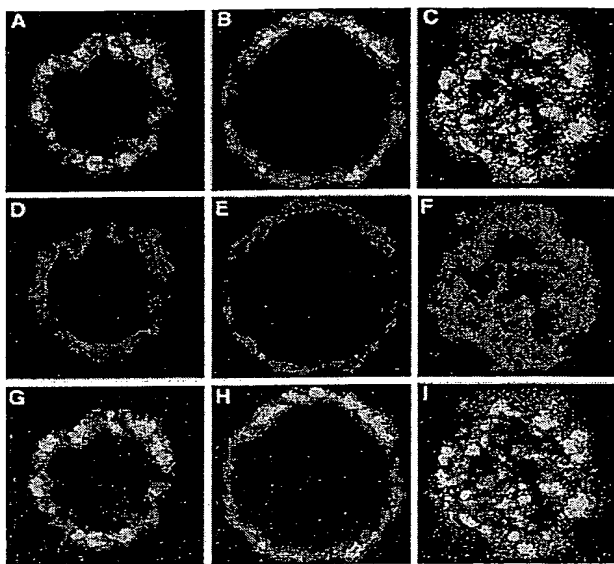


Fig. 4. Colocalization of CD25 with GM-1 ganglioside lipid raft marker labeled with FITC-cholera toxin B subunit on Kit225K6 T cells. Images of green and red fluorescence were collected in a Zeiss LSM 420 laser scanning confocal microscope (FITC-excitation: 488 nm; double dichroic: 488/543 nm; FITC-emission: 505–540 nm; Cy3-excitation: 543 nm; Cy3 emission: > 580 nm). Confocal images of double stained cells are shown at a 'close to bottom slice' (left column), at the 'middle cross section' (middle column) and at a 'top slice' (right column). The upper line (A, B, C) shows the fluorescence of FITC-CTX, the middle line (D, E, F) shows Cy3-anti-Tac Ig fluorescence and their pixel-registered overlays are shown in the bottom line of the figure (G, H, I). The yellow color in the overlay images represents membrane areas where the two labeled molecules are colocalized. (Field size: 15 × 15 microns; sampling: 512 × 512 pixels at eight bits.)

microscopic studies indicated a substantial level of colocalization of CD25 with GM-1, a lipid marker of rafts, labeled with fluorescent cholera toxin B subunit (CTX-B) (Fig. 4).

Clustering of IL-2R with CD48 and HLA glycoproteins in T cell membranes are cholesterol-sensitive

Disruption of the structural integrity of cholesterol/sphingolipid-rich microdomains is expected to abolish clustering of their protein constituents [21]. Therefore, two cell lines, the IL-2-dependent Kit225 K6 and the IL-2-independent HUT102B2 cells, were treated with water-soluble methyl- β -cyclodextrin (7 mM) to deplete their plasma membrane cholesterol [21,36]. Effect of cholesterol depletion on the microstructure of the plasma membrane was tested by measuring fluorescence anisotropy (r) of the DPH lipid probe sensing the orderedness/microviscosity of the membrane region in question. DPH fluorescence anisotropy remarkably decreased upon M β CD treatment in both cell lines (from 0.157 to 0.064 and from 0.149 to 0.082, respectively), reflecting a substantial membrane fluidization.

FRET on cholesterol-depleted T cell lines indicated largely decreased mutual vicinity between the IL-2R α chains (CD25) and CD48 or HLA glycoproteins (Table 1.) Changes of similar tendency were observed on HUT102B2

cells, as well (data not shown). No FRET could be detected between CD48 and TrfR either before or after M β CD-treatment on either cell lines, suggesting that the membrane regions containing TrfR are physically separated from the microdomains accumulating clusters of CD25, CD48, HLA-DR and GM-1.

Disruption of raft integrity abrogates the IL-2 stimulated tyrosine-phosphorylation signals

Stimulation of T cells through the IL-2R complex results in heterodimerization of the intracellular domains of β and γ_c chains followed by association with Jak, Syk (or src family) kinases. These, in turn, phosphorylate the receptor chains, forming docking sites for further downstream signaling molecules, such as STAT transcription activation factors [2]. Cytokine-stimulation is usually followed by a number of tyrosine-phosphorylation events (e.g. phosphorylation of receptor chains or diverse downstream signal components, cross-phosphorylation of Jaks, etc.), while STAT3/STAT5 phosphorylation is thought to be a signal specific to IL-2 (and IL-15) stimulation [2,37]. As hetero-oligomerization and a proper orientation of IL-2R subunits seems essential to docking and activation of STATs, we investigated here whether raft integrity is a necessary condition to a proper transduction of cytokine-stimulated phosphorylation signals.

Figure 5A shows the time course of a developing overall tyrosine phosphorylation pattern stimulated by IL-2 in Kit225K6 T cells, as assessed by immunoblotting. The major tyrosine-phosphorylated bands appeared in the 35–60 kDa region and the extent of phosphorylation increased in time, plateauing in \approx 15 min after IL-2 addition. The right panel of Fig. 5A clearly shows that pretreatment of the cells with cholesterol-extracting agent, M β CD, largely suppressed the extent of phosphorylation, nearly uniformly in the pattern.

Effect of cholesterol depletion on a signal step unique for IL-2 stimulation was also investigated. This was the tyrosine phosphorylation of STAT3/STAT5, monitored through binding of anti-(phospho-tyr-STAT3/STAT5) Ig. As Fig. 5B shows, stimulation of the Kit225K6 T cells with 1000 U·mL⁻¹ IL-2 resulted in a largely enhanced binding of anti-(P-tyrSTAT3) Ig (more than fourfold) and anti-(P-tyrSTAT5) Ig (more than sixfold), respectively, relative to their basal level (detected in control, unstimulated T cells). This enhancement was remarkably abolished when the membrane cholesterol of T cells was depleted by M β CD before IL-2 stimulation (Fig. 5B).

DISCUSSION

To investigate the molecular background of large scale cell surface clusters/domains of HLA and IL-2R observed recently by fluorescence (confocal, SNOM) and electron microscopies [12,38,39], nanometer scale molecular localities of the α , β and γ_c chains of IL-2R, class I HLA and HLA-DR molecules were measured by FRET techniques. Earlier FRET studies on class I HLA–CD25 interaction have already been reported [24,40]. In addition to this, our data show that the signaling β and γ_c chains are also in close molecular proximity to both class I HLA and HLA-DR molecules in the plasma membrane of human T cell lines of

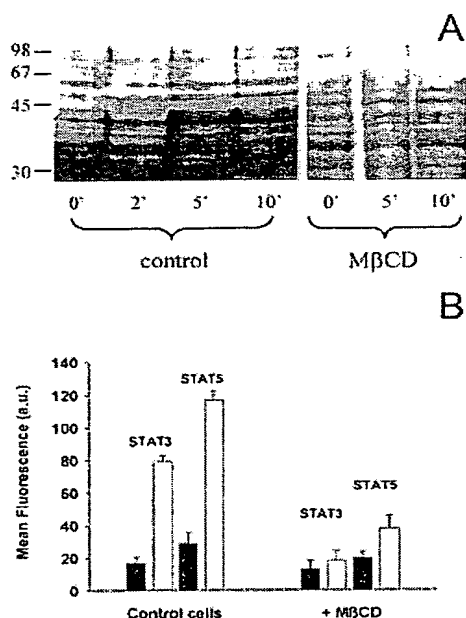


Fig. 5. Disruption of lipid rafts by cholesterol depletion abrogates IL-2 stimulated tyrosine-phosphorylation signals on T cells. (A) Detection of the overall tyrosine phosphorylation pattern in Kit225K6 T cells upon IL-2 stimulation. Parallel samples were obtained from cells pretreated with 7 mM MβCD. Aliquots were taken from the samples at the indicated times after IL-2 addition. After subjecting these aliquots to lysis, SDS PAGE and Western blotting, the membranes were incubated with horse-radish peroxidase conjugated antiphosphotyrosine antibody (ICN) and developed by ECL assay. (The X-ray films were digitized and normalized for the protein content of the membrane determined from amido-black absorbance). (B) Effect of cholesterol depletion on tyrosine phosphorylation/activation of STAT3/STAT5. The bars display means of flow cytometric fluorescence histograms of Kit225K6 T cells stained with FITC-anti-(rabbit IgG) Ig following binding of anti-(phosphotyrosine-STAT3) Ig or anti-(phosphotyrosine-STAT5) Ig. The data are displayed after subtraction of the background derived from isotype control staining and nonspecific binding of the second antibody. Error bars represent SEM values ($n \geq 3$). Black bars represent fluorescence proportional to binding of anti-(phospho-tyr-STAT3) Ig or anti-(phospho-tyr-STAT5) Ig in unstimulated cells, while white bars indicate its binding 15 min after IL-2 stimulation. Cell treatments are indicated below the abscissa.

leukemia/lymphoma origin. This might be characteristic of these cell lines overexpressing CD25 relative to resting peripheral T cells. FRET provided additional information about the possible interaction site between CD25 and class I HLA molecules in these protein clusters. The stronger FRET between CD25 and HLA-I heavy chain, compared with that between CD25 and β_2 m indicates that CD25 preferentially interacts with the heavy chain of class I HLA. This is consistent with the altered binding of W6/32, but not of L368 Ig, after IL-2 deprivation of T cells. IL-2 binding to CD25 likely masks the W6/32 mAb binding site on proximal HLA molecules. Although the physiological significance of the molecular vicinity/association of class I HLA and IL-2R chains is still left undefined by these data, regulatory cross-talk suggested for the class I HLA-insulin receptor interaction [41] cannot be excluded.

Taken together, considering the simultaneous nature of FRET from IL-2R chains to HLA molecules and the 'cross-FRET' between IL-2R chains [11], the present data strongly suggest that at least a fraction of these molecules is compartmented in a common membrane microdomain. These supramolecular clusters may be characteristic of human leukemia/lymphoma T cell membranes, as immunogold staining of IL-2R on peripheral resting murine T lymphocytes and cell lines did not show any clustered distribution [42], in contrast to our recent microscopic results on leukemia/lymphoma cells [12].

On the other hand, a fraction of cell surface CD25 was found also proximal to transferrin receptors, thought to be located outside lipid rafts [34,35] in these T cells, as shown by previous [43] and present FRET data. As class I and class II HLA molecules were also found partially associated with TrfRs on T cells [43], our data may reflect that a fraction of cell surface CD25 molecules (low affinity form of IL-2R) is associated with TrfR-positive membrane microdomains, as well. Association of CD25 with these TrfR-positive domains may provide an efficient endocytosis/recycling pathway for the excess α chains (CD25) not involved in signal transduction of these cells.

Our data convincingly show that all the constituents of the high affinity human IL-2R are preferentially associated with DRMs (rafts) containing CD48, in T cells of leukemia/lymphoma origin. Constitutive expression of human IL-2R β and γ chains in membrane rafts was confirmed by our experiments, a result similar to that observed in mouse T lymphoma cells [44]. On the other hand, our data also support association of human CD25 with lipid rafts, independently of its ligand (IL-2) occupation. Our detergent-resistance data, in good agreement with earlier FRET data [11], suggest that the preassembly of the three IL-2R chains in the plasma membrane of T leukemia/lymphoma cells is not induced by ligand binding, as in case of other growth factor receptors (e.g. EGFR) [8].

Furthermore, our data suggest that the transient supramolecular assemblies of IL-2R chains, CD48, HLA-glycoproteins and GM-1 gangliosides at the cell surface are promoted by lipid 'raft' microdomains [33], which are rich in cholesterol and glycosphingolipids. These membrane microdomains were recently reported to be essential in compartmentation of signaling components providing efficient responses to TcR or IgE receptor activation [13–15,35]. In the T cells investigated here, raft-disruption by cholesterol-depletion resulted in a largely reduced molecular coclustering of IL-2R chains with CD48 and HLA-DR, possibly via lateral dispersion of these raft components. Although association of HLA molecules with lipid rafts, in general, is still a poorly understood and controversial issue [14,45], they may contribute to stabilize these microdomains by a 'fencing effect' [46], through their dynamic coupling to the cytoskeletal matrix [47,48], even if they are localized at the periphery of rafts.

Association of the IL-2R chains with lipid rafts (containing CD48) may have several functional consequences in T cells. First, rafts may concentrate the α chains (CD25) in the vicinity of signaling IL-2R β and γ_c chains, forming a common signaling platform in the membrane, before cytokine stimulation. This 'focusing' effect may enhance the association rate of the high affinity receptor upon IL-2 binding, even if IL-2R α does not bind directly IL-2 [49,50].

This property may partly be responsible for the increased proliferation rate of leukemia/lymphoma T cells compared with normal peripheral T cells. Consistent with the present data, the recently observed 'preassembly' of IL-2R subunits [11] in leukemia/lymphoma T cells may be brought about by sorting a fraction of overexpressed α chains together with the constitutively expressed β and γ_c chains to common membrane microdomains via 'raft-mediated trafficking'. Compartmentation of the IL-2R chains by rafts in these cells may also assist in setting up the proper conformation of heterotrimer IL-2R and its association with further intracellular (or raft-associated) signaling molecules to gain full signaling capacity. This is possibly brought about by a conformation-dependent tightening of their interactions upon binding of the relevant cytokine [11].

Second, the GPI microdomains can also concentrate other cytokine receptor α chains (e.g. IL-4R α IL-7R α or IL-15R α) in the locality of common γ chains shared by them for signaling [2,6]. This hypothesis, however, requires further investigation with the above mentioned α chains.

Third, co-compartmentation of CD25 with CD48 may further provide a regulatory platform for GPI-anchored proteins in T cell physiology and growth. Recent work, reporting on inhibition of T cell growth but not of effector function upon immobilization of GPI-anchored proteins CD48, Thy1 or Ly6A/E by cross-linking with antibodies [51], is consistent with this hypothesis. The GPI-microdomains, which are rich in src-family kinases [13,14] may also promote/regulate assembly of the IL-2R subunits with these enzymes in case of signal pathways mediating activation-induced T cell death or survival [2].

The impact of raft-assisted membrane compartmentation on T cell growth signaling was demonstrated by the remarkably reduced IL-2 stimulated STAT3/STAT5 phosphorylation upon disruption of raft integrity. This effect may be brought about by the lateral dispersion of IL-2R subunits resulting in decoupling of the intracellular interaction (crosstalk) between Jaks associated to the β and γ_c chains, respectively. These interactions are known to be essential in the formation of docking sites for downstream signaling molecules, such as STATs, during signal transduction [2].

In conclusion, the present data are consistent with a model where a substantial fraction of IL-2R α (CD25), together with the constitutively expressed β and γ_c chains, is associated with cholesterol- and glycosphingolipid-rich membrane microdomains (rafts) in cell lines of human adult T cell lymphoma/leukemia origin, independently of the ligand occupation level of IL-2 receptors. These microdomains contain, among others, a potential regulatory protein of T cell growth, CD48. A pivotal role of cholesterol in maintaining such transient protein assemblies, including also HLA glycoproteins, was also demonstrated. Thus, IL-2R chains may represent a new example of the few transmembrane proteins found associated with lipid rafts [14]. It is still unclear which structural motifs result in targeting these polypeptide chains to rafts, as no report has so far been published regarding their acylation (palmitoylation), which is known to promote association with rafts [14,35]. Perhaps their relatively heavy N- or O-linked glycosylation makes them attractive for rafts through potential carbohydrate-carbohydrate interactions with GPI-anchored proteins as well as with the glycosylated

headgroups of glycosphingolipids occurring at high density in rafts.

All these properties may be characteristic of human T cell lines of leukemia/lymphoma origin, as a recent study in mouse cell lines [52] revealed a distinct role of lipid rafts in regulating IL-2 signaling, namely sequestration of CD25 by lipid rafts impeding interaction with the IL-2R β and γ chains. The observed difference between these and our results focuses attention on the constitutive or induced raft-association of the IL-2R subunits and therefore the regulatory role of lipid rafts in IL-2R signaling may be cell- or species-specific. This is further emphasized by another recent study [53] that reports on raft-association of the IL-2R β chain in transformed human NK and fibroblast cells. Thus, to better understand the role of lipid rafts in cell growth/viability-signaling of T cells, in general, and in the unregulated growth of leukemic T cells, in particular, similar comparative investigations seem necessary using mouse vs. human T cell lines and antigen-stimulated T cells from peripheral blood vs. uncultured cells isolated from T cell leukemia. The importance of this question is underlined by the recently reported progress in the IL-2 receptor-targeted immunotherapy of human leukemia/lymphoma [9].

ACKNOWLEDGEMENTS

The authors thank Drs T. Keresztes, A. Erdei, F. Erdődi, B. Lontay and M. Józsi for the valuable discussions and their help in sedimentation and immuno-precipitation experiments. The skillful technical assistance of A. Harangi, G. Őri, T. Lakatos and A. Lacasse is also gratefully acknowledged. This work was supported by Research Grants OTKA T30411 (S. D.), T34493 (J. M.), T030399 (J. Sz.), F020590 (L. B.), F025210, T037831 (G. V.), F034487 (A. B.) from the Hungarian Academy of Sciences, by FKFP 518/99 (J. M.) from the Hungarian Ministry of Education, by ETT 117/2001 (Gy. V.) from Hungarian Ministry of Health and Welfare, by GA AV CR A7052904 (V. H.) from the Czech Academy of Sciences and by Bolyai Research Scholarship of Hungarian Academy of Sciences for L. B. and G. V.

REFERENCES

1. Waldmann, T.A. (1991) The interleukin-2 receptor. *J. Biol. Chem.* **266**, 2681–2684.
2. Nelson, B.H. & Willerford, D.M. (1998) Biology of the interleukin-2 receptor. *Adv. Immunol.* **70**, 1–81.
3. Nakamura, Y., Russell, S.M., Mess, S.A., Friedmann, M., Erdos, M., Francois, C., Jacques, Y., Adelstein, S. & Leonard, W.J. (1994) Heterodimerization of the IL-2 receptor beta- and gamma-chain cytoplasmic domains is required for signalling. *Nature* **369**, 330–333.
4. Leonard, W.J. & O'Shea, J.J. (1998) Jaks and STATs: biological implications. *Annu. Rev. Immunol.* **16**, 293–322.
5. Tagaya, Y., Bamford, R.N., DeFilippis, A.P. & Waldmann, T.A. (1996) IL-15: a pleiotropic cytokine with diverse receptor/signaling pathways whose expression is controlled at multiple levels. *Immunity* **4**, 329–336.
6. DiSanto, J.P. (1997) Cytokines: shared receptors, distinct functions. *Curr. Biol.* **7**, R424–R426.
7. Hemar, A., Subtil, A., Lieb, M., Morelon, E., Hellio, R. & Dautry-Varsat, A. (1995) Endocytosis of interleukin 2 receptors in human T lymphocytes: distinct intracellular localization and fate of the receptor alpha, beta, and gamma chains. *J. Cell Biol.* **129**, 55–64.
8. Lemmon, M.A. & Schlessinger, J. (1994) Regulation of signal transduction and signal diversity by receptor oligomerization. *Trends Biochem. Sci.* **19**, 459–463.

9. Waldmann, T.A. (2000) T-cell receptors for cytokines: targets for immunotherapy of leukemia/lymphoma. *Ann. Oncol.* **11** (Suppl. 1), 101–106.
10. Kondo, S., Shimizu, A., Saito, Y., Kinoshita, M. & Honjo, T. (1986) Molecular basis for two different affinity states of the interleukin 2 receptor: affinity conversion model. *Proc. Natl Acad. Sci. USA* **83**, 9026–9029.
11. Damjanovich, S., Bene, L., Matkó, J., Alileche, A., Goldman, C.K., Sharrow, S. & Waldmann, T.A. (1997) Preassembly of interleukin 2 (IL-2) receptor subunits on resting Kit 225, K6 T cells and their modulation by IL-2, IL-7, and IL-15: a fluorescence resonance energy transfer study. *Proc. Natl Acad. Sci. USA* **94**, 13134–13139.
12. Vereb, G., Matkó, J., Vamosi, G., Ibrahim, S.M., Magyar, E., Varga, S., Szöllösi, J., Jenei, A., Gáspár, R.J., Waldmann, T.A. & Damjanovich, S. (2000) Cholesterol-dependent clustering of IL-2R α and its colocalization with HLA and CD48 on T lymphoma cells suggest their functional association with lipid rafts. *Proc. Natl Acad. Sci. USA* **97**, 6013–6018.
13. Xavier, R., Brennan, T., Li, Q., McCormack, C. & Seed, B. (1998) Membrane compartmentation is required for efficient T cell activation. *Immunity* **8**, 723–732.
14. Horejsi, V., Drbal, K., Cebecauer, M., Cerny, J., Brdicka, T., Angelisova, P. & Stockinger, H. (1999) GPI-microdomains: a role in signalling via immunoreceptors. *Immunol. Today* **20**, 356–361.
15. Sheets, E.D., Holowka, D. & Baird, B. (1999) Membrane organization in immunoglobulin E receptor signaling. *Curr. Opin. Chem. Biol.* **3**, 95–99.
16. Matkó, J., Szöllösi, J., Trón, L. & Damjanovich, S. (1988) Luminescence spectroscopic approaches in studying cell surface dynamics. *Q. Rev. Biophys.* **21**, 479–544.
17. Szöllösi, J., Trón, L., Damjanovich, S., Helliwell, S.H., Arndt-Jovin, D. & Jovin, T.M. (1984) Fluorescence energy transfer measurements on cell surfaces: a critical comparison of steady-state fluorimetric and flow cytometric methods. *Cytometry* **5**, 210–216.
18. Trón, L., Szöllösi, J., Damjanovich, S., Helliwell, S.H., Arndt-Jovin, D.J. & Jovin, T.M. (1984) Flow cytometric measurement of fluorescence resonance energy transfer on cell surfaces. Quantitative evaluation of the transfer efficiency on a cell-by-cell basis. *Biophys. J.* **45**, 939–946.
19. Matkó, J. & Edidin, M. (1997) Energy transfer methods for detecting molecular clusters on cell surfaces. *Methods Enzymol.* **278**, 444–462.
20. Jovin, T.M. & Arndt-Jovin, D.J. (1989) FRET microscopy: digital imaging of fluorescence resonance energy transfer. Applications in cell biology. In *Cell Structure and Function by Microspectrofluorimetry* (Kohen, E. & Hirschberg, J.G., eds), pp. 99–115. Academic Press, San Diego, CA, USA.
21. Varma, R. & Mayor, S. (1998) GPI-anchored proteins are organized in submicron domains at the cell surface. *Nature* **394**, 798–801.
22. Damjanovich, S., Matkó, J., Mátyus, L., Szabó, G.J., Szöllösi, J., Pieri, J.C., Farkas, T. & Gáspár, R.J. (1998) Supramolecular receptor structures in the plasma membrane of lymphocytes revealed by flow cytometric energy transfer, scanning force- and transmission electron-microscopic analyses. *Cytometry* **33**, 225–233.
23. Eicher, D.M. & Waldmann, T.A. (1998) IL-2R α on one cell can present IL-2 to IL-2R β / γ (c) on another cell to augment IL-2 signaling. *J. Immunol.* **161**, 5430–5437.
24. Szöllösi, J., Damjanovich, S., Goldman, C.K., Fulwyler, M.J., Aszalos, A.A., Goldstein, G., Rao, P., Talle, M.A. & Waldmann, T.A. (1987) Flow cytometric resonance energy transfer measurements support the association of a 95-kDa peptide termed T27 with the 55-kDa Tac peptide. *Proc. Natl Acad. Sci. USA* **84**, 7246–7250.
25. Arima, N., Kamio, M., Okuma, M., Ju, G. & Uchiyama, T. (1991) The IL-2 receptor α -chain alters the binding of IL-2 to the β -chain. *J. Immunol.* **147**, 3396–3401.
26. Szöllösi, J., Horejsi, V., Bene, L., Angelisova, P. & Damjanovich, S. (1996) Supramolecular complexes of MHC class I, MHC class II, CD20, and tetraspan molecules (CD53, CD81, and CD82) at the surface of a B cell line JY. *J. Immunol.* **157**, 2939–2946.
27. Yguerabide, J. (1994) Theory for establishing proximity relations in biological membranes by excitation energy transfer measurements. *Biophys. J.* **66**, 683–693.
28. Damjanovich, S., Bene, L., Matkó, J., Mátyus, L., Krasznai, Z., Szabó, G., Pieri, C., Gáspár, R.J. & Szöllösi, J. (1999) Two-dimensional receptor patterns in the plasma membrane of cells. A critical evaluation of their identification, origin and information content. *Biophys. Chem.* **82**, 99–108.
29. Bodnár, A., Jenei, A., Bene, L., Damjanovich, S. & Matkó, J. (1996) Modification of membrane cholesterol level affects expression and clustering of class I HLA molecules at the surface of JY human lymphoblasts. *Immunol. Lett.* **54**, 221–226.
30. Shinitzky, M. & Barenholz, Y. (1978) Fluidity parameters of lipid regions determined by fluorescence polarization. *Biochim. Biophys. Acta* **515**, 367–394.
31. Ilangumaran, S., Arni, S., van Echten-Deckert, G., Borisch, B. & Hoessli, D.C. (1999) Microdomain-dependent regulation of Lck and Fyn protein-tyrosine kinases in T lymphocyte plasma membranes. *Mol. Biol. Cell* **10**, 891–905.
32. Fleisher, T.A., Dorman, S.E., Anderson, J.A., Vail, M., Brown, M.R. & Holland, S.M. (1999) Detection of intracellular phosphorylated STAT-1 by flow cytometry. *Clin. Immunol.* **90**, 425–430.
33. Simons, K. & Ikonen, E. (1997) Functional rafts in cell membranes. *Nature* **387**, 569–572.
34. Harder, T. & Simons, K. (1999) Clusters of glycolipid and glycosylphosphatidyl-inositol-anchored proteins in lymphoid cells: accumulation of actin regulated by local tyrosine phosphorylation. *Eur. J. Immunol.* **29**, 556–562.
35. Langlet, C., Bernard, A.M., Drevot, P. & He, H.T. (2000) Membrane rafts and signaling by the multichain immune recognition receptors. *Curr. Opin. Immunol.* **12**, 250–255.
36. Ilangumaran, S. & Hoessli, D.C. (1998) Effects of cholesterol depletion by cyclodextrin on the sphingolipid microdomains of the plasma membrane. *Biochem. J.* **335**, 433–440.
37. Johnston, J.A., Bacon, C.M., Finbloom, D.S., Rees, R.C., Kaplan, D., Shibuya, K., Ortaldo, J.R., Gupta, S., Chen, Y.Q. & Giri, J.D. (1995) Tyrosine phosphorylation and activation of STAT5, STAT3, and Janus kinases by interleukins 2 and 15. *Proc. Natl Acad. Sci. USA* **92**, 8705–8709.
38. Jenei, A., Varga, S., Bene, L., Mátyus, L., Bodnár, A., Bacsó, Z., Pieri, C., Gáspár, R.J., Farkas, T. & Damjanovich, S. (1997) HLA class I and II antigens are partially co-clustered in the plasma membrane of human lymphoblastoid cells. *Proc. Natl Acad. Sci. USA* **94**, 7269–7274.
39. Hwang, J., Gheber, L.A., Margolis, L. & Edidin, M. (1998) Domains in cell plasma membranes investigated by near-field scanning optical microscopy. *Biophys. J.* **74**, 2184–2190.
40. Harel-Bellan, A., Krief, P., Rimsky, L., Farrar, W.L. & Mishal, Z. (1990) Flow cytometry resonance energy transfer suggests an association between low-affinity interleukin 2 binding sites and HLA class I molecules. *Biochem. J.* **268**, 35–40.
41. Ramalingam, T.S., Chakrabarti, A. & Edidin, M. (1997) Interaction of class I human leukocyte antigen (HLA-I) molecules with insulin receptors and its effect on the insulin-signaling cascade. *Mol. Biol. Cell* **8**, 2463–2474.
42. Breitfeld, O., Kuhlcke, K., Lother, H., Hohenberg, H., Mannweiler, K. & Rutter, G. (1996) Detection and spatial distribution of IL-2 receptors on mouse T-lymphocytes by immunogold-labeled ligands. *J. Histochem. Cytochem.* **44**, 605–613.

43. Mátyus, L., Bene, L., Heiligen, H., Rausch, J. & Damjanovich, S. (1995) Distinct association of transferrin receptor with HLA class I molecules on HUT-102B and JY cells. *Immunol. Lett.* **44**, 203–208.
44. Hoessli, D.C., Poincelet, M. & Rungger-Brandle, E. (1990) Isolation of high-affinity murine interleukin 2 receptors as detergent-resistant membrane complexes. *Eur. J. Immunol.* **20**, 1497–1503.
45. Chiu, I., Davis, D.M. & Strominger, J.L. (1999) Trafficking of spontaneously endocytosed MHC proteins. *Proc. Natl Acad. Sci. USA* **96**, 13944–13949.
46. Kusumi, A. & Sako, Y. (1996) Cell surface organization by the membrane skeleton. *Curr. Opin. Cell Biol.* **8**, 566–574.
47. Woda, B.A. & Woodin, M.B. (1984) The interaction of lymphocyte membrane proteins with the lymphocyte cytoskeletal matrix. *J. Immunol.* **133**, 2767–2772.
48. Geppert, T.D. & Lipsky, P.E. (1991) Association of various T cell-surface molecules with the cytoskeleton. Effect of cross-linking and activation. *J. Immunol.* **146**, 3298–3305.
49. Grant, A.J., Roessler, E., Ju, G., Tsudo, M., Sugamura, K. & Waldmann, T.A. (1992) The interleukin 2 receptor (IL-2R): the IL-2R alpha subunit alters the function of the IL-2R beta subunit to enhance IL-2 binding and signaling by mechanisms that do not require binding of IL-2 to IL-2R alpha subunit. *Proc. Natl Acad. Sci. USA* **89**, 2165–2169.
50. Roessler, E., Grant, A., Ju, G., Tsudo, M., Sugamura, K. & Waldmann, T.A. (1994) Cooperative interactions between the interleukin 2 receptor alpha and beta chains alter the interleukin 2-binding affinity of the receptor subunits. *Proc. Natl Acad. Sci. USA* **91**, 3344–3347.
51. Marmor, M.D., Bachmann, M.F., Ohashi, P.S., Malek, T.R. & Julius, M. (1999) Immobilization of glycosylphosphatidylinositol-anchored proteins inhibits T cell growth but not function. *Int. Immunol.* **11**, 1381–1393.
52. Marmor, M.D. & Julius, M. (2001) Role of lipid rafts in regulating interleukin-2 receptor signaling. *Blood* **98**, 1489–1497.
53. Lamaze, C., Dujeancourt, A., Baba, T., Lo, C.G., Benmerah, A. & Dautry-Varsat, A. (2001) Interleukin 2 receptors and detergent-resistant membrane domains define a clathrin-independent endocytic pathway. *Mol. Cell* **7**, 661–671.

Flow cytometric resonance energy transfer measurements support the association of a 95-kDa peptide termed T27 with the 55-kDa Tac peptide

(fluorescence energy transfer/interleukin 2 receptor)

JANOS SZÖLLÖSI*, SANDOR DAMJANOVICH*, CAROLYN K. GOLDMAN†, MACK J. FULWYLER‡, ADORJAN A. ASZALOS§, GIDEON GOLDSTEIN¶, PATRICIA RAO¶, MARY ANNE TALLE¶, AND THOMAS A. WALDMANN†||

*Department of Biophysics, Medical University School of Debrecen, H-4012 Debrecen, Hungary; †Metabolism Branch, National Cancer Institute, National Institutes of Health, Bethesda, MD 20892; ‡Laboratory for Cell Analysis, Department of Laboratory Medicine, University of California San Francisco, San Francisco, CA 94143; §Food and Drug Administration, Washington, DC 20204; and ¶Immunology Division, Ortho Pharmaceutical Corporation, Raritan, NJ 08869

Contributed by Thomas A. Waldmann, July 1, 1987

ABSTRACT Two monoclonal antibodies (OKT27 and OKT27b) have been produced that react with distinct epitopes of a 95-kDa peptide. The T27 antigen is widely distributed, being expressed on B lymphocytes, monocytes, and adult T-leukemic cells but not on polymorphonuclear leukocytes or platelets. There was a low level of T27 expression on resting T cells that increased on T-cell activation. In preliminary studies, the OKT27b antibody coprecipitated a 55-kDa peptide, as well as the 95-kDa peptide, from the radiolabeled cells of the HuT 102B2 cell line. Preclearance with anti-Tac, a monoclonal antibody to the 55-kDa peptide of the multichain interleukin 2 receptor, removed the 55-kDa but not the 95-kDa peptide from subsequent OKT27b immunoprecipitates of HuT 102B2 extracts, suggesting the possibility that the T27 peptide was associated with the Tac peptide. However, the precipitation of the p55 Tac peptide by OKT27b was quite inconsistent. Thus, additional information was sought using a flow cytometric energy transfer technique to provide a physical estimation of the proximity between the Tac and the T27 peptides. The flow cytometric version of the fluorescence resonance energy transfer technique permits the determination of inter- and intramolecular distances at 2- to 10-nm levels on a cell-by-cell basis. Using this approach, there was a mean energy transfer of 7.3% with HuT 102B2 cells when fluorescein isothiocyanate anti-Tac served as the donor and tetramethylrhodamine isothiocyanate OKT27 served as the acceptor. In contrast, there was no energy transfer in comparable studies observed when fluorescein anti-Tac and rhodamine anti-transferrin receptor antibodies were used. These observations support the conclusion that there is a close nonrandom proximity in HuT 102B2 cells between the 95-kDa peptide identified by the OKT27 monoclonal antibody and the p55 Tac peptide of the multichain interleukin 2 receptor.

T lymphocytes stimulated with antigen or mitogen produce interleukin 2 (IL-2) (1, 2). T-cell growth is dependent on the interaction of IL-2 with high-affinity IL-2 receptors that are not present on resting cells but are induced and expressed on T cells after activation (3-5). There are at least two classes of IL-2 receptors that differ markedly in their affinities for IL-2 (6). Both classes of receptors share the same Tac peptide (55 kDa) (4, 5). To define the molecular basis for high- and low-affinity receptors and to determine the mechanism whereby IL-2 communicates a signal to the nucleus, we have investigated the possibility that the IL-2 receptor is a complex with multiple peptide chains in addition to the one

identified by anti-Tac (7). Using crosslinking methodology, we have identified a non-Tac IL-2 binding peptide of 75 kDa and have proposed that the 75-kDa IL-2 binding peptide is associated with the 55-kDa Tac peptide to form the high-affinity IL-2 receptor complex (7).

Recently, two additional monoclonal antibodies, OKT27 and OKT27b, were developed in an effort to identify distinct human T-cell activation antigens. These antibodies, which are the subject of the present report, identify two distinct epitopes of a peptide (T27) of ≈ 95 kDa. As part of these studies, the OKT27b monoclonal antibody inconsistently precipitated a 55-kDa peptide from the radiolabeled cells of the HuT 102B2 cell line that expressed the Tac peptide. In these studies, preclearance with anti-Tac removed the 55-kDa, but not the 95-kDa, peptide from subsequent OKT27b immunoprecipitation of the radiolabeled HuT 102B2 cell extracts. This observation suggested that the T27 protein could be associated with the IL-2 receptor complex. However, the precipitation of the p55 Tac peptide by T27b was very inconsistent. Thus, we wished to obtain further information concerning the relationship between the p55 Tac and T27 peptides. For this purpose, the relative spatial distribution of the Tac and T27 proteins was analyzed by a fluorescence resonance energy transfer method. This technique has been successfully applied in biochemistry for determining inter- and intramolecular distances at the 2- to 10-nm level (8-11). A flow cytometric version of fluorescence resonance energy transfer was introduced recently with the ability to determine the average distance relationships—i.e., proximity between fluorescently tagged monoclonal antibodies in the cell membrane on a cell-by-cell basis (12-14).

In our study, monoclonal antibodies directed against the Tac and T27 proteins were suitably labeled with fluorescein isothiocyanate (FITC) and tetramethylrhodamine isothiocyanate (TRITC). Using these probes and the flow cytometric energy transfer (FCET) method, we determined the relative spatial distribution of Tac peptide and the epitope of the T27 protein identified by OKT27 in the cell membrane of the HuT 102B2 cell line and have obtained direct physical evidence for association of the 95-kDa T27 peptide with the Tac peptide.

MATERIALS AND METHODS

Monoclonal Antibodies. The production and specificity of anti-Tac antibody to the 55-kDa peptide of the IL-2 receptor

Abbreviations: FCET, flow cytometric energy transfer; FITC, fluorescein isothiocyanate; F-anti-Tac, FITC-labeled anti-Tac; IL-2, interleukin 2; PHA, phytohemagglutinin; R-OKT27, rhodamine-labeled OKT27; TRITC, tetramethylrhodamine isothiocyanate.

||To whom reprint requests should be addressed.

The publication costs of this article were defrayed in part by page charge payment. This article must therefore be hereby marked "advertisement" in accordance with 18 U.S.C. §1734 solely to indicate this fact.

was described (5). The OKT27 and OKT27b antibodies are IgG2a monoclonal antibodies that were products of two independent fusions. The OKT27 antibody was the product of a fusion between P3 × 63Ag8U1 myeloma cells and spleen cells from CA F₁ mice that had been immunized with human T4 cells stimulated with purified protein derivative. The OKT27b antibody was the product of a fusion between P3 × 68Ag8.653 mouse myeloma cells and spleen cells from mice stimulated with human T lymphocytes activated in a mixed lymphocyte reaction. Monoclonal antibodies designated as L368 and W6/32 were kindly provided by Frances Brodsky (Becton-Dickinson Immunocytometry Systems, Mountain View, CA).

Cells. The HuT 102B2 cell line, originally derived from a human adult T-cell lymphoma and associated with the human T-cell lymphotropic virus I (HTLV-I), was grown in RPMI 1640 medium with 20% fetal calf serum and antibiotics.

Immunofluorescence Analysis. The percentages of cells expressing antigen reactive with the T-cell activation antigen monoclonal antibodies were determined by indirect immunofluorescence as described by Matheison and coworkers (15).

Cell-Surface Labeling, Detergent Extraction, Immunoprecipitation, and NaDodSO₄/PAGE Analysis. Viable whole cells were radiolabeled with sodium ¹²⁵I using a modification of a lactoperoxidase technique (16). Cells were washed twice and then lysed with isotonic immunoprecipitation buffer and immunoprecipitated by the method of Goldman and Liu (17). Samples were loaded onto a 12.5% polyacrylamide gel containing 0.1% NaDodSO₄ and electrophoresed according to the method of Laemmli (18).

Labeling of Antibodies for Energy Transfer Experiments. The labeling procedure was as described (19, 20). As determined by spectrophotometric and spectrofluorimetric measurements, a dye-to-protein labeling ratio between 2 and 4 was obtained for fluorescein and between 1 and 3 for rhodamine.

Energy Transfer Experiments. A Becton-Dickinson FACS 440 flow cytometer equipped with dual-laser excitation was used to determine energy transfer between FITC- and TRITC-labeled proteins of the cell surface. A complete technical description of the correlated data acquisition and analysis has been given elsewhere (13). The labeled cells were excited sequentially at 488 and 514 nm; by using suitable filter combinations, we detected fluorescence emission at 535 nm (with a bandpath width of 15 nm) and above 590 nm. Four intensities were collected: the fluorescence at 535 and >590 nm excited at 488 nm, the forward angle 488 nm-light-scatter signal, and the fluorescence emission >590 nm excited at 514 nm. Correction parameters were derived from data obtained with single-labeled cells. All parameters were collected in list mode, and the analysis was carried out according to the protocol described (13, 14). The method evaluated the efficiency (*E*) of the fluorescence resonance energy transfer for each cell. *E*, the transfer efficiency, is expressed as a percentage of the excitation energy taken up by the donor (fluorescein) molecules and tunneled without radiation to the acceptor (rhodamine) molecules. *E* is directly related to the average donor-acceptor distance according to the following equation:

$$E = R_0^{-6} / (R_0^{-6} + R^{-6}), \quad [1]$$

where *R* is the actual average distance of the donor and acceptor molecules on a cell-by-cell basis, and *R*₀ is a characteristic spectroscopic parameter of the donor and acceptor pair defined by the distance between the donor and acceptor where the emission probability of the donor's excitation state by fluorescence of the donor or by transfer to the acceptor is 50% (Eq. 1). Thus, the proximity of labeled

antibodies is expressed as a frequency distribution histogram of *E* over the cell population.

RESULTS

Characteristics of Proteins Precipitated by OKT27 and OKT27b. To characterize the proteins precipitated by OKT27 and OKT27b, Triton X extracts of HuT 102B2 cells, surface-labeled with ¹²⁵I, were incubated with monoclonal antibodies, immunoprecipitated with *Staphylococcus aureus* cells, and then electrophoresed under reducing conditions through NaDodSO₄/polyacrylamide gels. Both OKT27 and OKT27b immunoprecipitated an intense band with a calculated mass of 95 kDa (Fig. 1). The 95-kDa band was not present in OKT27 precipitates of radiolabeled extracts that had been precleared with OKT27b, indicating that the antibodies identified the same peptide. This conclusion as well as the conclusion that OKT27 and OKT27b identify different epitopes of the same peptide was confirmed with a "sandwich" ELISA using these antibodies and an extract of the cell line Raji that expresses the T27 peptide (data not shown). In contrast, preclearance with OKT27b did not remove the bands obtained by the precipitation of radiolabeled HuT 102B2 cell extracts with antibodies that identify peptides with a similar molecular radius (i.e., an anti-transferrin receptor antibody) and F10-44-2 [an antibody of the CDw44 lineage-nonspecific cluster defined at the Third Leukocyte Differentiation Antigen Workshop (21)]. As noted previously, in analyses of the same radioiodinated HuT 102B2 extracts, anti-Tac precipitated an intense area from 50 to 60 kDa with much less intense bands at 75 and 180 kDa. Preclearance with T27b did not reduce the intensity of these bands precipitated by anti-Tac. However, in preliminary studies OKT27b precipitated a 55-kDa band as well as the 95-kDa band. The addition of anti-Tac in a preclearance study removed the 55-kDa but not the 95-kDa band from subsequent OKT27b immunoprecipitates of HuT 102B2 extracts. Although these studies suggested an association between the p55 peptide precipitated by anti-Tac and the 95-kDa peptide precipitated by OKT27b, the precipitation of a 55-kDa peptide by the OKT27b monoclonal antibody was very inconsistent; in most studies, no band at p55 was observed.

Immunofluorescence Analysis. A relatively low proportion of resting T cells bore either the Tac or the T27 antigens as assessed by indirect immunofluorescence (Table 1). However, the majority of freshly obtained leukemic cells as well as

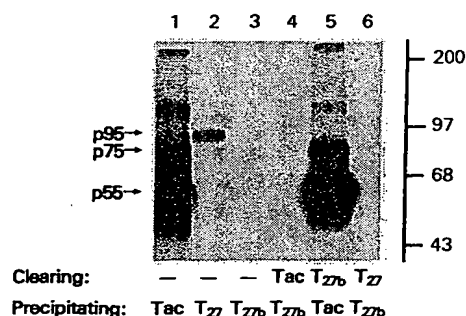


Fig. 1. Characteristics of proteins precipitated by OKT27 and OKT27b. Triton extracts of HuT 102B2 cells labeled with ¹²⁵I were incubated with the monoclonal antibodies indicated, immunoprecipitated with *S. aureus* cells, and then electrophoresed under reducing conditions through NaDodSO₄/polyacrylamide gels. In those cases indicated, the extracts were precleared with anti-Tac, OKT27b, or OKT27, and the supernatants were then immunoprecipitated with the monoclonal antibodies indicated and electrophoresed as indicated above. Numbers on right are kDa.

Table 1. Expression of T27 and Tac antigens on normal cells, leukemic cells, and cell lines

Cells	% positive, mean \pm SEM (individual values)	
	OKT27	Anti-Tac
Fresh normal cells		
E rosette ⁺ (T enriched) (<i>n</i> = 12)	25 \pm 4	8 \pm 1
E rosette ⁻ nonadherent (B enriched) (<i>n</i> = 2)	(39, 39)	(2, 4)
E rosette ⁻ (monocyte gated) (<i>n</i> = 9)	62 \pm 10	ND*
T cells cultured 48 hr with PHA (<i>n</i> = 2)	84 \pm 3	77 \pm 6
Clonal T cells		
Adult T-cell leukemia (<i>n</i> = 7)*	44 \pm 11 (0, 65, 33, 47, 81, 18, 46)	60 \pm 6 (52, 29, 77, 72, 57, 75, 55)
Cell lines		
Adult T-cell leukemia (HuT 102, HuT 78, patient M.C., patient E.D.)	(89, 74, 85, 50) (0)	(89, 14, 89, 78) (82)
Adult T-cell leukemia (MT-1)		
ALL T-cell leukemia (<i>n</i> = 5) (T-cell precursor)	27 \pm 12	ND
EBV-transformed B-cell lines (<i>n</i> = 8)	82 \pm 3	ND
MLA-144 (gibbon ape T-cell leukemia)	(0)	(0)
K562 (human chronic myelogenous leukemia)	(82)	(1)
U937 (human monocytic leukemia)	(83)	(11)
Pre-B-cell lines (<i>n</i> = 4)	90 \pm 4	ND

ND, not done; EBV, Epstein-Barr virus.

*One patient expressed the Tac but not the T27 antigen.

the cell lines prepared from patients with HTLV-I-associated adult T-cell leukemia expressed the T27 as well as the Tac antigen. In addition, T-cell precursor lines derived from patients with acute T-cell leukemia expressed the T27 antigen. The T27 antigen was not lineage specific but was widely distributed, being expressed on populations enriched for normal B cells, Epstein-Barr virus-transformed B-cell lines, freshly obtained monocytes, and the monocytic cell line U937. In addition, certain non-lymphoid non-monocytic lines expressed the T27 antigen, whereas granulocytes and platelets did not. Although for a number of cell populations expression of Tac and T27 was concordant, there were rare cell populations that expressed the Tac antigen but not the T27 antigen (e.g., MT-1 cell line). More frequently, cell populations were identified that did not express the Tac antigen yet expressed the more widely distributed T27 antigen. As noted above, only a modest proportion of the freshly obtained T cells expressed either the Tac or T27 antigens. Furthermore, even the cells expressing the antigens manifested low staining intensity. However, there was a marked increase in both the proportion of cells expressing these antigens as well as the intensity of the staining per cell after phytohemagglutinin (PHA) stimulation of isolated T cells, indicating that the T27 antigen, like the Tac antigen, can be viewed as an early activation antigen when T cells are considered. Specifically, the mean fluorescence units for cells stained with OKT27 rose from a preactivation level of 1.2 units to a peak value of 7.3 units 2 days after PHA

stimulation, and then falling to 2.7 units by day 10. The comparable values for anti-Tac at the same time periods were 1.1, 9.8, and 3.4 units.

Proximity Measurements Between Tac Epitope of the 55-kDa IL-2 Receptor Peptide and T27 Epitope of the 95-kDa T27 Peptide. The distribution of the binding sites for FITC anti-Tac (F-anti-Tac) and rhodaminated OKT27 (R-OKT27) antibodies was investigated on HuT 102B2 cells by using energy transfer measurements in a flow cytometer. The F-anti-Tac served as donor, and the R-OKT27 served as acceptor. As controls for determining correction coefficients, cell samples were labeled with either F-anti-Tac or R-OKT27 alone. Simultaneously, the cells were labeled with both conjugated antibodies to measure energy transfer. The frequency distributions of F-anti-Tac and R-OKT27 fluorescence of single-labeled cells are shown in Fig. 2A and B. The energy transfer distribution, shown in Fig. 2C, with a mean value of 7.3% indicates that the two monoclonal antibodies and their respective binding sites are in close proximity. Nine independent experiments with cells harvested independently showed a rather standard average transfer efficiency of around 7% (Table 2). The relatively broad distribution of the antigen identified by OKT27 is also shown in Fig. 3A, where the energy transfer efficiency of the F-anti-Tac and R-OKT27 donor-acceptor pair was plotted against the ratio of the donor to acceptor. The left side of the plot in Fig. 3A shows an

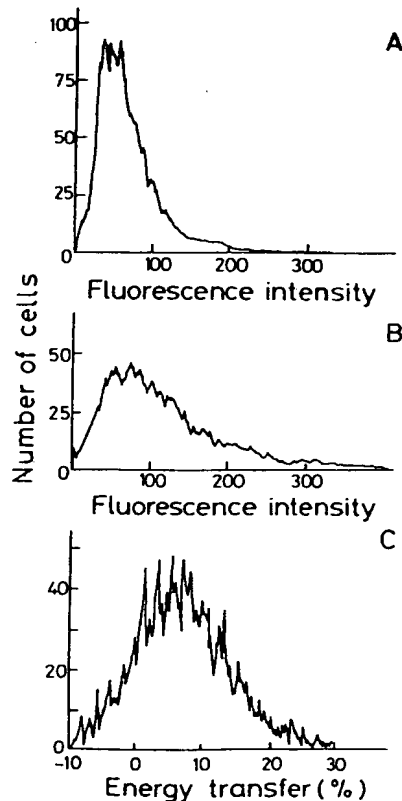


FIG. 2. Frequency distribution histograms of F-anti-Tac (A) and R-OKT27 (B) antibody-labeled HuT 102B2 cells. (C) Energy transfer efficiency distribution with a mean of 7.3 when the cells were labeled simultaneously with both antibodies. During the labeling at 0°C, the antibody concentration was kept at saturation level in all three cases. Approximately 5000 cells were analyzed per distribution.

Table 2. Energy transfer efficiency values (E) between donor-acceptor pairs

Donor	Acceptor	E , %
F-anti-Tac	R-OKT27	6.7, 4.2, 8.4, 7.3, 6.2, 7.5, 7.0, 9.3, 7.5
F-OKT27	R-OKT27	8.1, 11.0, 10.2
F-anti-TfR	R-OKT27	2.3
F-anti-TfR	R-anti-TfR	8.4
F-anti-Tac	R-anti-TfR	0.1
F-OKT27	R-anti-TfR	0.6
F-L368	R-L368	2.1
F-anti-Tac	R-W6/32	9.6, 16.0, 9.3
F-OKT27	R-W6/32	8.5, 5.8, 6.8

Anti-TfR, anti-transferrin receptor.

upward curvature, indicating the higher energy transfer in case of lower donor-to-acceptor ratio as is predicted by former theoretical and experimental work (13, 22). In Fig. 3B, a plot similar to that of Fig. 3A is presented. However, in this particular case, we measured the energy transfer between F-L368 and R-W6/32 directed against different peptides of the HLA class I complex. The monoclonal antibody L368 is directed against β_2 -microglobulin, and the W6/32 monoclonal antibody is directed against the main framework peptide of every HLA class I molecule. Thus, the binding of the two noncompeting monoclonal antibodies was always stoichiometric in a 1:1 ratio, as is predicted by the model in the inset of Fig. 3B. Despite a significant transfer efficiency indicating the closely correlated quasi-intramolecular binding sites, the energy transfer efficiency did not show a dependence on the donor-to-acceptor ratio, in contrast to the observation with OKT27 and anti-Tac.

Energy Transfer Experiments in Combination with Other Monoclonal Antibodies. The majority of the T27 antigens are in an aggregated form containing associated homopolymers on the cell surface with energy transfer between T27 and identical T27 antigens on an associated T27 peptide. Other combinations of intra- and intermolecular donor-acceptor pairs with anti-HLA and other antibodies frequently showed energy transfer. In the case of β_2 -microglobulin and HLA class I, intramolecular energy transfer was detected (Fig. 3B) as predicted from the known proximity of the β_2 -microglobulin and the HLA class I peptides. Energy transfer was also observed between F-anti-Tac and R-W6/32, as well as between F-OKT27 and R-W6/32 (Table 2; Fig. 4). This finding is consistent with the very high density of HLA antigen on the cell surface, providing an opportunity for chance association between these antibodies. A contrasting pattern was observed on examination of combinations of anti-transferrin receptor antibodies with different antibodies. The 8.4% energy transfer between transferrin receptors suggests a dimeric or polymeric structure (Table 2). On the other hand, no energy transfer was observed between F-anti-

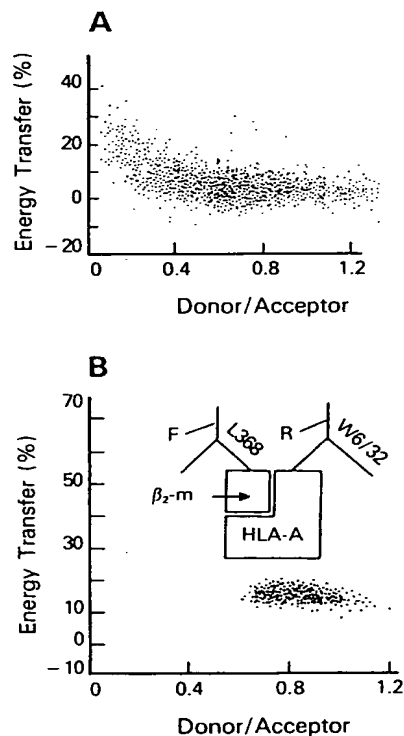


FIG. 3. (A) Relative distribution of F-anti-Tac and R-OKT27 antibodies at the cell surface. The dot plot shows that, with decreasing donor-to-acceptor ratio (left side of the population), the transfer efficiency is increasing. (B) Fluorescence energy transfer distribution between two closely related antibodies directed against two separate peptides of the HLA class I complex as depicted (*inset*) did not show any change in the energy transfer distribution upon decreasing the donor-to-acceptor ratio.

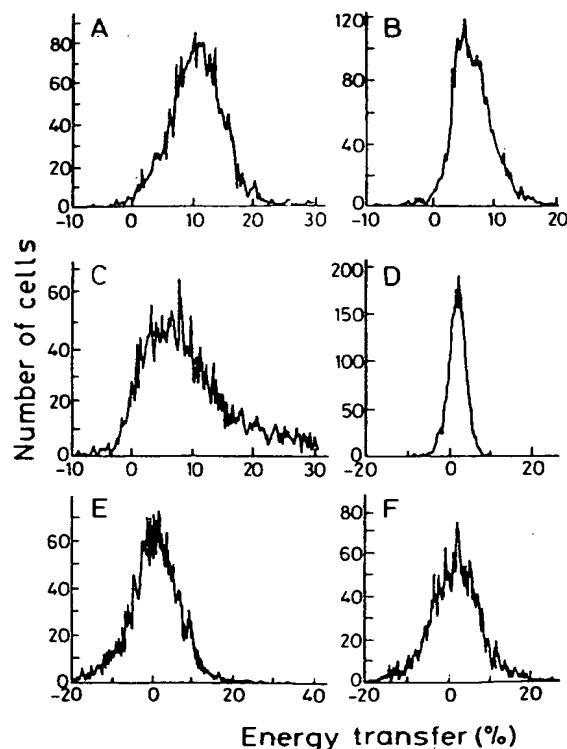


FIG. 4. Frequency distribution of energy transfer efficiency between fluoresceinated and rhodaminated antibodies on the surface of HuT 102B2 cells. The donor-acceptor pairs were as follows: (A) F-OKT27 and R-OKT27 (mean, 10.7%); (B) F-OKT27 and R-W6/32 (mean, 6.8%); (C) F-anti-Tac and R-W6/32 (mean, 9.3%); (D) F-L368 and R-L368 (mean, 1.2%); (E) F-anti-Tac and R-anti-transferrin receptor (mean, 0.9%); (F) F-anti-transferrin receptor and R-OKT27 (mean, 2.3%). Only A, B, and C showed significant transfer.

transferrin receptor and R-OKT27 antibodies. Furthermore, there was no energy transfer between F-anti-Tac and R-anti-transferrin receptor antibodies.

DISCUSSION

In this study, a peptide (T27) defined by two monoclonal antibodies (OKT27 and OKT27b) was identified. Both monoclonal antibodies identified a peptide of 95 kDa. On the basis of studies using preclearance of radiolabeled cell-surface membrane peptides from HuT 102 and a sandwich ELISA, the two antibodies were shown to identify two different epitopes of the same peptide. In selected studies, the OKT27b monoclonal antibody coprecipitated a 55-kDa peptide that could be precleared with anti-Tac. Thus, additional information was sought concerning the relationship of the Tac and T27 peptides. In a series of independent studies, fluorescence recovery after photobleaching was used to define the diffusion properties of the peptides identified by anti-Tac and OKT27 antibodies. Pretreatment of HuT 102B2 cells with the OKT27 monoclonal antibody resulted in the immobilization of the Tac peptide in >30% of cells (A.A.A., S.D., T.A.W., and M. Edidin, unpublished observations). This observation supports the view that there is a molecular association between the Tac and T27 peptides on HuT 102B2 cells.

To provide a physical estimation of the proximity of the Tac peptide and T27 peptide, FCET measurements were performed. The application of the FCET method requires a minimum number of labeled cell-surface elements (13, 14). The HuT 102B2 cell line, which has a high number of IL-2 receptors, offered an excellent experimental target for our investigation on the proximity of the Tac and T27 antigens. The studies outlined in Fig. 2 demonstrate the close proximity of the Tac and T27 antigens. We could not measure distance relationships of donor and acceptor molecules using the anti-Tac antibody as the acceptor, presumably because a smaller number of antigens recognized by anti-Tac were present in the HuT 102B2 cell preparation used when compared with the epitopes identified by OKT27. Antigens in higher abundance are preferably used as acceptors in energy transfer experiments (13, 14). The number of Tac antigens and the number of OKT27 targets are sufficiently high to permit fluorescence energy transfer measurements but not so high as to cause artifactual energy transfer. The results of a series of positive and negative control studies using different donor-acceptor combinations provide support for the view that there is a molecular association of the Tac and T27 epitopes.

It is clear that not all of the T27 peptides identified by OKT27 are associated with the Tac antigen. There are cells that express this T27 antigen that are Tac negative and that do not bind IL-2. Reciprocally, there are IL-2 binding cells that express the p55 Tac peptide yet are nonreactive with the OKT27 antibody. In addition, the energy transfer between F-anti-Tac and R-OKT27 increased at a decreasing donor-to-acceptor ratio, in contrast to the 1:1 stoichiometry ratio observed with two antibodies to different epitopes of the HLA complex.

Taken as a whole, the measurements in these studies suggest a close proximity of the Tac peptide and the T27 peptide. Specifically, the 55-kDa Tac peptide was intermittently coprecipitated by OKT27b antibody. In addition, in photobleaching recovery studies, the Tac antigen on HuT 102B2 cells was immobilized by pretreatment with OKT27. Finally, the biophysical measurement using FCET revealed a close proximity of the Tac and T27 peptides. Further biochemical and immunological experiments are necessary to define any role that might be played by the T27 peptide and by the proximity relationship of this peptide and the Tac peptide in the process of lymphocyte activation and differentiation.

The work of J.S., S.D., and M.J.F. was supported jointly by the National Science Foundation (INT-8405545) and the Hungarian Academy of Sciences under the U.S.-Hungarian Cooperative Science Program.

1. Morgan, D. A., Ruscetti, F. W. & Gallo, R. C. (1976) *Science* 193, 1007-1008.
2. Smith, K. A. (1980) *Immunol. Rev.* 51, 337-357.
3. Robb, R. J., Munck, A. & Smith, K. A. (1981) *J. Exp. Med.* 154, 1455-1474.
4. Waldmann, T. A. (1986) *Science* 232, 727-732.
5. Uchiyama, T., Broder, S. & Waldmann, T. A. (1981) *J. Immunol.* 126, 1393-1397.
6. Robb, R. J., Greene, W. C. & Rusk, C. M. (1984) *J. Exp. Med.* 160, 1126-1146.
7. Tsudo, M., Kozak, R. W., Goldman, C. K. & Waldmann, T. A. (1987) *Proc. Natl. Acad. Sci. USA* 84, 4215-4218.
8. Stryer, L. (1979) *Annu. Rev. Biochem.* 47, 819-846.
9. Fairclough, R. H. & Cantor, C. R. (1978) *Methods Enzymol.* 48, 347-379.
10. Dale, R. E., Eisinger, J. & Blumber, W. E. (1979) *Biophys. J.* 26, 161-194.
11. Jovin, T. M. (1979) in *Flow Cytometry and Sorting*, eds. Melamed, M. R., Mullaney, P. F. & Mendelsohn, M. L. (Wiley, New York), pp. 137-165.
12. Damjanovich, S., Tròn, L., Szöllösi, J., Zidovetzki, R., Vaz, W. L. C., Regateiro, F., Arndt-Jovin, D. J. & Jovin, T. M. (1983) *Proc. Natl. Acad. Sci. USA* 80, 5985-5989.
13. Tròn, L., Szöllösi, J., Damjanovich, S., Helliwell, S. H., Arndt-Jovin, D. J. & Jovin, T. M. (1984) *Biophys. J.* 45, 939-946.
14. Szöllösi, J., Tròn, L., Damjanovich, S., Helliwell, S. H., Arndt-Jovin, D. J. & Jovin, T. M. (1984) *Cytometry* 5, 210-216.
15. Matheison, B. J., Sharrow, S. O., Campbell, P. S. & Asofsky, R. (1979) *Nature (London)* 277, 478-480.
16. Ledbetter, J. A. L., Evans, R. L., Lipinski, M., Cunningham-Rundles, C., Good, R. A. & Herzenberg, L. A. (1981) *J. Exp. Med.* 153, 310-323.
17. Goldman, N. D. & Liu, T.-Y. (1987) *J. Biol. Chem.* 262, 2363-2368.
18. Laemmli, U. K. (1970) *Nature (London)* 227, 680-685.
19. Spack, E. G., Jr., Packard, B., Wier, M. L. & Edidin, M. (1986) *Anal. Biochem.* 158, 233-237.
20. DePetrìs, S. (1978) *Methods Membr. Biol.* 9, 1-201.
21. Cobbold, S., Hale, G. & Waldmann, H. (1987) in *Leucocyte Typing III*, ed. McMichael A. J. (Oxford Univ., Oxford), pp. 788-803.
22. Wolber, P. K. & Hudson, B. S. (1979) *Biophys. J.* 28, 197-210.

The p75 peptide is the receptor for interleukin 2 expressed on large granular lymphocytes and is responsible for the interleukin 2 activation of these cells

(Tac peptide/lymphokine-activated killer cells)

MITSURU TSUDO*, CAROLYN K. GOLDMAN*, KATHLEEN F. BONGIOVANNI*, WING C. CHAN†, ELLIOTT F. WINTON†, MASATO YAGITA§, ELIZABETH A. GRIMM§, AND THOMAS A. WALDMANN*

*Metabolism Branch, National Cancer Institute, Bethesda, MD 20892; †Departments of Medicine and of Pathology and Laboratory Medicine, Emory University School of Medicine, Atlanta, GA 30322; and §Department of Tumor Biology, M. D. Anderson Hospital, Houston, TX 77030

Contributed by Thomas A. Waldmann, April 15, 1987

ABSTRACT There are at least two interleukin 2 (IL-2) binding peptides: one is the M_r 55,000 peptide (p55) reactive with the anti-Tac monoclonal antibody, and the other is a M_r 75,000 non-Tac IL-2 binding peptide (p75). Independently existing Tac or p75 peptides represent low-affinity IL-2 receptors, whereas high-affinity IL-2 receptors are expressed when both peptides are present and associated in a receptor complex. It has long been known that normal large granular lymphocytes (LGL) or leukemic cells from the patients with abnormal expansions of LGL can be activated by IL-2 not only to more-potent natural killer cells but also to effectors of lymphokine-activated killer (LAK) activity, although they do not express the Tac peptide. In the present study, using cross-linking methodology, we found that normal LGL and leukemic LGL from all individuals tested expressed the p75 IL-2 binding peptide but did not express the Tac peptide. These LGL leukemia cells made proliferative responses to IL-2 but required a much higher concentration than that required for the proliferation of normal phytohemagglutinin-stimulated T lymphoblasts that express high-affinity receptors. Furthermore, the addition of IL-2 to Tac-negative LGL leukemic cells augmented transcription of the Tac gene and induced the Tac peptide. Neither the IL-2-induced proliferation nor the up-regulation of Tac gene expression was inhibited by the addition of anti-Tac. These results strongly suggest that the p75 peptide is responsible for IL-2-induced activation of LGL and that the p75 peptide alone can mediate an IL-2 signal. Thus, the p75 peptide may play an important role in the IL-2-mediated immune response not only by participating with the Tac peptide in the formation of the high-affinity receptor complex on T cells but also by contributing to the initial triggering of LGL activation so that these cells become efficient natural killer and lymphokine-activated killer cells.

Large granular lymphocytes (LGL) are lymphocytes that display abundant cytoplasm with many azurophilic granules (1-4). These cells are phenotypically heterogeneous according to the expression of the T3 (CD3) (5) or the Leu-11 (CD16, receptors for the Fc portion of IgG) (6) antigens. Although LGL constitute only a minor subset of normal peripheral blood lymphocytes, virtually all natural killer (NK) activity is attributed to this population (1, 2, 4). In addition, a number of patients with an abnormal expansion of LGL have been described (7-11). Their phenotypes are also heterogeneous, reflecting the variety of normal LGL (11). Several lines of evidence suggest that normal LGL (12-15) and leukemic LGL (7, 9-11) can respond directly to interleukin 2 (IL-2) at relatively high concentrations, with enhanced NK activity,

γ -interferon production, and eventually proliferation, without the need of other stimuli. Furthermore, it has been reported that LGL can be stimulated by IL-2 to generate cytotoxic cells termed lymphokine-activated killer cells, or LAK cells, that can lyse NK-resistant tumor targets (16).

There are at least two forms of the cellular receptors for IL-2—one with a high affinity ($K_d = 10^{-11}$ M) and the other with a much lower affinity (10^{-8} M) (17). Both of these share the same Tac peptide (M_r 55,000) (18, 19) defined by the anti-Tac monoclonal antibody. This observation of such a great difference in affinity led to an investigation of the possibility that the IL-2 receptor is a complex receptor with multiple peptides in addition to the Tac peptide. These studies culminated in (i) the demonstration of a non-Tac IL-2 binding peptide with a M_r of 75,000 (p75) and (ii) our suggestion that this p75 peptide associates with the p55 Tac peptide on activated T cells to form a high-affinity receptor complex (20, 21). Sharon *et al.* (22) also have demonstrated a M_r 70,000–75,000 IL-2 binding peptide on activated T cells. Unlike activated T cells, the number of IL-2 receptors, as assessed by analysis with the anti-Tac antibody, is negligible on resting peripheral blood lymphocytes (17, 18) and on normal LGL (12, 13, 15) or leukemic LGL (9, 10). Nevertheless, as noted above, these Tac-negative LGL can be stimulated to make a number of responses to IL-2. Furthermore, up-regulation of the Tac peptide by IL-2 has been demonstrated for a number of cell types, including some that initially express few if any Tac molecules (23–25). These observations have led to a number of questions including the following ones. How can non-Tac-expressing cells such as LGL be stimulated by IL-2 to become effective killer cells? Why do LGL require a much higher concentration of IL-2 for activation than that required for saturation of high-affinity receptors (12, 15)? What IL-2-mediated signals transduced from cell-surface receptors are sufficient to up-regulate the Tac gene expression? These unsolved questions lead us to the view that a triggering process exists in which the Tac peptide is not involved. In the present study we addressed this issue specifically by investigating the role played in this process by the p75 non-Tac IL-2 binding peptide.

We demonstrate that the p75 IL-2 binding peptide, but not the Tac peptide, is expressed on normal LGL and LGL leukemia cells and discuss the possibility that the p75 peptide alone is sufficient to transduce the IL-2 signal in such cells. In addition, we provide evidence that the up-regulation of Tac peptide gene expression can be mediated by the interaction of IL-2 with the p75 peptide alone.

MATERIALS AND METHODS

Cell Separation. Normal LGL were separated by using a slight modification of a method described previously (2). Briefly, peripheral blood mononuclear cells were isolated using Ficoll-Paque (Pharmacia), followed by removal of cells adherent to plastic surfaces and to nylon-wool columns. Nonadherent cells were fractionated by centrifugation on discontinuous gradients consisting of 45%, 50%, and 55% Percoll (Pharmacia). Low-density and midfraction lymphocytes were isolated from the top and from the interface between 45% and 50% Percoll, respectively. LGL in the low-density fraction were further purified by removal of cells forming rosettes with sheep erythrocytes at 29°C for 1 hr. The resulting LGL preparations, whose recovery was ≈ 8 –10% of the initial peripheral blood mononuclear cell preparation, contained $>80\%$ LGL as determined by morphologic analysis of Wright-Giemsa-stained slides.

LGL Leukemia Cells. Eight patients with LGL leukemia were studied. The diagnosis was made considering clinical features, hematologic characteristics, and cell-surface phenotypes (8, 11).

Antibodies and IL-2. The Leu series of monoclonal antibodies was purchased from Becton Dickinson Monoclonal Center. Anti-Leu-11 (CD16) reacts with the Fc receptor for IgG expressed on NK cells and neutrophils (6). Anti-NKH-1 (Leu-19) reacts with a 220-kDa protein of unknown function expressed on NK cells and on a subset of monocytes (26). Anti-T11 (CD2) (Coulter) reacts with the receptor for sheep erythrocytes. Anti-Tac monoclonal antibody was purified from hybridoma ascites by using protein A-Sepharose (Pharmacia). Flow cytometry with a FACS (fluorescence-activated cell sorter) analyzer (Becton Dickinson) was performed as described (20). Recombinant human IL-2 from *Escherichia coli* (27) was a generous gift from Cetus (Emeryville, CA).

Proliferative Response of LGL Leukemia Cells to IL-2. Leukemic cells (1×10^5) in 200 μ l of RPMI 1640 medium containing 10% fetal calf serum were cultured in a 96-well plate for 72 hr in the presence of a 1:4 dilution series of IL-2 in triplicate. Proliferation was measured by the incorporation of 1 μ Ci (1 Ci = 37 GBq) of [3 H]thymidine (6.7 Ci/mmol, New England Nuclear) per well during the last 6 hr of the culture. We also studied activated normal peripheral blood mononuclear cells that had been cultured with 0.1% phytohemagglutinin (PHA-P, Difco) for 7 days.

Cross-Linking Study. 125 I-labeled human recombinant IL-2 (28.6–44 μ Ci/ μ g, New England Nuclear) was chemically cross-linked with intact cells by the methods described previously (20, 21). Cells (5 – 10×10^6) were incubated for 1 hr at 4°C with 5 nM 125 I-labeled IL-2 and with unlabeled proteins as indicated and then cross-linked with 1 mM disuccinimidyl suberate (Pierce).

RNA Transfer Blot Analysis. The levels of mRNA encoding the Tac peptide on LGL leukemia cells were evaluated by using a radiolabeled Tac cDNA probe (28). LGL leukemia cells were cultured for 24 hr at 2×10^6 cells per ml in RPMI 1640 medium containing 10% fetal calf serum in the absence or presence of 5 nM IL-2 and 500 nM (75 μ g/ml) anti-Tac antibody. After the isolation of total RNA by the method of Chirgwin *et al.* (29), 10 μ g of RNA was electrophoresed on formaldehyde gels, transferred to nitrocellulose membranes (Schleicher & Schuell), baked at 80°C for 2 hr, and hybridized with the Tac cDNA probe radiolabeled with [32 P]dCTP from New England Nuclear. Hybridizations were performed overnight in a solution containing $4 \times$ NaCl/Cit ($1 \times = 150$ mM NaCl/15 mM sodium citrate), 10% dextran sulfate, 40% formamide, 7 mM Tris (pH 7.6), 1% $\times 100$ Denhardt's solution (Denhardt's solution = 0.02% Ficoll 400/0.02% polyvinylpyrrolidone/0.02% bovine serum albumin), and 20 μ g of salmon sperm DNA per ml. Membranes were washed

three times in $2 \times$ NaCl/Cit containing 0.1% NaDodSO₄ at room temperature, followed by two washes in $1 \times$ NaCl/Cit containing 0.1% NaDodSO₄ at 52°C, and then were autoradiographed.

RESULTS

Expression of the p75 Peptide on Normal LGL. Human peripheral blood mononuclear cells depleted of B lymphocytes and monocytes were enriched for LGL using Percoll sedimentation followed by rosetting with sheep erythrocytes (termed E⁺ and E⁻ population). The resulting low-density E⁻ population, which will be referred to as LGL, contained $>80\%$ large granular lymphocytes as determined by morphologic analysis. The proportions of these cells reactive with monoclonal antibodies were 40% for T3 (CD3), 30–40% for Leu-11 (CD16), and 40% for NKH-1. These LGL showed higher NK activity against K562 target cells than did the other cell populations examined—i.e., unfractionated, midfraction, and low-density E⁺ fraction lymphocytes (data not shown). The midfraction cells from the Percoll gradient represented purified preparations of T cells that were $>90\%$ Leu-1 (CD5) reactive. To determine whether these freshly prepared lymphocyte populations expressed the IL-2 binding peptide, cross-linking studies were performed. Cells (1×10^7) were incubated with 5 nM 125 I-labeled IL-2, covalently cross-linked with 1.0 mM disuccinimidyl suberate, and analyzed by NaDodSO₄/PAGE under reducing conditions. Unfractionated cells and the midfraction T cells expressed a faint but distinct labeling of a M_r 90,000 band and a fainter labeling of a M_r 70,000 band (Fig. 1), representing the p75 and p55 Tac peptides, respectively, cross-linked with IL-2 [M_r 15,000 (30)]. These observations indicate that certain resting lymphocytes, including T cells, constitutively express a low level of both IL-2 binding peptides. Furthermore, PHA-activated lymphoblasts cross-linked with 1 nM 125 I-labeled IL-2 expressed a M_r 90,000 band as well as a more heavily

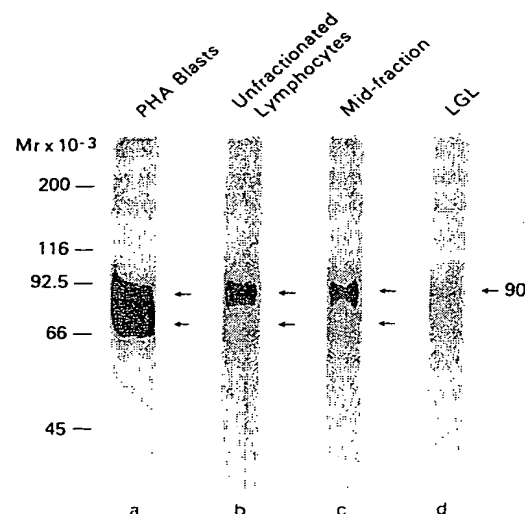


FIG. 1. 125 I-labeled IL-2 receptor complexes produced by covalently cross-linking 125 I-labeled IL-2 to normal lymphocytes. Lanes: a, lymphoblasts activated with PHA for 3 days; b, fresh unfractionated lymphocytes depleted of monocytes and B cells; c, midfraction (mainly T cells) from a Percoll sedimentation; d, LGL. Cells were incubated with 1 nM 125 I-labeled IL-2 for PHA-activated blasts or 5 nM for the other populations and then cross-linked with disuccinimidyl suberate, solubilized, and electrophoresed on NaDodSO₄/PAGE under reducing conditions. The standards used were myosin (M_r 200,000), β -galactosidase (M_r 116,000), phosphorylase b (M_r 92,500), bovine serum albumin (M_r 66,000), and ovalbumin (M_r 45,000).

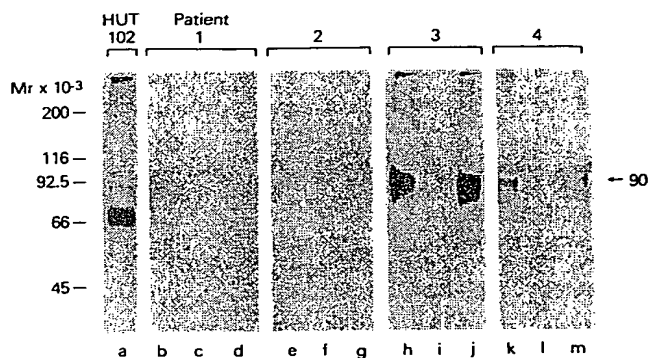


FIG. 2. ^{125}I -labeled IL-2 receptor complexes produced by covalently cross-linking ^{125}I -labeled IL-2 to LGL leukemia cells from four patients and HUT 102 cells, a human T lymphotropic virus type I-induced human T-cell line. Patients 1 and 2 had type A and patients 3 and 4 had type B expression of LGL. Cells were incubated with 1 nM ^{125}I -labeled IL-2 for HUT 102 or 5 nM for leukemic cells in the absence (lanes a, b, e, h, and k) and presence (lanes c, f, i, and l) of 200-fold excess of unlabeled IL-2 or 500-fold molar excess of anti-Tac antibody (lanes d, g, j, and m).

labeled M_r 70,000 band, indicating a greater number of Tac peptides than p75 IL-2 binding peptides. In contrast to resting and activated T lymphocytes, normal LGL cross-linked with radiolabeled IL-2 yielded the M_r 90,000 but not the M_r 70,000 band, indicating that they express the p75 but not the p55 Tac IL-2 binding peptide.

Expressing of the p75 Peptide on LGL Leukemia Cells. Since IL-2 has been reported to induce LGL leukemia cells to manifest biological effects (7–11), the leukemic cells of eight patients with LGL leukemia were examined to determine which type of IL-2 receptor on the leukemic cells is responsible for these effects. All cases manifested an expansion of LGL. These eight cases could be classified into two subtypes on the basis of their phenotype as described by Chan *et al.* (11). In five of the cases with T_H or T_H lymphoproliferative disease (type A), the abnormal cells were of the T-cell lineage and expressed the CD2 (T11), CD3 (Leu-4) and CD8 (Leu-2a) antigens, whereas the other three cases with LGL leukemia (type B) consisted of cells lacking the CD3 and CD8 antigens but expressing NKH-1. None of the cases expressed the Tac

antigen, consistent with previous reports (9, 10). However, cross-linking studies revealed that LGL leukemia cells from all eight patients, regardless of type, uniformly expressed the p75 IL-2 binding peptide and did not express the p55 Tac peptide. The autoradiograms of four representative cases are shown in Fig. 2. The labeling was shown to be specific by the demonstration that the addition of a 200-fold molar excess of unlabeled IL-2 during the incubation with labeled IL-2 completely abolished the labeling of the M_r 90,000 band. In contrast, the addition of even a 500-fold molar excess of anti-Tac antibody did not abolish the labeling. In some cases, an unknown specific labeling was observed at M_r 57,000, yielding a M_r 42,000 peptide after subtraction of the M_r 15,000 of IL-2.

Proliferative Response of LGL Leukemia Cells to IL-2. To determine whether the IL-2 receptor expressed on LGL leukemia cells is a functional IL-2 receptor, we examined the proliferative response of these cells to IL-2. Normal PHA-stimulated blasts that express both high- and low-affinity IL-2 receptors (17) manifested a good proliferative response to IL-2 (Fig. 3A). A maximal response was observed when these cells were incubated with 100 pM IL-2, and 50% of the maximal thymidine incorporation was achieved on addition of 20–60 pM IL-2, consistent with a previous report suggesting that the proliferative response in activated T lymphoblasts is mediated through the interaction of IL-2 with its high-affinity receptors (17). LGL leukemia cells from the two patients examined also manifested a good proliferative response. However, the pattern of the dose-response curve was very different from that with normal PHA lymphoblasts. The LGL leukemic cells required >5 nM IL-2 for a maximal response and 4 nM (patient 1) or 0.6 nM (patient 2) to obtain 50% of the maximal response, suggesting that the IL-2 response of these cells is not mediated through the multichain high-affinity IL-2 receptor. Next, we examined the effect on IL-2-induced proliferation of the addition of anti-Tac antibody that blocks IL-2 binding to the p55 Tac peptide. The IL-2 concentrations chosen for these studies were those required for 50% of the maximal response, and a 500-fold molar excess of anti-Tac antibody was added. The IL-2-induced proliferation of LGL leukemia cells was not inhibited by anti-Tac (Fig. 3B, patients 1 and 2), whereas there was a 90% inhibition of thymidine uptake for normal PHA-stimulated lymphoblasts, suggesting that the p55 Tac peptide was not involved in the IL-2-induced proliferation of LGL leu-

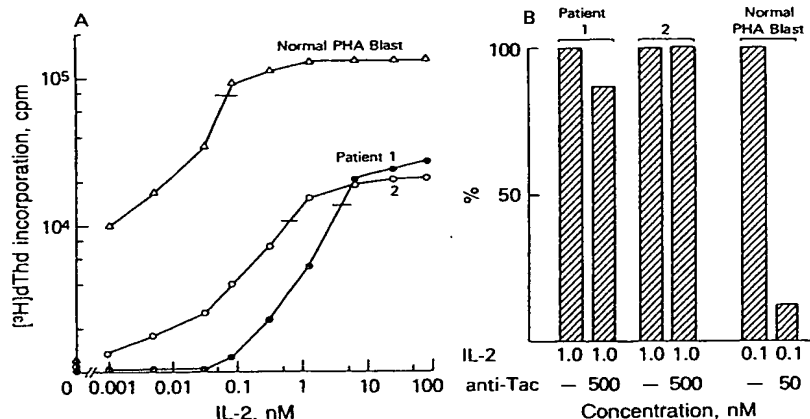


FIG. 3. (A) Proliferative response to IL-2 of normal PHA-activated lymphoblasts and type A LGL leukemia cells from two patients. Cells (1×10^5 per well) were cultured in triplicate with 1:4 dilution series of IL-2 for 72 hr, and ^3H thymidine incorporation was measured for the last 6 hr. (B) Inhibition by anti-Tac antibody of the proliferative response to IL-2. The concentrations of IL-2 were chosen so that a half-maximal response was achieved. Cells (1×10^5 per well) were cultured with IL-2 in the indicated concentrations in the absence or presence of 500-fold molar excess of anti-Tac antibody for 72 hr. One hundred percent ^3H thymidine incorporations for patients 1 and 2 and for normal PHA-stimulated blasts (average of three donors) were 6394 ± 457 cpm, $10,153 \pm 565$ cpm, and $58,435 \pm 1589$ cpm, respectively (mean \pm SEM).

kemia cells in our short-term cultures and that the p75 peptide alone can mediate the IL-2 proliferative signal in such cells.

IL-2 Augments Transcription of the Tac Gene and Induces the Tac Peptide on LGL. IL-2 has been reported to up-regulate the expression of the Tac peptide on a number of cell types (23–25). To investigate the possibility that IL-2 can up-regulate the expression of the Tac peptide on LGL leukemia cells, such cells were cultured with IL-2 for 3 days in the presence or absence of the anti-Tac antibody. After 3-day cultures, the cells were washed with 10 mM citrate buffer, pH 4.0/0.14 M NaCl to remove IL-2 and antibody bound to cells and were stained with the anti-Tac antibody and examined by flow cytometry. In the two cases tested, the proportion of Tac-positive cells increased when cultured with IL-2 (Table 1). This up-regulation of Tac peptide expression was not prevented by the addition of the anti-Tac antibody, and, interestingly, seemed to be enhanced. These data suggest that, even with Tac-negative cells, IL-2 is able to induce Tac peptide expression on certain LGL. To extend these studies of the IL-2-induced up-regulation of the Tac peptide, total RNA was isolated from LGL leukemia cells after stimulation with IL-2 for 24 hr and was subjected to RNA blotting analysis with a cDNA probe for the Tac peptide (Fig. 4). Tac mRNA was induced by IL-2 stimulation of LGL leukemia cells, whereas fresh leukemia cells or cells cultured with medium alone did not express the Tac mRNA. Furthermore, the addition of the anti-Tac antibody together with IL-2 enhanced the Tac mRNA expression, when compared to that of cells cultured with IL-2 alone, consistent with the enhanced cell surface expression of the Tac peptide described above.

These data support the conclusion that the interaction of IL-2 with the p75 peptide alone is a sufficient signal for the up-regulation of transcription of mRNA and expression of the IL-2 receptor peptide identified by the anti-Tac antibody.

DISCUSSION

The high-affinity IL-2 receptor on T cells appears to be a multichain receptor complex with at least two IL-2 binding peptides, the p55 Tac and the p75 peptide (20–22). Each peptide by itself can bind IL-2 with a low affinity, whereas high-affinity receptors are expressed when both peptides are present and associated in a receptor complex. In the case of normal PHA-activated lymphoblasts or with human T-cell lymphotropic virus type I-associated T-cell lines such as HUT 102, the number of high-affinity receptors seems to be restricted by the number of p75 peptides available to associate with the 10- to 50-fold more numerous Tac peptides.

In the present study, using cross-linking methodology, we defined the IL-2 binding peptide composition of LGL leukemia cells as well as freshly prepared peripheral blood LGL that are associated with NK and LAK activity. Unfractionated lymphocytes and midfraction (mainly T cells) from a Percoll sedimentation technique expressed both the p55 and p75 peptides faintly but distinctly, although the quantity of Tac peptides expressed was much less than that on PHA-activated lymphoblasts. In contrast, the LGL population obtained from normal peripheral blood expressed the p75 peptide alone. That is, this population expressed an IL-2

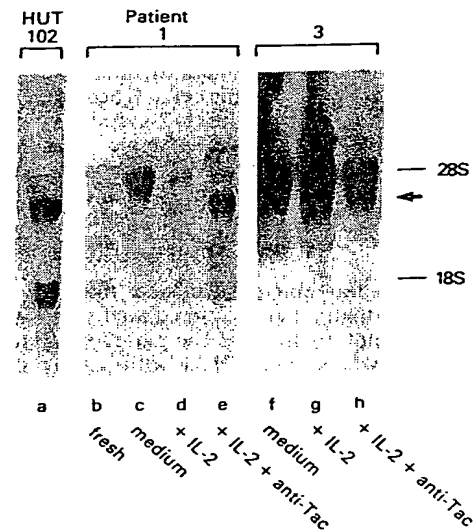


FIG. 4. IL-2-induced Tac mRNA expression on LGL leukemia cells. LGL leukemia cells studied were freshly obtained prior to culture or cultured with medium alone (lanes c and f), 5 nM IL-2 (lanes d and g), or 5 nM IL-2 plus a 100-fold molar excess of anti-Tac antibody (lanes e and h) for 24 hr. Then, total RNA was extracted and analyzed by RNA transfer blots. In lane a, HUT 102 was used as a positive control. The mRNA for the patients encoding the Tac peptide migrated in the band (3.5 kb) indicated by the arrow on the right. The upper bands observed represent nonspecific binding to 28S ribosomal RNA in these non-poly(A)-selected preparations.

receptor that was not recognized by the anti-Tac monoclonal antibody. Furthermore, all eight cases of LGL leukemia examined manifested the p75 peptide but did not manifest the Tac peptide. The low-affinity Tac peptide with a 13-amino acid cytoplasmic tail, when expressed alone, is not sufficient to mediate a functional IL-2 signal (28). In the present study we defined whether the p75 peptide, when expressed alone on LGL leukemia cells, is an effective functional IL-2 receptor. We took advantage of p75-expressing, Tac-non-expressing LGL leukemia cells to demonstrate that these cells proliferated in response to IL-2 and that this proliferation was not inhibited by even a 500-fold molar excess of anti-Tac antibody. PHA-activated blasts appear to respond to IL-2 through high-affinity receptors, since fmol-to-pmol quantities of IL-2 were sufficient for proliferation (Fig. 3). In contrast to such PHA-activated lymphoblasts, LGL leukemia cells required 10- to 80-fold more IL-2 to induce proliferation. Thus, it appears that the proliferative signal of IL-2 was not mediated through high-affinity receptors in our short-term cultures of LGL leukemia cells.

Several investigators have reported findings regarding the IL-2-induced augmentation of NK activity that were difficult to explain when only the Tac peptide was considered. Trinchieri *et al.* (12) reported a dose-dependent enhancement of NK activity in peripheral blood lymphocytes cultured for 18 hr in the presence of IL-2 at >20 ng/ml (i.e., >1.3 nM). This IL-2 concentration was 10-fold greater than that required for half-optimal proliferation of CTLL cells in a standardized assay. Furthermore, anti-Tac did not inhibit the IL-2-mediated enhancement of NK activity. Similarly, using NK-enriched populations, Ortaldo *et al.* (13) and Lanier *et al.* (15) reported NK activation by a high dose of IL-2 that was not inhibited by addition of the anti-Tac antibody. In addition, Phillips and Lanier (26) have shown that the majority of LAK activity is mediated by NK cells that express the NKH-1 (Leu-19) antigen and that high doses of IL-2 (>500 units per ml) are required for the optimal generation of

Table 1. Induction of Tac antigen on LGL leukemia cells by IL-2

Culture	Tac-positive cells, % of cultured cells	
	Patient 1	Patient 3
Medium alone	3	<1
With IL-2	14	45
With IL-2/anti-Tac	32	46

cytotoxicity. These phenomena cannot be explained simply by the view that IL-2 mediates its biological effects only through high-affinity receptors that include the Tac peptide (17). In the case of LGL leukemia cells, Koizumi *et al.* (9) and Chan *et al.* (11) demonstrated the IL-2-induced augmentation of NK activity of Tac-negative leukemic cells. Moreover, Pistoia *et al.* (31) have reported the establishment of Tac-negative IL-2-dependent cytotoxic cell lines from patients with LGL leukemia, although they speculated that the undetectable level of the Tac antigen is attributable to cell growth.

Supported by the above-mentioned findings, our data strongly suggest that: (i) an IL-2-mediated signaling process exists that does not involve the Tac peptide; and (ii) the p75 peptide alone, which binds IL-2 with a low affinity, is responsible for this Tac peptide-independent signal transduction. It is possible that the IL-2 signal is mediated only through multichain high-affinity receptors when activated T cells that manifest both Tac and p75 peptides are considered. However, this is not the case for normal or leukemic LGL.

One of the major findings in the present study concerns the up-regulation of the Tac peptide by IL-2 on LGL leukemia cells. As shown in Table 1 and Fig. 4, we demonstrated, both at the protein level and at the mRNA level, that the Tac peptide was newly expressed by the initially Tac-negative LGL leukemia cells following the stimulation with IL-2. Reem and Yeh (23), using dexamethasone to block IL-2 secretion, suggested that IL-2 receptor expression on activated T cells is itself positively influenced by IL-2. Similarly, we demonstrated that the addition of IL-2 to a cloned IL-2 receptor-expressing normal B-cell line led to the induction of an increased number of receptors identified by anti-Tac (24). Furthermore, Depper *et al.* (25), taking advantage of the physiological decline in IL-2 receptor expression in lectin-activated lymphocytes, have suggested that IL-2 augments transcription of the IL-2 receptor (Tac) gene through high-affinity receptors because this phenomenon was mediated by concentrations of IL-2 sufficient to saturate only the high-affinity receptors. However, in these systems cells already expressing the Tac peptide and also high-affinity receptors were examined. The pattern of expression in the two cases of LGL leukemia we examined was quite different. Without involvement of the Tac peptide, it appears that IL-2 can provide the Tac-inducing signal through the p75 peptide. Once the Tac peptide is expressed, it may become noncovalently associated with the p75 peptide and thus generate the high-affinity receptor enabling these LGL to respond to low concentrations of IL-2. It is possible that, after this stage of activation and induction of the Tac peptide, the effect of low concentrations of IL-2 may be inhibited by the anti-Tac antibody.

The observation in the present report that most T-cell functions require both the Tac and p75 peptides, whereas the initial activation of LAK and NK functions of LGL require only the p75 peptide for interaction with IL-2, has potential implications for LAK cell therapy that depend on the cells or molecules required for effective therapy and those that cause toxicity (32). If the effective therapy is mediated by the LAK cells and some of the toxicity is mediated by interaction of IL-2 with T cells, then insights concerning different peptide receptors for IL-2 used by T cells and LAK cells suggest new therapeutic approaches for the LAK therapy of patients with cancer. One approach would be to use molecular engineering to generate altered IL-2 molecules that would retain those epitopes required for binding and signaling through the p75 peptide but no longer retain those elements of the molecule required for binding to the Tac peptide. Such engineered IL-2-related molecules might retain their capability to initiate activation of LGL into the LAK effectors without simulta-

neously activating T lymphocytes through the high-affinity receptor.

In summary, LGL from normal individuals as well as leukemic LGL express the p75 IL-2 binding peptide but do not express the Tac peptide. The interaction of IL-2 with these LGL that manifest the p75 IL-2 binding peptide alone provides a sufficient signal for the proliferation of these cells and for the induction of expression of the Tac peptide. Thus, the p75 IL-2 binding peptide may play an important role in the IL-2-mediated immune response not only by participating in the formation of the high-affinity receptor in cooperation with the Tac peptide but also by contributing to the initial triggering of LGL activation.

We thank the Celus Corp. (Emeryville, CA) for providing human recombinant IL-2.

1. Saksela, E., Timonen, T., Ranki, A. & Hayry, P. (1979) *Immunol. Rev.* 44, 71-123.
2. Timonen, T., Ortaldo, J. R. & Herberman, R. B. (1981) *J. Exp. Med.* 153, 569-582.
3. Grossi, C. E., Cadoni, A., Zicca, A., Leprini, A. & Ferrarini, M. (1982) *Blood* 59, 277-283.
4. Trinchieri, G. & Perussia, B. (1984) *Lab. Invest.* 50, 489-513.
5. Ortaldo, J. R., Sharrow, S. O., Timonen, T. & Herberman, R. B. (1981) *J. Immunol.* 127, 2401-2409.
6. Lanier, L. L., Le, A. M., Phillips, J. H., Warner, N. L. & Babcock, G. F. (1983) *J. Immunol.* 131, 1789-1796.
7. Hooks, J. J., Haynes, B. F., Detrick-Hooks, B., Diehl, L. F., Gerrard, T. L. & Fauci, A. S. (1982) *Blood* 59, 198-201.
8. Reynolds, C. W. & Foon, K. A. (1984) *Blood* 64, 1146-1158.
9. Koizumi, S., Seki, H., Tachinami, M., Taniguchi, M., Matsuda, A., Taga, K., Nakarai, T., Kato, E., Taniguchi, N. & Nakamura, H. (1986) *Blood* 68, 1065-1073.
10. Pistoia, V., Prasthofer, E. F., Tilden, A. B., Barton, J. C., Ferrarini, M., Grossi, C. E. & Zuckerman, K. (1986) *Blood* 68, 1095-1100.
11. Chan, W. C., Link, S., Mawle, A., Check, I., Brynes, R. K. & Winton, E. F. (1986) *Blood* 68, 1142-1153.
12. Trinchieri, G., Matsumoto-Kobayashi, M., Clark, S. C., Seehra, J., London, L. & Perussia, B. (1984) *J. Exp. Med.* 160, 1147-1169.
13. Ortaldo, J. R., Mason, A. T., Gerard, J. P., Henderson, L. E., Farrer, W., Hopkins, W. F., Herberman, R. B. & Rabin, H. (1984) *J. Immunol.* 133, 779-783.
14. Ito, K., Tilden, A. B., Kumagai, K. & Balch, C. M. (1985) *J. Immunol.* 134, 802-807.
15. Lanier, L. L., Benike, C. J., Phillips, J. H. & Engleman, E. G. (1985) *J. Immunol.* 134, 794-801.
16. Grimm, E. A. & Rosenberg, S. A. (1984) in *Lymphokines* eds. Pick, E. & Landy, M. (Academic, New York), Vol. 9, pp. 279-311.
17. Robb, R. J., Greene, W. C. & Rusk, C. M. (1984) *J. Exp. Med.* 160, 1126-1146.
18. Uchiyama, T., Broder, S. & Waldmann, T. A. (1981) *J. Immunol.* 126, 1393-1397.
19. Waldmann, T. A. (1986) *Science* 232, 727-732.
20. Tsudo, M., Kozak, R. W., Goldman, C. K. & Waldmann, T. A. (1986) *Proc. Natl. Acad. Sci. USA* 83, 9694-9698.
21. Tsudo, M., Kozak, R. W., Goldman, C. K. & Waldmann, T. A. (1987) *Proc. Natl. Acad. Sci. USA* 84, 4215-4218.
22. Sharon, M., Klausner, R. D., Cullen, B. R., Chizzonite, R. & Leonard, W. J. (1986) *Science* 234, 859-863.
23. Reem, G. & Yeh, N. H. (1984) *Science* 225, 429-430.
24. Waldmann, T. A., Goldman, C. K., Robb, R. J., Depper, J. M., Leonard, W. J., Sharrow, S. O., Bongiovanni, K. F., Korsmeyer, S. J. & Greene, W. C. (1984) *J. Exp. Med.* 160, 1450-1466.
25. Depper, J. M., Leonard, W. J., Drogula, C., Kronke, M., Waldmann, T. A. & Greene, W. C. (1985) *Proc. Natl. Acad. Sci. USA* 82, 4230-4234.
26. Phillips, J. H. & Lanier, L. L. (1986) *J. Exp. Med.* 164, 814-825.
27. Wang, A., Lu, S. D. & Mark, D. (1984) *Science* 224, 1431-1433.
28. Leonard, W. J., Depper, J. M., Crabtree, G. R., Rudikoff, S. R., Pumphrey, J., Robb, R. J., Kronke, M., Svetlik, P. B., Pfeffer, N. J., Waldmann, T. A. & Greene, W. C. (1984) *Nature (London)* 311, 626-631.
29. Chirgwin, J. M., Przybyla, A. E., MacDonald, R. J. & Rutter, W. J. (1979) *Biochemistry* 18, 5294-5299.
30. Taniguchi, T., Matsui, H., Fujita, T., Takaoka, C., Kashima, N., Yoshimoto, R. & Hamuro, J. (1983) *Nature (London)* 302, 305-310.
31. Pistoia, V., Caroll, A. J., Prasthofer, E. F., Tilden, B., Zuckerman, K. S., Ferrarini, M. & Grossi, C. E. (1986) *J. Clin. Immunol.* 6, 457-466.
32. Rosenberg, S. A., Lotze, M. T., Muul, L. M., Leitman, S., Chang, A. E., Ettinghausen, S. E., Matory, Y. L., Skibber, J. M., Shiloni, E., Vetto, J. T., Seipp, C. A., Simpson, C. & Reichert, C. M. (1985) *N. Engl. J. Med.* 313, 1485-1492.

Demonstration of a non-Tac peptide that binds interleukin 2: A potential participant in a multichain interleukin 2 receptor complex

MITSURU TSUDO, ROBERT W. KOZAK, CAROLYN K. GOLDMAN, AND THOMAS A. WALDMANN

Metabolism Branch, National Cancer Institute, National Institutes of Health, Bethesda, MD 20892

Contributed by Thomas A. Waldmann, September 10, 1986

ABSTRACT The interleukin 2 (IL-2) receptor system plays a key role in the T-cell immune response. Although IL-2 binding was reported to be restricted to the Tac peptide, we have identified an IL-2 binding peptide that does not react with anti-human IL-2 receptor monoclonal antibodies, including anti-Tac on MLA 144, a gibbon ape T-cell line. The MLA 144 cell line expressed 6800 IL-2 binding sites per cell with a low ($K_d = 14$ nM) affinity for human recombinant IL-2. Using cross-linking methodology, we demonstrated that the IL-2 binding peptide on MLA 144 is larger (M_r 75,000) than the Tac peptide, which has a M_r of 55,000. An IL-2 binding peptide of similar size (M_r 75,000) was also identified in addition to the Tac peptide (M_r 54,000-57,000) on Hut 102, a human T-cell lymphotropic virus I-induced T-cell leukemia line, and phytohemagglutinin-activated normal human and gibbon ape lymphoblasts. Anti-Tac antibody did not block the binding of 125 I-labeled IL-2 to MLA 144 cells. However, this antibody abolished the binding of 125 I-labeled IL-2 not only to the Tac peptide on Hut 102 cells and normal lymphoblasts but also to the M_r 75,000 IL-2 binding peptide, suggesting that this latter peptide is associated with the Tac peptide to form the high-affinity IL-2 receptor complex.

T lymphocytes stimulated with antigen or mitogen produce interleukin 2 (IL-2) (1). T-cell growth is dependent on the interaction of IL-2 with high-affinity IL-2 receptors, which are not present on resting cells but are induced and expressed on T cells following activation (2). Analysis of the structure and function of the human IL-2 receptor was greatly facilitated by the production of a monoclonal antibody, designated anti-Tac, that identifies the IL-2 receptor (3, 4). The anti-Tac antibody blocks the binding of radiolabeled IL-2 to activated T cells (5) and IL-2 at high concentrations blocks the binding of 3 H-labeled anti-Tac to activated T cells (6). Furthermore, passage of radiolabeled proteins from phytohemagglutinin (PHA)-activated lymphoblasts through either an IL-2-coupled Affi-Gel or anti-Tac-coupled Sepharose column effectively removed molecules reactive with the alternative support (7). Finally, three groups (8-10) showed that cDNAs encoding the Tac peptide directed the synthesis of an IL-2 binding peptide in eukaryotic cells. These studies support the view that the Tac peptide contains an IL-2 binding site and that the ability to bind IL-2 is limited to the Tac peptide. However, this view presents a series of questions that have not been resolved. First, radiolabeled binding studies indicate that there are high (10^{-12} M in K_d) and low (10^{-8} M)-affinity receptors that are recognized by the same anti-Tac antibody (11). What is the structural basis for this great difference in affinity ($>10^3$ in K_d)? Furthermore, the deduced amino acids from the IL-2 receptor cDNAs indicated that the intracytoplasmic domain of the Tac peptide has only 13 amino acids, too small for enzymatic activity (8-10). How then does this short chain transduce a signal to the nucleus?

EL-4, a mouse thymoma line, or CTLL-2, a mouse cytotoxic cell line transfected with Tac cDNAs, expressed human high-affinity receptors (12, 13), whereas mouse L cells or fibroblast line transfectants expressed only low-affinity receptors (14). Why does the Tac cDNA show cell-type-specific reconstitution of the high-affinity IL-2 receptor? Finally, how can certain Tac-negative cells (e.g., natural killer cells or precursors of lymphokine-activated killer cells) make nonproliferative responses to IL-2 (15, 16)? These questions led us to consider the possibility that the IL-2 receptor was not a single peptide but rather a receptor complex that includes the Tac peptide as well as an unidentified non-Tac peptide. In the present study, we have identified a non-Tac IL-2 binding peptide that has a M_r of 75,000 (p75), which is larger than the M_r 55,000 Tac peptide (5, 17) on MLA 144, a gibbon ape T-cell line (18). An IL-2 binding peptide similar in size (M_r 75,000) has also been identified on Hut 102, a human T-cell lymphotropic virus I-induced T-cell leukemia line, and on PHA-activated normal lymphoblasts.

MATERIALS AND METHODS

Cells. Hut 102 and MLA 144 cells were maintained in RPMI 1640 medium containing 10% fetal calf serum. Lymphoblasts were generated from human and gibbon ape peripheral blood mononuclear cells isolated by Ficoll-Paque (Pharmacia) by culturing the cells (2×10^6 per ml in RPMI 1640 medium containing 10% fetal calf serum) with 0.1% PHA-P (Difco) for 2 or 3 days.

IL-2 Binding Assay. The binding of radioiodinated IL-2 to cells was measured according to the methods described by Robb *et al.* (11) with a slight modification. 125 I-labeled human recombinant IL-2 was purchased from New England Nuclear [NEX 229, specific activity: 28.6-44.4 μ Ci/ μ g (1 Ci = 37 GBq)]. For the detection of low-affinity receptors, recombinant unlabeled IL-2 (Cetus, Emeryville, CA) was combined with iodinated IL-2 to obtain a final concentration of 50 nM, resulting in a final specific activity of 2.9-4.4 μ Ci/ μ g. To remove endogenous IL-2 prior to the binding assay, MLA 144 cells were incubated for 20 s in 10 mM sodium citrate, pH 4.0/0.14 M NaCl followed by centrifugation for 15 s at $10,000 \times g$. After the washing, cells ($1-2.5 \times 10^6$) were incubated with serial dilutions of 125 I-labeled IL-2 for 1 hr at 4°C in a total volume of 100 μ l of RPMI 1640 medium containing 10% fetal calf serum and 25 mM Hepes (pH 7.3). Then, cells were centrifuged for 15 s at $10,000 \times g$ and resuspended in 100 μ l of the same medium. The cell suspension was centrifuged through a 150- μ l layer of a mixture of 20% olive oil/80% di-*n*-butyl phthalate (Sigma) for 2 min at $10,000 \times g$. The tips of the tubes containing the cell pellets were cut off and the radioactivity was measured in a γ -counter. Nonspecific binding was determined in the presence of a 200-fold excess of unlabeled IL-2. Specific binding was obtained by subtracting nonspecific binding from total binding.

Abbreviations: IL-2, interleukin 2; PHA, phytohemagglutinin.

Flow Cytometry. After the acid treatment described above, cells (1×10^6) were incubated with saturating amounts of monoclonal antibodies for 30 min at 4°C. A negative control was incubated with normal mouse serum (1:300). Then, cells were washed twice with phosphate-buffered saline (PBS) containing 3% fetal calf serum and 0.05% sodium azide followed by incubation with saturating amounts of fluorescein isothiocyanate-conjugated goat anti-mouse Ig (Coulter) for 30 min at 4°C. After washing twice, cells were analyzed by a FACS analyzer (Becton Dickinson).

Cross-Linking Study. 125 I-labeled IL-2 was chemically cross-linked with cell membranes or intact cells as described (19, 20) with minor modifications. Cell membranes were isolated according to the methods described by August *et al.* (21). Briefly, cells ($1-4 \times 10^8$) were suspended in 10 ml of 0.25 M sucrose/10 mM Tris, pH 7.4, containing 0.2 mM MgCl_2 , 0.2 mM CaCl_2 , 1 mM phenylmethylsulfonyl fluoride, and 1 μ g of antipain per ml. The suspension was homogenized with a Brinkmann Polytron for 2 min at setting 7. After centrifugation at $600 \times g$ for 10 min, the supernatant was centrifuged at $12,000 \times g$ for 30 min. The $12,000 \times g$ supernatant was adjusted to 0.1 M NaCl and centrifuged at $100,000 \times g$ for 90 min at 4°C. The $100,000 \times g$ pellet was suspended in PBS, stored in aliquots at -70°C , and used as the membrane fraction. Membranes (0.1–0.5 mg) were incubated for 1 hr at 4°C with 5 nM 125 I-labeled IL-2 and unlabeled proteins as indicated in a total volume of 100 μ l of PBS containing 10% fetal calf serum and 25 mM Hepes (pH 7.3). The incubation mixtures were centrifuged at $10,000 \times g$ for 4 min. The pellets were resuspended in 100 μ l of PBS and centrifuged at $10,000 \times g$ for 6 min through a 1-ml layer of 2.5% sucrose in PBS. The pellets were suspended in 250 μ l of PBS, and 25 mM disuccinimidyl suberate (Pierce) in dimethyl sulfoxide was added to a final concentration of 0.5 mM. After the incubation at room temperature for 15 min, the reaction was quenched by adding 750 μ l of 10 mM Tris, pH 7.4/1 mM EDTA/0.14 M NaCl. After 5 min, membranes were pelleted by centrifugation at $10,000 \times g$ for 4 min. The pellets were solubilized with 50 μ l of NaDodSO₄ sample buffer (6.25 mM Tris, pH 6.8/10% glycerol/1% NaDodSO₄) containing 5% 2-mercaptoethanol, boiled for 5 min, and subjected to NaDodSO₄/polyacrylamide gel electrophoresis (PAGE) using a 7.5% acrylamide gel. Autoradiograms were obtained from the dried gels after exposure for 1–4 days. For cross-linking to intact cells, cells ($2-5 \times 10^6$) were incubated for 1 hr at 4°C with 5 nM 125 I-labeled IL-2 in a total volume of 200 μ l of RPMI 1640 medium containing 10% fetal calf serum and 25 mM Hepes (pH 7.3). After centrifugation ($10,000 \times g$, 1 min) through 10% sucrose in PBS, cross-linking was carried out as described above. Cells were solubilized with 50 μ l of PBS containing 1% Triton X-100 and 1 mM phenylmethylsulfonyl fluoride. After the centrifugation ($10,000 \times g$, 5 min), the supernatants were mixed with the same volume of 2 \times concentrated NaDodSO₄ sample buffer containing 10% 2-mercaptoethanol.

Immunoprecipitation. After the cross-linking of 125 I-labeled IL-2, Hut 102 membranes were solubilized with 1% Triton X-100/PBS and immunoprecipitated as described (6) with anti-Tac or 7G7/B6 monoclonal antibody. Anti-Tac and 7G7/B6 were purified by protein A-Sepharose (Pharmacia) from hybridoma ascites fluid. Control UPC 10 (mouse IgG2a) was purchased from Sigma.

RESULTS

MLA 144, a cell line originally established from a gibbon ape with a spontaneous lymphosarcoma, is a constitutive producer of IL-2 (18, 22, 23). As described (2, 24), MLA 144 expresses IL-2 receptors as assessed by binding of human biosynthetically labeled IL-2. To confirm this finding, we

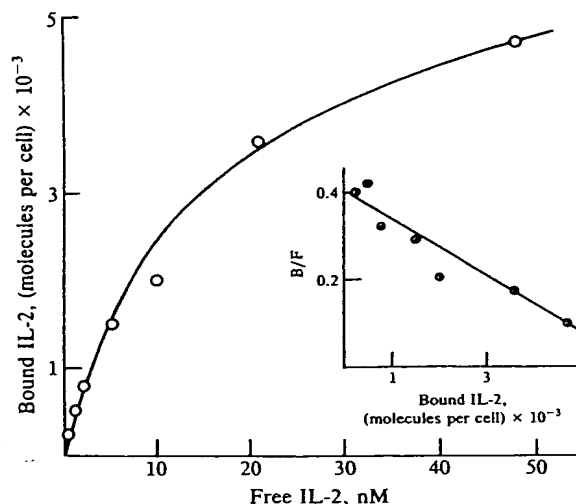


FIG. 1. Binding of 125 I-labeled IL-2 to MLA 144. (Inset) Scatchard transformation of data. B/F, bound/free. The calculated number of binding sites was 6100 per cell and the $K_d = 1.5 \times 10^{-8}$ M in this particular experiment.

performed an 125 I-labeled recombinant IL-2 binding assay. A representative binding curve and Scatchard analysis is shown in Fig. 1. The linear feature of the Scatchard plots obtained supports the view that MLA 144 expresses only low-affinity receptors with a K_d of 14 ± 3 nM ($n = 5$). The receptor number was 6800 ± 2200 per cell (mean \pm SEM). Furthermore, no high-affinity receptors were detected using high-affinity conditions (low concentrations of IL-2). In contrast, Hut 102, a human T-cell leukemia virus 1-induced T-cell leukemia line, expressed $17,900 \pm 2400$ high- and $454,000 \pm 109,000$ low-affinity receptors per cell with K_d values of 57 ± 21 pM ($n = 4$) and 37 ± 14 nM ($n = 4$), respectively (data not shown).

Since MLA 144 is a primate T-cell line, we determined whether this cell line was reactive with monoclonal antibodies to the human IL-2 receptor, which are known to react with the non-human primate IL-2 receptor as well. As shown in Table 1, MLA 144 expressed the Leu-1 antigen (pan T cell) and the transferrin receptor. However, it was not reactive with anti-Tac or with 7G7/B6, a monoclonal antibody that binds to the same M_r 55,000 peptide (p55) as anti-Tac but to a distinct epitope not involved in IL-2 binding (25). In addition, two other commercially available monoclonal antibodies to the human IL-2 receptor (anti-IL-2R, Coulter and Becton Dickinson) failed to react with MLA 144. To clarify whether the absence of the Tac antigen on MLA 144 cells is simply due to the difference in species or, instead, whether gibbon ape lymphocytes have the capacity to synthesize the Tac antigen, we cultured normal peripheral blood lymphocytes from gibbon apes with PHA for 2 days and tested their reactivity with anti-Tac. As shown in Table 2, gibbon ape

Table 1. Flow cytometric analysis of antigens on MLA 144

Antibody	Positive cells, %
Leu-1	47
Leu-2a	7
Leu-3a	0
Anti-transferrin receptor	96
Anti-Tac	0
7G7/B6	0
Anti-IL-2R	
Coulter	0
Becton Dickinson	0

Table 2. Expression of Tac antigen on gibbon ape lymphocytes activated with PHA

Animal	Tac-positive cells, %	
	Medium alone	PHA
1	8	61
2	8	49
3	11	75

Tac-positive cells were cultured with medium alone or with PHA.

PHA blasts strongly expressed the Tac antigen. This suggested that the IL-2 binding peptide of MLA 144 is different from the Tac peptide.

Cross-linking studies were performed to define the size of the surface molecule on MLA 144 cells responsible for IL-2 binding. As shown in Fig. 2 (lanes k-o), when 125 I-labeled IL-2 (5 nM) was incubated with MLA 144 plasma membranes, covalently cross-linked with 0.5 mM disuccinimidyl suberate, and analyzed by NaDodSO₄/PAGE under reducing conditions, a labeled band with a M_r of 90,000 was observed. This binding was shown to be specific by the finding that 200-fold excess unlabeled IL-2 present during the incubation completely abolished the band (lane l). As expected from the results of flow cytometric analysis, the addition of anti-Tac (lane m), 7G7/B6 (lane n), or a control mouse IgG2a, UPC 10 (lane o), did not affect the labeling. Since the M_r of IL-2 is 15,000 (26), the calculated M_r of the IL-2 binding peptide on MLA 144 membranes is 75,000, much larger than the Tac peptide (M_r 55,000) (6, 17).

Since it is well known that IL-2 receptors as well as the Tac antigen are abundantly expressed on human PHA blasts and Hut 102 (11), we performed cross-linking studies using membrane fractions of Hut 102 and PHA blasts. As shown in Fig. 2, the labeling of two bands was observed in both cases (lanes a and f). A more heavily labeled lower band migrated at M_r 69,000 for Hut 102 and M_r 72,000 for PHA blasts. The calculated size of these IL-2 binding peptides (M_r 54,000 and 57,000, respectively) after subtracting the molecular weight of IL-2 (M_r 15,000) is in good agreement with the reported molecular weight of the Tac peptide (6, 17). Indeed, these

lower bands were clearly abolished by the addition of anti-Tac during the incubation with 125 I-labeled IL-2 (lanes c and h). Of interest, an IL-2 binding peptide similar in size to that of MLA 144 was also identified in these cells. Upper and lower bands appear specific for IL-2, since excess unlabeled IL-2 abolished the labeling (lanes b and g). Surprisingly, the radioactivity reflecting binding to the upper species was greatly reduced by anti-Tac (lanes c and h). It is unlikely that the upper species possesses the Tac epitope, since anti-Tac did not immunoprecipitate the M_r 75,000 protein (6, 17). Thus, it is conceivable that this non-Tac IL-2 binding peptide is closely associated with the Tac peptide and that its IL-2 binding site in these complexes is sterically hidden by anti-Tac. As expected, these two bands were not affected by 7G7/B6 or the control UPC 10.

To confirm that the Tac peptide contributes to form the lower band but not the upper band, the following experiments were performed. After cross-linking 125 I-labeled IL-2 with Hut 102 membranes, Triton X-100-solubilized materials were immunoprecipitated with anti-Tac or the 7G7/B6 antibody. As shown in Fig. 3, anti-Tac did not precipitate any radioactivity (lane c), consistent with the findings (6) that IL-2 blocks the binding of anti-Tac. The eluate from 7G7/B6 showed only a M_r 70,000 band (lane e), indicating that the M_r 90,000 band does not contain the 7G7/B6 epitope, a non-IL-2 binding epitope of the Tac peptide.

Cross-linking studies using gibbon ape PHA lymphoblasts were performed to determine whether normal gibbon ape lymphoblasts express two species of IL-2 binding peptides. In this case, intact cells were incubated with 125 I-labeled IL-2 and subjected to cross-linking. As shown in Fig. 4, the results were quite similar to those of human PHA blasts—that is, M_r 90,000 and 70,000 bands were observed and were sensitive to inhibition by unlabeled IL-2 and anti-Tac.

DISCUSSION

In the present study, we have reported a previously unidentified peptide that binds IL-2. The absence of the distinct antigens identified by anti-Tac or 7G7/B6 on this molecule is not explained by the difference in species, since gibbon ape

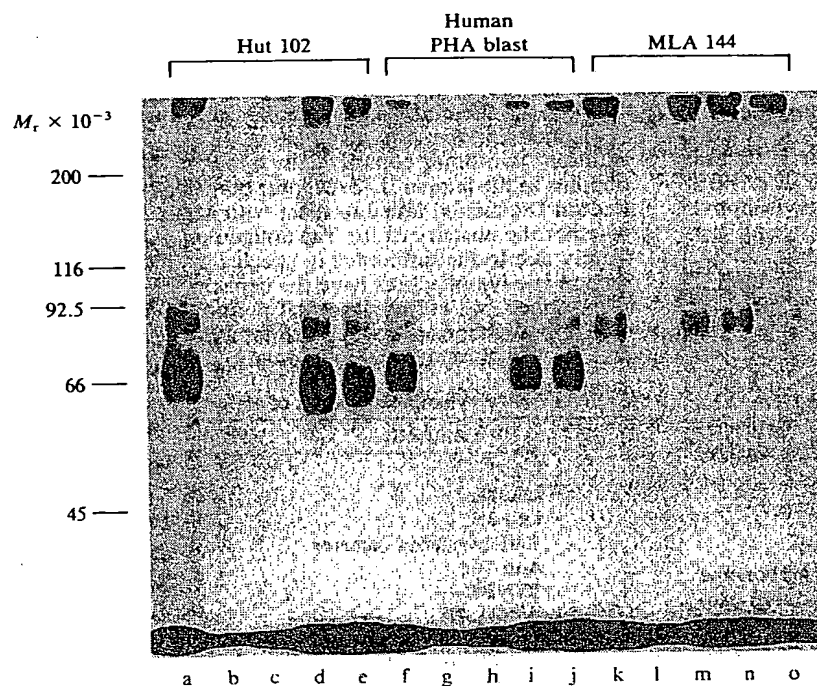


FIG. 2. Autoradiogram showing 125 I-labeled IL-2 receptor complexes produced by chemical cross-linking 125 I-labeled IL-2 to the plasma membranes of Hut 102, human PHA lymphoblasts, and MLA 144. Membranes were incubated with 125 I-labeled IL-2 in the absence (lanes a, f, and k) or presence of a 200-fold excess of unlabeled IL-2 (lanes b, g, and l), 500-fold molar excess of anti-Tac antibody (lanes c, h, and m), 500-fold molar excess of 7G7/B6 antibody (lanes d, i, and n), or 500-fold molar excess of control mouse IgG, UPC 10 (lanes e, j, and o) and then cross-linked, solubilized, and run on NaDodSO₄/PAGE under reducing conditions. Standards were myosin (M_r 200,000), β -galactosidase (M_r 116,000), phosphorylase b (M_r 92,500), bovine serum albumin (M_r 66,000), ovalbumin (M_r 45,000), and carbonic anhydrase (M_r 31,000).

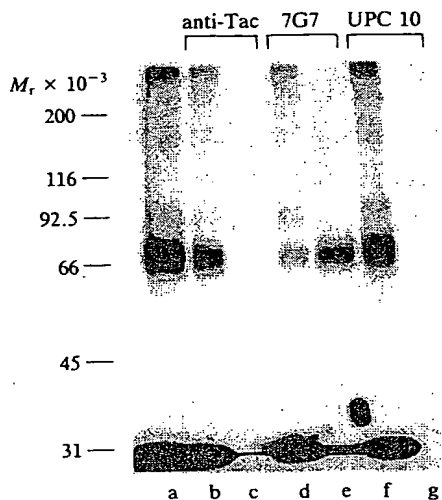


FIG. 3. Autoradiogram showing the immunoprecipitation with anti-Tac, 7G7/B6, and UPC 10. After cross-linking ^{125}I -labeled IL-2 with Hut 102 membranes, solubilized materials were precipitated with antibody-coupled protein A-Sepharose. Lanes: a, no treatment (control); c, e, and g, eluates from the indicated antibody-coupled protein A-Sepharose; b, d, and f, effluents.

lymphocytes can be induced to express the Tac antigen. Furthermore, the molecular weight of this new peptide (M_r 75,000) is much larger than that of the Tac peptide (M_r 55,000), making it unlikely that this peptide is a product of the Tac gene that underwent point mutation. Moreover, no mRNA for the Tac gene was expressed in MLA 144, as assessed by RNA transfer blot analysis (data not shown). Thus, we conclude that the p75 IL-2 binding peptide is a molecule that is completely distinct from the Tac peptide.

Interestingly, an IL-2 binding peptide of similar size was

also identified in Hut 102 and PHA blasts from humans and gibbon apes. Because this upper band of these cells was abolished by the addition of anti-Tac during the incubation with ^{125}I -labeled IL-2, one might consider the possibility that the M_r 90,000 band represents the Tac peptide (M_r 55,000) that bound two IL-2 molecules (M_r 15,000) to make a M_r 90,000 band. Two IL-2 binding sites per Tac peptide could reflect binding to two homologous regions of the peptide encoded by the second and fourth exons of the Tac gene reported by Leonard and coworkers (27). However, our experiments shown in Fig. 3 mitigate against this possibility. Neither anti-Tac nor 7G7/B6 antibody immunoprecipitated the M_r 90,000 protein. If the M_r 90,000 band represented the M_r 55,000 Tac peptide and two bound IL-2 molecules, it should have been precipitated by 7G7/B6, a monoclonal antibody that identifies a non-IL-2 binding epitope of the M_r 55,000 peptide.

Thus, there appear to be at least two peptides that bind IL-2 in Hut 102 cells and normal human and gibbon ape PHA blasts. The lesser radioactivity of the higher molecular weight bands on NaDodSO₄/PAGE suggests that there are fewer p75 IL-2 receptor peptides than Tac peptides. The p75 was not detected in freshly prepared human peripheral blood mononuclear cells, suggesting that this peptide as well as the Tac peptide is induced in the process of activation. The majority of the p75 on the cell surface would appear to be intimately associated with the Tac peptide, since anti-Tac blocks the binding of IL-2 to this peptide (Fig. 2). It is very likely that an IL-2 binding peptide on MLA 144 corresponds to the upper band of gibbon ape PHA blasts. MLA 144 expresses only one type of peptide that binds IL-2 with low affinity.

The structural difference that distinguishes high- from low-affinity IL-2 receptors remains undefined. We favor a multichain model for the high-affinity IL-2 receptor, in which a receptor complex composed of at least the Tac and the p75 peptides forms the high-affinity receptor responsible for ligand internalization and signal transduction. In this model, an independently existing Tac or p75 peptide would therefore represent low-affinity receptors, whereas high-affinity receptors would be expressed when both IL-2 binding peptides are expressed and associated in a receptor complex. In accord with this view, cells bearing the p75 peptide alone (e.g., MLA 144) or the Tac peptide alone (unpublished observation) express only low-affinity receptors, whereas cell lines (e.g., Hut 102) that express both receptor peptides manifest high-affinity receptors as well.

We have examined this model using the observations of Weissman *et al.* (28) and Fujii *et al.* (29), who showed that ^{125}I -labeled IL-2 underwent internalization at 37°C only through binding to high-affinity but not to low-affinity receptors. We examined the effect of ^{125}I -labeled IL-2 internalization on the band pattern of IL-2 binding peptides. After the incubation of Hut 102 or human PHA blasts with ^{125}I -labeled IL-2 at 4°C for 30 min, the cells were incubated at 37°C for another 30 min and subjected to cross-linking. The upper bands of Hut 102 and PHA blasts disappeared with only a modest decrease of the radioactivity of the lower bands (data not shown), suggesting that a higher molecular weight receptor complex that included the p75 that bound ^{125}I -labeled IL-2 was internalized and therefore was not cross-linked with disuccinimidyl suberate.

A number of multichain cell-surface receptors have been defined. The acetylcholine receptor is a well-defined multichain receptor, which is a pentameric membrane protein composed of four subunits: α_2 , β , γ , δ . Mishina *et al.* (30) succeeded in reconstructing the functional acetylcholine receptor by injecting mRNA of the four subunits into *Xenopus* oocytes. They concluded that all subunits were required to elicit a normal nicotinic response to acetylcho-

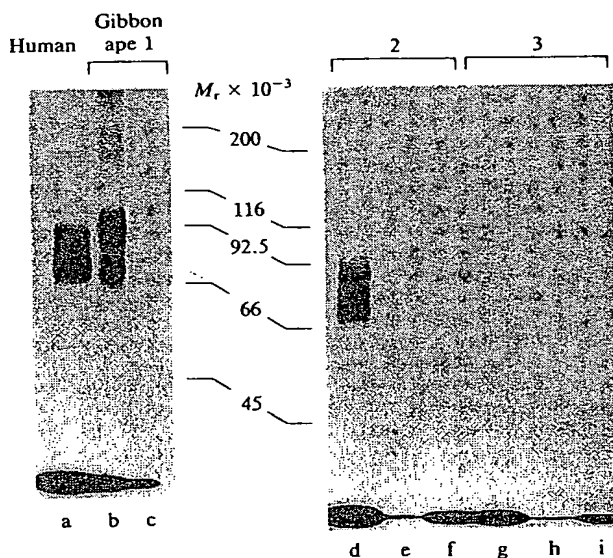


FIG. 4. Autoradiogram showing the ^{125}I -labeled IL-2 receptor complex produced by chemically cross-linking ^{125}I -labeled IL-2 to intact PHA blasts from one human and three gibbon apes. Cells were incubated with ^{125}I -labeled IL-2 in the absence (lanes a, b, d, and g) and presence of a 200-fold excess of unlabeled IL-2 (lanes c, e, and h) or 500-fold molar excess of anti-Tac antibody (lanes f, g, and i) then cross-linked, solubilized, and run on NaDodSO₄/PAGE under reducing conditions.

line, whereas only α -subunits were indispensable for α -bungarotoxin binding activity. Hosang and Shooter (31) reported that the nerve growth factor receptor system of chicken sensory neurons that possess high- and low-affinity receptors exhibited two major labeled bands with M_r 145,000 and 105,000 on cross-linking with ^{125}I -labeled nerve growth factor, whereas non-neuronal cells, which possess only low-affinity receptors, exhibited only the M_r 105,000 component. Although the ligand in many complex receptors binds to only one of the peptides of the complex, immunoglobulins and T-cell antigen receptors represent complex receptors with simultaneous binding of ligand to different distinct chains of the receptor complexes.

Although a M_r 145,000 species consisting of all of the three molecules (the Tac peptide, the non-Tac peptide, and IL-2) has not as yet been identified in cross-linking studies, the multichain model for the high-affinity IL-2 receptor is attractive. Further characterization of the M_r 75,000 IL-2 binding peptide should extend our understanding of the binding of IL-2 to activated T cells.

The IL-2 used was a kind gift of the Cetus Corporation, Emeryville, CA. The gibbon ape blood was obtained from Yerkes Regional Primate Research Center, Emory University, Atlanta, GA. R.W.K. was supported by the ADA Clarence E. Rice Fellowship and by Public Health Service Grant 1F32 CA07974-01 awarded by the National Cancer Institute, Department of Health and Human Services.

1. Smith, K. A. (1980) *Immunol. Rev.* 51, 337-357.
2. Robb, R. J., Munk, A. & Smith, K. A. (1981) *J. Exp. Med.* 154, 1455-1474.
3. Uchiyama, T., Broder, S. & Waldmann, T. A. (1981) *J. Immunol.* 126, 1393-1397.
4. Waldmann, T. A. (1986) *Science* 232, 727-732.
5. Leonard, W. J., Depper, J. M., Uchiyama, T., Smith, K. A., Waldmann, T. A. & Greene, W. C. (1982) *Nature (London)* 300, 267-269.
6. Leonard, W. J., Depper, J. M., Robb, R. J., Waldmann, T. A. & Greene, W. C. (1983) *Proc. Natl. Acad. Sci. USA* 80, 6957-6961.
7. Robb, R. J. & Greene, W. C. (1983) *J. Exp. Med.* 158, 1332-1337.
8. Leonard, W. J., Depper, J. M., Crabtree, G. R., Rudikoff, S., Pumphrey, J., Robb, R. J., Krönke, M., Svetlik, P. B., Pfeffer, N. J., Waldmann, T. A. & Greene, W. C. (1984) *Nature (London)* 311, 626-631.
9. Nikaido, T., Shimizu, A., Ishida, N., Sabe, H., Teshigawara, K., Maeda, M., Uchiyama, T., Yodoi, J. & Honjo, T. (1984) *Nature (London)* 311, 631-635.
10. Cosman, D., Ceretti, D. P., Larsen, A., Park, L., March, C., Dower, S., Gillis, S. & Urdal, D. (1984) *Nature (London)* 312, 768-771.
11. Robb, R. J., Greene, W. C. & Rusk, C. M. (1984) *J. Exp. Med.* 160, 1126-1146.
12. Hatakeyama, M., Minamoto, S., Uchiyama, T., Hardy, R. R., Yamada, G. & Taniguchi, T. (1985) *Nature (London)* 318, 467-470.
13. Kondo, S., Shimizu, A., Maeda, M., Tagaya, Y., Yodoi, J. & Honjo, T. (1986) *Nature (London)* 320, 75-77.
14. Greene, W. C., Robb, R. J., Svetlik, P. B., Rusk, C. M., Depper, J. M. & Leonard, W. J. (1985) *J. Exp. Med.* 162, 363-368.
15. Ortaldo, J. R., Mason, A. T., Gerard, J. P., Henderson, L. E., Farrer, W., Hopkins, R. F., Herberman, R. B. & Rabin, H. (1984) *J. Immunol.* 133, 779-783.
16. Grim, E. A. & Rosenberg, S. A. (1984) *Lymphokine* (Academic, New York), Vol. 9, pp. 279-311.
17. Wano, Y., Uchiyama, T., Fukui, K., Maeda, M., Uchino, H. & Yodoi, J. (1984) *J. Immunol.* 132, 3005-3010.
18. Kawakami, T. G., Huff, S. D., Buckley, P. M., Dungworth, D. L. & Snyder, S. P. (1972) *Nature (London) New Biol.* 235, 170-171.
19. Kasuga, M., Van Obberghen, E., Nissley, S. P. & Rechler, M. M. (1981) *J. Biol. Chem.* 256, 5305-5308.
20. Faltynek, C. R., Branca, A., McCandless, S. & Baglioni, C. (1983) *Proc. Natl. Acad. Sci. USA* 80, 3269-3273.
21. August, G. P., Nissley, S. P., Kasuga, M., Lee, L., Greenstein, L. & Rechler, M. M. (1983) *J. Biol. Chem.* 258, 9033-9036.
22. Rabin, H., Hopkins, R. F., Ruscetti, F. W., Neubauer, R. H., Brown, R. L. & Kawakami, T. G. (1981) *J. Immunol.* 127, 1852-1856.
23. Chen, S. J., Holbrook, N. J., Mitchell, K. F., Vallone, C. A., Greengard, J. S., Crabtree, G. R. & Lin, Y. (1985) *Proc. Natl. Acad. Sci. USA* 82, 7284-7288.
24. Smith, K. A. (1982) *Immunobiology (Stuttgart)* 161, 157-173.
25. Rubin, L. A., Kurman, C. C., Biddison, W. E., Goldman, N. D. & Nelson, D. L. (1985) *Hybridoma* 4, 91-102.
26. Taniguchi, T., Matsui, H., Fujita, T., Takaoka, C., Kashima, N., Yoshimoto, R. & Hamuro, J. (1983) *Nature (London)* 302, 305-310.
27. Leonard, W. J., Depper, J. M., Kanehisa, M., Krönke, M., Pfeffer, N. J., Svetlik, P. B., Sullivan, M. & Greene, W. C. (1985) *Science* 230, 633-639.
28. Weissman, A. M., Harford, J. B., Svetlik, P. B., Leonard, W. J., Depper, J. M., Waldmann, T. A., Greene, W. C. & Klausner, R. D. (1986) *Proc. Natl. Acad. Sci. USA* 83, 1463-1466.
29. Fujii, M., Sugamura, K., Sano, K., Nakai, M., Sugita, K. & Hinuma, Y. (1986) *J. Exp. Med.* 163, 550-562.
30. Mishina, M., Kurosaki, T., Morimoto, Y., Noda, M., Yamamoto, T., Terao, M., Lingstrom, J., Takahashi, T., Kuno, M. & Numa, S. (1984) *Nature (London)* 307, 604-608.
31. Hosang, M. & Shooter, E. M. (1985) *J. Biol. Chem.* 260, 655-662.

Cholesterol-dependent clustering of IL-2R α and its colocalization with HLA and CD48 on T lymphoma cells suggest their functional association with lipid rafts

G. Vereb*, J. Matkó*, G. Vámosi†, S. M. Ibrahim*, E. Magyar‡, S. Varga‡, J. Szöllősi*, A. Jenei*, R. Gáspár, Jr.*, T. A. Waldmann§, and S. Damjanovich*||

*Department of Biophysics and Cell Biology, †Cell Biophysics Research Group of the Hungarian Academy of Sciences, ‡Central Research Service Laboratory, University of Debrecen, Medical and Health Sciences Center, P.O.B. 39, 4012 Debrecen, Hungary; §Metabolism Branch, National Cancer Institute, National Institutes of Health, Bethesda, MD 20892

Contributed by T. A. Waldmann, February 29, 2000

Immunogold staining and electron microscopy show that IL-2 receptor α -subunits exhibit nonrandom surface distribution on human T lymphoma cells. Analysis of interparticle distances reveals that this clustering on the scale of a few hundred nanometers is independent of the presence of IL-2 and of the expression of the IL-2R β -subunit. Clustering of IL-2R α is confirmed by confocal microscopy, yielding the same average cluster size, ≈ 600 –800 nm, as electron microscopy. HLA class I and II and CD48 molecules also form clusters of the same size. Disruption of cholesterol-rich lipid rafts with filipin or depletion of membrane cholesterol with methyl- β -cyclodextrin results in the blurring of cluster boundaries and an apparent dispersion of clusters for all four proteins. Interestingly, the transferrin receptor, which is thought to be located outside lipid rafts, exhibits clusters that are only 300 nm in size and are less affected by modifying the membrane cholesterol content. Furthermore, transferrin receptor clusters hardly colocalize with IL-2R α , HLA, and CD48 molecules (crosscorrelation coefficient is 0.05), whereas IL-2R α colocalizes with both HLA and CD48 (crosscorrelation coefficient is between 0.37 and 0.46). This codustering is confirmed by electron microscopy. The submicron clusters of IL-2R α chains and their codustering with HLA and CD48, presumably associated with lipid rafts, could underlie the efficiency of signaling in lymphoid cells.

IL-2 receptor | HLA glycoproteins | transferrin receptor | receptor clustering | electron microscopy

Cytokines regulating immune responses have their specific private receptor but may also share public receptors with other cytokines. IL-2 secreted by T lymphocytes when stimulated with antigen or mitogens is essential for T cell growth (1, 2). The private receptor for IL-2 is the IL-2R α -subunit, exhibiting relatively low affinity for IL-2 compared with the IL-2R $\alpha\beta\gamma$ heterotrimer, which is considered a fully functional receptor (3). We have recently shown in a fluorescence resonance energy transfer study that the IL-2R α , β , and γ -subunits are preassembled even on the surface of unstimulated Kit 225 K6 T lymphoma cells and cannot, therefore, be considered a transient signaling assembly (4). It is still unclear how IL-2R α is recruited to the less abundant β and γ chains to form the functionally active receptor.

Similar assemblies (nonrandom colocalization) of cell-surface antigens and receptors have been reported previously for lymphoid cells, as reviewed in ref. 5. Such supramolecular formations on the nanometer level have been explored primarily by using flow cytometric energy transfer (6), joined by other mostly fluorescence-based techniques that assess lateral or rotational mobility of membrane proteins or assemblies thereof (7–9). Possibly functional protein-association patterns were discovered,

including the di/oligomerization of HLA I and II molecules on activated T cells and lymphoid cell lines (10–13), the hetero-association between HLA I and HLA II glycoproteins (14), or HLA I and the IL-2R α -subunit (15). These observations argue against independent freely moving membrane proteins postulated by the fluid mosaic membrane model; instead, a segregated “corrallled” structure may be the valid hypothesis, with specific molecules confined to specific regions (5).

Various studies directed at the plasma membrane have provided evidence for the existence of such distinct domains in the submicron range (12, 16–18); for a most recent overview, see ref. 19. From the biochemical point of view, these domains appear as detergent insoluble/resistant glycolipid-enriched membrane domains [DRMs, DIGs, or GEMs (20)] and are often termed lipid rafts (21). Physically, they are expected to be represented by cell-surface patches found for both lipid and protein molecules (22). The physical and chemical forces giving rise to such domains are under intensive investigation (8, 23). One presumes that several intracellular, extracellular, and intramembrane constraints and forces influence the size and distribution of these clusters, one being the cholesterol content of the membrane area in question (21, 24). There is indeed evidence that changing the cholesterol composition of the cell membrane alters the association pattern and signaling properties of various molecules (24, 25). Such a change can be brought about by treating the cell membrane with filipin, a polyene antibiotic specifically complexing cholesterol (26), or by extracting cholesterol from the membrane by methyl- β -cyclodextrin (27).

The physiological significance of the lateral microdomain organization of biological membranes is not clear yet. One can assume that a larger-scale local accumulation of receptors and their signal transduction machinery (28, 29) may enhance the efficiency of transmembrane signaling by providing a focusing effect. We have previously shown patchy aggregation of platelet-derived growth factor receptors on glioblastoma cells (18) as well as assemblies of up to 1,000 erbB2 molecules on various mammary tumor cell lines (30). Also, in addition to the molecular association of MHC class I and class II glycoproteins on lymphoma cells, we have observed their submicron-scale clusters and codusters (12, 16). Given this knowledge, as well as the evidence that MHC class I glycoproteins are in the molecular vicinity of IL-2R α on some cell lines (15), in the present study

Abbreviations: TrfR, transferrin receptor; Cy3, sulfoindocyanine-succinimidyl ester.

||To whom reprint requests should be addressed. E-mail: dami@jaguar.dote.hu.

The publication costs of this article were defrayed in part by page charge payment. This article must therefore be hereby marked “advertisement” in accordance with 18 U.S.C. §1734 solely to indicate this fact.

we have undertaken to investigate the higher-order clustering of IL-2R α on Kit 225 K6 and MT-1 lymphoma cells and the possible heteroassociation of IL-2R α with MHC glycoproteins on the submicron-micron scale. To shed light on the possible role of lipid rafts (19, 21) in organizing these receptor assemblies, we have examined the colocalization of IL-2R α and MHC molecules with CD48, a glycosylphosphatidylinositol-linked T cell membrane protein reported to associate with rafts (20) and with the transferrin receptor (TrfR) that is excluded from glycosphingolipid-enriched membrane microdomains (31, 32). Furthermore, we have tested the influence of membrane cholesterol composition on the submicron-scale clustering of these molecules by extracting cholesterol with methyl- β -cyclodextrin or complexing cholesterol *in situ* with filipin.

Materials and Methods

Cell Culture and Treatment. Kit 225 K6 and MT-1 T cell lines were cultured in RPMI-1640 medium (5% CO₂) supplemented with 10% FCS and antibiotics. To maintain the growth of Kit 225 K6 cells, 20 units/ml recombinant IL-2 was added every 48 h. Resting cells were obtained by culturing for 72 h in IL-2-free medium. Filipin III (Sigma; 0.1 mg/ml) was used to complex cholesterol in the cell membrane. Incubation (10⁶ cells/ml) for 1 h at 37°C was followed by washing twice in PBS. Cholesterol extraction was achieved by treating 10⁶ cells/ml with 7 mM methyl- β -cyclodextrin (Sigma) for 1 h at 37°C, and its efficiency was assessed from the decrease of fluorescence polarization of the trimethylamine-diphenylhexatriene membrane probe (25).

mAbs. The IL-2R α -subunit, MHC class I and II were labeled with α Tac, W6/32, and L-243, respectively (4, 12). Anti-CD48 (MEM102) and anti-TrfR (MEM75) were a generous gift of V. Horejsi (Institute of Molecular Genetics, Academy of Science, Czech Republic). Fab fragments were prepared from mAbs as previously described (33). Whole mAbs or Fab fragments were conjugated with fluorescein or rhodamine succinimidyl esters having long linkers (XF or XR, Molecular Probes) or sulfonindocyanine-succinimidyl ester (Cy3, monofunctional, Amersham Pharmacia) as described earlier (14, 15).

Labeling of Cells with mAbs. Cells (10⁶/ml) suspended in ice-cold PBS were labeled in the dark for 40 min at 4°C. Optimal antibody concentrations were determined from saturation curves. Antibodies were air fuded (20,000 \times g, 30 min) before labeling. Labeled cells were washed in cold PBS and either fixed with 1% formaldehyde, used unfixed immediately, or further processed for electron microscopy.

Labeling of Cells with Colloidal Gold for Electron Microscopy. Labeling with the first Fab (see above) was followed by incubation with polyclonal secondary antibodies conjugated to gold beads of 10- or 30-nm diameter (Aurogamig G-10, against the heavy and light chains, or Aurogamig G-30 against the Fc fragment; from Amersham Pharmacia) for 40 min. After washing with PBS (10 min, 250 \times g) the cells were fixed with 2% paraformaldehyde for 1 h and then with 2% glutaraldehyde in 0.1 M sodium cacodylate buffer (pH 7.2) over night on ice. For sequential double labeling, the first antibody was a Fab followed by Aurogamig G-10, and then the unused binding sites of the polyclonal antibodies were blocked for 5 min with the Fab fragments used for primary labeling. mAbs against the second target epitope were whole antibodies that were tagged with Aurogamig G-30 against the Fc fragment. These beads will label only that fraction of the second target epitope that is not hidden by the first cohort of beads tagging the first target epitope (16).

Electron Microscopy. After immunogold labeling, cells were spread on poly-L-lysine-coated Formvar grids, dehydrated in

ascending ethanol series, and air dried from ether. Gold beads were counted in a JEOL electron microscope (JEM 100 B microscope operated at 100 kV) on the periphery and thinner parts of cells, where transparency allowed a good contrast.

Calculation of Actual and Expected Cell-Surface Distribution of Gold-Labeled Antigens. For a random distribution of the gold particles, the statistics of the number of beads per unit area should be Poissonian (12, 16). The average density of gold particles was calculated from their number and the area over which they were distributed. The area assigned to one bead on average was taken as the unit, and thus the parameter λ of the assumed Poisson distribution was taken as 1. The number of beads counted in each unit area on the cell surface was used to calculate the actual distribution.

Comparison of Characteristic Interparticle Distances of Colloidal Gold Labels. Scanned images of electron micrographs were processed by using a custom-written program developed in the LABVIEW (National Instruments, Austin, TX) environment. The coordinates of recognized labeling particles were used to produce the distribution of all interparticle distances in the sample.

Confocal Microscopy. Cells were labeled with fluorescent Fab fragments, fixed in 1% formaldehyde or left unfixed in control experiments, and attached to poly-L-lysine-coated slides. A Zeiss LSM 420 laser scanning confocal microscope was used for measurements. Cy3 and XR were excited at 543 nm, XF at 488 nm. For double-labeled samples in crosscorrelation studies, a 510- to 525-nm narrow bandpass emission filter was used to detect XF fluorescence instead of the usual 510 nm long pass. Confocal sections (512 \times 512 pixel, 0.6 μ m thin) were obtained with a pinhole setting of 25, \times 5–8 zoom, through a \times 100 (numerical aperture = 1.3) objective. The intensity distribution of surface labeling was generated from the three-dimensional reconstruction of sections by using a projection algorithm in NIH IMAGE (National Institutes of Health, Bethesda, MD). In addition to the reconstructed free surfaces of cells, single confocal sections of each cell, flattened against the glass slide, were also analyzed.

Determination of Cluster Size from Confocal Images. Average cluster size was determined from both projected surface distributions and flattened single confocal images by using the two-dimensional autocorrelation function

$$G(\rho, \varphi) = \langle f(r, \Theta) f(r + \rho, \Theta + \varphi) \rangle, \quad [1]$$

where the angle brackets indicate summation over the whole domain of the ρ radius and φ angle. The autocorrelation image was calculated by taking the inverse Fourier transform of the two-dimensional power spectrum matrix of the original images. Because in our case we do not expect the distribution to be anisotropic, $G(\rho, \varphi)$ is independent of φ . Consequently, an angle-invariant autocorrelation function $G(\rho)$ can be generated by averaging $G(\rho, \varphi)$ over the range $0 \leq \varphi < 2\pi$. $G(\rho)$ is fitted to the equation

$$G(\rho) = \sum_i A_i e^{-(\rho/R_i)^2}, \quad [2]$$

where the R_i characteristic radii serve as an adequate measure of the mean size (half-width at the 1/e height of a Gaussian distribution) of each class of clusters distinguishable on the basis of its size (22). Calculation of $G(\rho)$ and fitting Eq. 3 by using the Levenberg-Marquardt algorithm were performed with a custom-written program developed in the LABVIEW environment. Using two exponentials gave a good fit with small residuals. The smaller value of R_i , generally in the 100- to 500-nm range, was

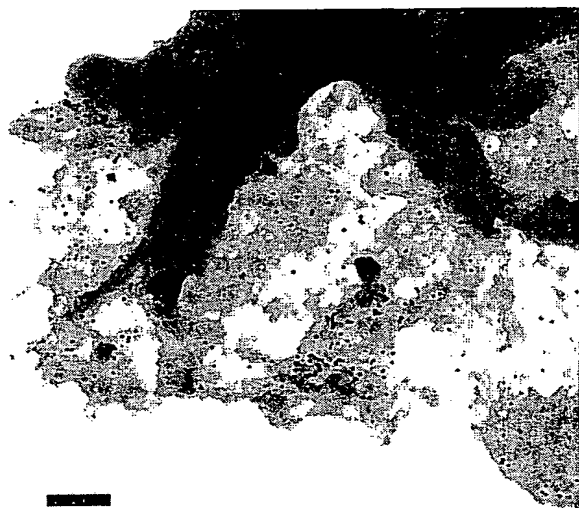


Fig. 1. Nonrandom distribution of IL-2R α on Kit 225 K6 cells revealed by colloidal gold labels. Kit 225 K6 cells were labeled with anti-Tac as primary antibody and then with 30 nm colloidal gold conjugated to the secondary antibodies. A representative electron micrograph of the periphery of a cell is shown. The distribution of gold labels appears to be nonrandom. Bar = 470 nm.

taken as the radius of submicron-sized clusters, in coherence with individual cluster sizes measured directly on the images. The larger value of R_i , several microns in magnitude, was assumed to be characteristic for background fluctuation (30).

Determining Colocalization from Image Crosscorrelation. Colocalization of pairs of cell-surface antigens was determined from confocal images of double-labeled cells. For a pair of images x and y , the crosscorrelation coefficient was calculated as

$$C = \frac{\sum_i \sum_j (x_{ij} - \langle x \rangle)(y_{ij} - \langle y \rangle)}{\sqrt{\sum_i \sum_j (x_{ij} - \langle x \rangle)^2 \sum_i \sum_j (y_{ij} - \langle y \rangle)^2}}, \quad [3]$$

where x_{ij} and y_{ij} are fluorescence pixel values at coordinates i, j in images x and y . Only those pixels were used for the summation

that were above detection threshold in both images. The theoretical maximum is $C = 1$ for identical images, and a value close to 0 implies disparate localization of the label. A program in LABVIEW was written to register and threshold image pairs and compute the crosscorrelation coefficient.

Results

Immunogold Labeling and Electron Microscopy Reveal a Submicron-Level Clustering of IL-2R α -Subunits on K6 Cells. Fig. 1 shows immunogold-labeled IL-2R α on Kit225 K6 cells. Clusters of several gold beads can be observed in addition to singly placed labels and larger areas with no label at all. Counting the labels, we constructed the actual probability distribution (Fig. 2a, diamonds) and compared it to the theoretical Poissonian (Fig. 2a, closed circles). It is clear that there are a larger number of unit areas with no label than that expected for a Poissonian, and that unit areas with four or more gold labels are more abundant as well. Because of this disproportion, unit areas close to the expected Poissonian parameter (i.e., those with one, two, and three labels) are lesser in number than predicted for a random distribution. The observed and expected distributions are different beyond a confidence level of 99.99 by using the χ^2 test. Thus, the localization of labels follows a nonrandom distribution, manifesting as clustering on the submicron scale.

Quantitative Assessment of Interparticle Distances Reveals No Difference in the Higher-Level Clustering of IL-2R α on IL-2 Fed and Starved K6 Cells and MT-1 Cells. Because the receptor clusters are not expected to be anisotropic, the calculation of a relevant autocorrelation function that can be used to quantify cluster size simplifies to constructing the distribution histogram of all interparticle distances, without regard to the direction of localization. Such a distribution histogram is presented in Fig. 2b (diamonds) for the sample shown in Fig. 1. It is compared to a simulated distribution of the same number of particles randomly scattered over the same area (closed circles). The actual distribution is comprised of two peaks, whereas the randomly generated particle pattern shows a single Poissonian peak. The first peak of the actual distribution likely corresponds to the average interparticle distance within the small clusters of gold beads, whereas the second peak characterizes the average distance to labels outside the cluster. These average distances describe quantitatively the submicron-level receptor patterns on various T cells. In Fig. 2c, we see that in the case of Kit 225 K6 cells, the distance distribution is not influenced by IL-2 deprivation. Furthermore, the average distances within the clusters are the same in the case of MT-1 cells as for the K6 line.

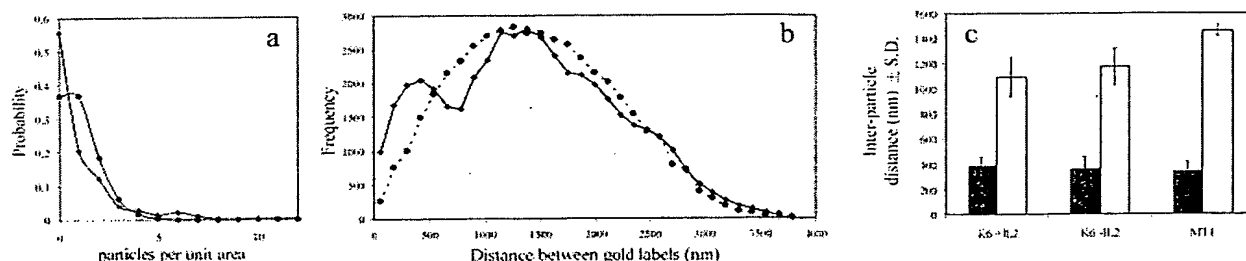


Fig. 2. Quantitative analysis of the distribution of gold labels on IL-2R α -subunits. (a) Gold labels shown in Fig. 1 were counted ($n = 406$), and the unit area was defined such that the expected value of gold labels per unit area was one. The image was divided into equal squares of one unit area each and the actual distribution of labels among the squares determined. The probability distribution of the particle density per unit area is plotted for the actual finding (\diamond) and compared to a Poisson distribution with parameter $\lambda = 1$ (\bullet). (b) The coordinates of all labels in Fig. 1 were determined, and the distribution of all interparticle distances was plotted (\diamond). A model distribution was also generated assuming Poissonian statistics (dashed line, \bullet). In contrast to the single peak of the expected random distribution, the measured distribution has two peaks. The first peak, around 400 nm, represents the characteristic distance of gold labels within clusters. (c) Characteristic distances for gold labels determined as in *b* are plotted for Kit 225 K6 (K6 + IL2), IL-2-starved Kit 225 K6 (K6 - IL2), and MT-1 cells. Characteristic distances within clusters are represented by filled columns, and average distances within the whole sample area are shown with open columns. Data are mean \pm SD from six independent experiments.

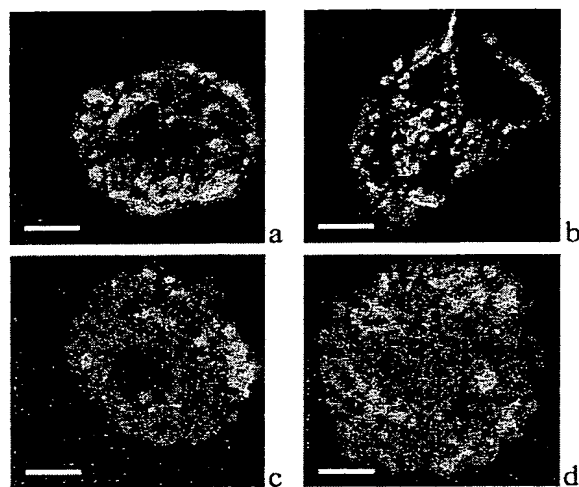


Fig. 3. Confocal laser-scanning microscopy of Cy3-labeled IL-2R α and TrfR. Kit 225 K6 cells were labeled with Cy3-conjugated α Tac Fab against the IL-2R α -subunit (a, c, and d) or XR-conjugated MEM-75 against the TrfR (b). Cells in c and d were treated with filipin and methyl- β -cyclodextrin, respectively. Confocal slices of 0.6 μ m thickness were obtained. Surface fluorescence distribution was reconstructed from z directional projection of image slices. Bar = 4 μ m. A patchy receptor distribution can be observed with clusters of 200- to 1,200-nm diameter depending on the type of receptor and the treatment.

Confocal Laser-Scanning Microscopy of Hydrated Samples Confirms the Presence of Submicron IL-2R α Clusters on MT-1 and Kit225 K6 Cells. Confocal laser-scanning microscopy was used to confirm the presence of submicron IL-2R α clusters on MT-1 and K6 cells. Cells were labeled on ice with Fab fragments to visualize receptors without inducing aggregation artifacts. Fig. 3 shows images of Kit 225 K6 cells labeled with Cy3-conjugated α Tac (Fig. 3a) or XR-conjugated MEM-75 against the TrfR (Fig. 3b). A patchy receptor distribution is observed with clusters of 500–800 nm for the IL-2R α and 200–300 nm for the TrfR. Controls on prefixed and live cells indicate that this clustering is not caused by the labeling procedure. Cluster diameter for the IL-2R α determined from $G(\rho)$ (Eqs. 1 and 2) was \approx 600 nm (see also Fig. 4). This implies that the minimum and maximum distances between immunogold labels within a cluster would be 0 and 600 nm, averaging to \approx 300, which corresponds well to the \approx 380-nm average interparticle distance within clusters determined in electron microscopy (Fig. 2).

Cluster Size of IL-2R α , HLA Glycoproteins, and CD48 Depends on the Integrity of Cholesterol-Rich Lipid Rafts. Interestingly, clusters of the TrfR are significantly smaller in size (250 nm) than those of IL-2R α . TrfR is thought to be localized outside rafts (31), whereas several src-family kinases that play a role in T cell activation are detected in association with rafts (21, 32). To check whether these cholesterol-rich regions could be held responsible for keeping together the islets of IL-2R α -subunits, we have examined the change of cluster size after modifying the membrane cholesterol content with cyclodextrin or filipin. Fig. 3 c and d show that cluster boundaries become blurred, and their size increases on both treatments. Thus, modulation of cholesterol content seems to break up the tightness of IL-2R α clusters. The increase in cluster size is significant in both cases (Fig. 4, filled columns) and is paralleled by a decrease of absolute fluorescence intensities, indicating dispersion of the labeled proteins. The same observations can be made for MT-1 cells (data not shown).

As Fig. 4 shows, both class I and II MHC glycoproteins and the raft marker CD48 behave similarly to IL-2R α : their cluster size

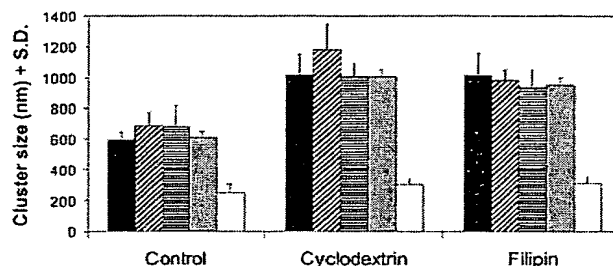


Fig. 4. Cluster sizes of IL-2R α , HLA class I and II, CD48, and TrfR and their modulation by membrane cholesterol content. Cluster sizes on Kit 225 K6 cells determined from the angle-averaged autocorrelation function are presented for IL-2R α (filled columns), HLA class I (crosshatched columns), and class II (striped columns), CD48 (gray columns), and TrfR (open columns). The effect of modulating the cholesterol content of the membrane is also displayed: with the exception of TrfR, all receptor clusters exhibit a significant increase of cluster size on both cholesterol depletion by cyclodextrin or *in situ* complexation of cholesterol by filipin. ($n > 9$, from three independent experiments).

is comparable to that of IL-2R α (control group, crosshatched, striped, and gray columns) and is dispersed significantly on cyclodextrin and filipin treatment. On the other hand, TrfR not only possesses smaller clusters in control cells, but its cluster size hardly changes on either of the treatments modifying membrane cholesterol (open columns). The same molecules behave similarly on the surface of MT-1 cells (data not shown).

Crosscorrelation Analysis of Confocal Images Reveals Partial Coclustering of IL-2R with MHC and CD48 Molecules, but Not with TrfR. Because flow cytometric energy transfer measurements gave evidence of nanometer-level proximity between IL-2R α and MHC antigens, we have used double labeling with fluorescent Fabs in confocal microscopy to investigate the colocalization of IL-2R α with MHC glycoproteins. Fig. 5a shows the colocalization of IL-2R α (green) and HLA class II (red). Because of the high degree of colocalization (crosscorrelation coefficient $C = 0.37$; see Fig. 6), many pixels of the image appear orange when the red and green channels are overlaid. Fig. 5b demonstrates that IL-2R α (green) and TrfR (red) images from the same cell exhibit disparate localization of these two receptors. Accordingly, their crosscorrelation coefficient is very low ($C = 0.05$). In similar experiments, the crosscorrelation coefficient was measured for a set of receptor pairs (Fig. 6). While IL-2R α colo-

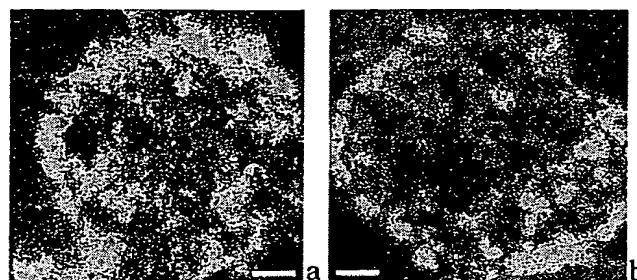


Fig. 5. IL-2R α exhibits submicron-scale colocalization with MHC II but not with TrfR. A representative confocal fluorescence image of the colocalization of IL-2R α and HLA class II is shown in a. IL-2R α and HLA class II are labeled with XF (green) and XR (red), respectively. Because of the high degree of colocalization, many pixels appear orange when the two channels are fused. b demonstrates that IL-2R α (green) and TrfR (red) codetected in a similar experiment are mostly localized at different areas of the plasma membrane. Bar = 2 μ m.

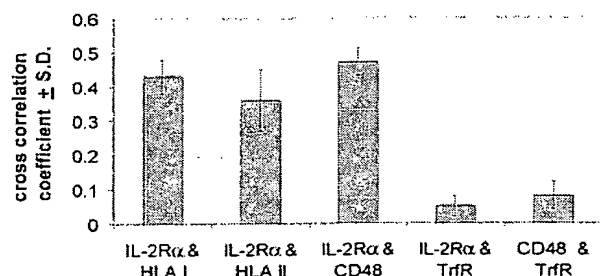


Fig. 6. IL-2R α staining crosscorrelates with MHC glycoproteins and CD48 but not with TrfR. Kit 225 K6 cells were double labeled with pairs of antibodies against IL-2R α , HLA class I and II, CD48, and TrfR. The crosscorrelation coefficient is measured for the following receptor pairs: IL-2R α and HLA class I, IL-2R α and HLA class II, IL-2R α and CD48, IL-2R α and TrfR, and CD48 and TrfR. While IL-2R α colocalizes with HLA class I and II and CD48, a raft marker, neither IL-2R α nor CD48 colocalizes with TrfR ($n = 7$).

calizes with HLA class I, II, and CD48, neither IL-2R α nor CD48 colocalizes with TrfR. A similar colocalization pattern was observed on MT-1 cells. This is consistent with a selective association of IL-2R α , MHC, and the raft marker CD48 with cholesterol-rich membrane rafts that are perturbed by filipin or cyclodextrin treatment and the observation that TrfR clusters are virtually unaffected by the modification of membrane cholesterol.

Sequential Immunogold Labeling and Electron Microscopy Confirm the Higher-Level Partial Colocalization of IL-2R α and MHC. Earlier we have developed a strategy to examine coclustering of class I and class II MHC antigens on lymphoid cells (16). Fig. 7 shows an example of IL-2R α labeled with 10 nm gold followed by 30 nm gold tags on MHC-I molecules on the surface of Kit225 K6 cells. Although there are also some labels that are not proximal to the other labeling species, many of the small and large beads are seen coclustered. A similar partial colocalization of IL-2R α and MHC-II was observed on both Kit 225 K6 and MT-1 cells (data not shown). Thus, the coclustering deduced from confocal images is supported by electron microscopic evidence.

When the surface density of 30-nm gold labels on IL-2R α is

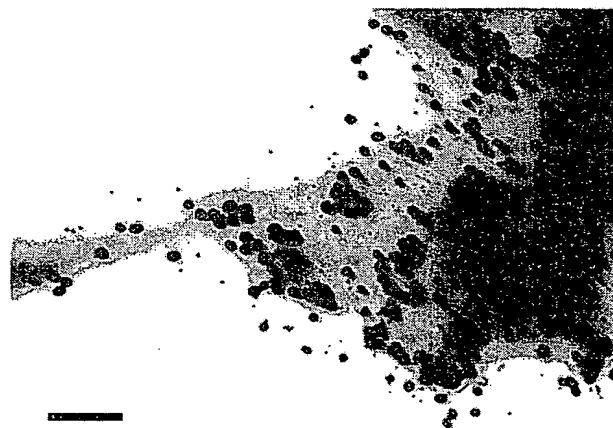


Fig. 7. Electron microscopy confirms the partial coclustering of IL-2R α and MHC molecules. Immunogold labeling followed the sequence: α Tac Fab—10 nm AuroGamig—blocking by α Tac Fab—W6/32 whole antibody—30 nm AuroGamig (anti-Fc). Electron microscopy shows that the selective labels against the IL-2R α and the MHC are partially, although not completely, colocalized, thus confirming the confocal microscopic data (Bar = 200 nm).

averaged for several cells, 25/ μ m² are seen. If IL-2R α is labeled after covering MHC class II molecules with L243 Fab and 10-nm gold beads, the detectable 30-nm labels on IL-2R α decrease to 13/ μ m². This is consistent with the idea that the interaction of MHC-II and IL-2R α at the molecular level allows detection of only about 50% of the IL-2R α after having shielded those α -subunits that are in the vicinity of MHC-II antigens. A similar \approx 50% coclustering ratio could be determined for IL-2R α in relation to MHC class I molecules on these cells. This observation is in line with the crosscorrelation coefficient of 0.37–0.43 seen between fluorescent labels on IL-2R α and MHC antigens.

Discussion

Recently, we have presented fluorescence resonance energy transfer efficiency data indicating spontaneous assembly of the α -, β -, and γ -subunits of the multisubunit IL-2 receptor on Kit 225 K6 T lymphoma cells even in the absence of IL-2 (4). Here we show by using immunogold labeling in electron microscopy that this molecular-level assembly of the IL-2 receptor is extended to a higher hierarchical level, i.e., on the several hundred nanometer scale in the plasma membrane of human T lymphoma cells. The distribution of colloidal gold labels attached to IL-2R α was significantly different from a hypothetical random Poissonian pattern ($P > 0.9999$). The distribution of interparticle distances also showed two peaks, one close to that expected for the single peak of a Poissonian pattern and another at smaller distances, likely corresponding to the average cluster radius of 350–380 nm.

Clusters of similar size were observed both on Kit 225 K6 cells, which have an absolute requirement of IL-2 for their growth, and on MT-1 cells, which do not express the β -subunit of the IL-2 receptor and grow independently of IL-2. Also, IL-2 deprivation of Kit 225 K6 cells had no effect on cluster size. Thus the molecular interactions producing submicron-scale clusters seem to be largely independent of the presence of the IL-2R β -subunits or the specific ligand IL-2.

Confocal laser-scanning microscopy of both fixed and live cells confirmed the submicron clusters observed with electron microscopy. Also, the cluster size deduced from electron microscopy corresponded well to that seen in confocal slices and surface reconstructions. The cluster sizes measured are on the same order of magnitude as the areas of confined diffusion determined from single particle tracking for ganglioside GM1 and the Thy-1 antigen (34); furthermore, they are comparable to those assessed for ErbB2 (30) and platelet-derived growth factor receptor molecules (18) by scanning near-field optical microscopy.

Such high degree of receptor aggregation has been found both as a ligand-induced phenomenon (35) and as a stably maintained structure with yet undetermined lifetimes. The latter frequently occurs under polarizing conditions, especially in the nervous system (36) or in the neuromuscular junction (37). However, similar receptor clustering can also be found on cells that are nonpolarized, e.g., lymphoid cells. Earlier we have demonstrated higher hierarchical-level distribution patterns of the MHC class I (12) and class II molecules (16). These findings have been corroborated recently by data revealing anomalous diffusion of MHC I and II molecules (11, 38).

The present experiments significantly support the view that such above-nanometer-level codistribution patterns could be common among various receptor types even on nonpolarized cells. The existence of lipid rafts in the plasma membrane can easily have a central role in maintaining such receptor superstructures (21). Besides glycosphingolipids, cholesterol has been postulated as an important functional component of lipid rafts. Consistent with this, modifying membrane cholesterol content was shown to influence signaling by raft-associated molecular assemblies (24, 39). We found that specifically complexing cholesterol *in situ* with filipin or extracting it from the membrane with cyclodextrin changes the higher level colocalization patterns by dispersing and blurring the

clusters of both IL-2R α , HLA I, II, and the raft protein CD48. At the same time, flow cytometric energy transfer measurements have shown that IL-2R α is in the nanometer-scale proximity of both MHC-I and MHC-II on Kit 225 K6 and MT-1 cells (fluorescence resonance energy transfer efficiency was in the range of 12–21%; unpublished data). These data together support the notion that IL-2R α and MHC proteins may be partially confined to lipid rafts. In accordance with this hypothesis, a significant crosscorrelation of different color fluorescent labels on pairs of CD48 and these molecules was found, whereas the submicron clusters of the TrfR, which is not a constituent of rafts (31, 32), were significantly smaller and did not colocalize with either IL-2R α or CD48.

The combined application of fluorescence resonance energy transfer, electron microscopy, confocal laser-scanning microscopy, and image processing suggests that both small receptor islands and larger rafts can accommodate the IL-2 receptor α -subunit together with HLA class I and class II glycoproteins. The importance of the organizing role of lipid rafts is underlined by the finding that caveola-like domains serve as concentrators of various signal transduction machineries (28, 40), and several small cytoplasmic kinases, a group vastly important in the signal transduction of T lymphocytes (20, 41), are bound to lipid rafts (21, 29, 42). Thus, the clusters on both the molecular and the submicron level could underlie the efficiency of signaling in lymphoid cells and might play a role in the directed secretion of lymphokines and in specific internalization pathways.

MHC class II, recently reported to coaggregate with lipid rafts on stimulation by crosslinking (43), and class I molecules seem to be partially recruited into the signaling platform of IL-2R

subunits and CD48 formed by rafts. Although it is believed so far that posttranslational modification (fatty acylation, glycosylphosphatidylinositol linkage) is a specific predictor for targeting lipid rafts (20), for transmembrane proteins with (MHC molecules) or without (IL-2R α) intracellular tails, it is hard to predict their partitioning behavior based on their sequence. In these domains, MHC molecules may provide a stabilizing effect through their direct cytoskeletal connections (44). In addition, MHC class I molecules may also contribute to this biochemical switchboard as potential regulators of IL-2 receptor signaling by an intracellular tyrosine phosphorylation crosstalk, as reported for the insulin receptor recently (45).

Coimmobilization of GPI-anchored raft proteins, including CD48, on T cells has been reported to inhibit recruitment of IL-2R α chains with the signaling β and γ -subunits, but not the association of β and γ chains with the Janus kinases (46). In light of our data showing a “focusing” effect of rafts for IL-2R α , this might be due to coimmobilization of IL-2R α and/or a steric blocking of its interaction with the β and γ . Thus, T cell rafts related to cell-surface clusters of the proteins investigated here may promote IL-2R-mediated signaling by recruiting the α -chains into a signaling platform regardless of their ligand binding and, on the other hand, may also have a control on T cell growth (46) through the colocalized GPI-linked proteins (CD48 or Thy-1).

This research was supported by grants Hungarian National Research Fund (OTKA) F025210, T23873, T30411, T19372, T30399, T029947 and Fund for Higher Education Research (FKFP) 0518/99 and 327/2000.

- Waldmann, T. A. (1986) *Science* 232, 727–732.
- Waldmann, T. A. (1991) *J. Biol. Chem.* 266, 2681–2684.
- Nakamura, Y., Russell, S. M., Mess, S. A., Friedmann, M., Erdos, M., Francois, C., Jacques, Y., Adelstein, S. & Leonard, W. J. (1994) *Nature (London)* 369, 330–333.
- Damjanovich, S., Bene, L., Matkó, J., Alileche, A., Goldman, C. K., Sharrow, S. & Waldmann, T. A. (1997) *Proc. Natl. Acad. Sci. USA* 94, 13134–13139.
- Damjanovich, S., Gáspár, R., Jr. & Pieri, C. (1997) *Q. Rev. Biophys.* 30, 67–106.
- Damjanovich, S., Trón, L., Szöllösi, J., Zidovetzki, R., Vaz, W. L. C., Regateiro, F., Arndt-Jovin, D. J. & Jovin, T. M. (1983) *Proc. Natl. Acad. Sci. USA* 80, 5985–5989.
- Edidin, M., Zuniga, M. C. & Scheetz, M. (1994) *Proc. Natl. Acad. Sci. USA* 91, 3378–3382.
- Jacobson, K., Sheets, E. D. & Simson, R. (1995) *Science* 268, 1441–1442.
- Cherry, R. J., Smith, P. R., Morrison, I. E. & Fernandez, N. (1998) *FEBS Lett.* 430, 88–91.
- Bene, L., Balázs, M., Matkó, J., Most, J., Dierich, M. P., Szöllösi, J. & Damjanovich, S. (1994) *Eur. J. Immunol.* 24, 2115–2123.
- Cherry, R. J., Wilson, K. M., Triantafyllou, K., O'Toole, P., Morrison, I. E., Smith, P. R. & Fernandez, N. (1998) *J. Cell Biol.* 140, 71–79.
- Damjanovich, S., Vereb, G., Schaper, A., Jenei, A., Matkó, J., Starink, J. P., Fox, G. Q., Arndt-Jovin, D. J. & Jovin, T. M. (1995) *Proc. Natl. Acad. Sci. USA* 92, 1122–1126.
- Matkó, J., Bushkin, Y., Wei, T. & Edidin, M. (1994) *J. Immunol.* 152, 3355–3360.
- Szöllösi, J., Damjanovich, S., Balázs, M., Nagy, P., Trón, L., Fulwyler, M. J. & Brodsky, F. M. (1989) *J. Immunol.* 143, 208–213.
- Szöllösi, J., Damjanovich, S., Goldman, C. K., Fulwyler, M. J., Aszalós, A., Goldstein, G., Rao, P. & Waldmann, T. A. (1987) *Proc. Natl. Acad. Sci. USA* 84, 7246–7250.
- Jenei, A., Varga, S., Bene, L., Mátyus, L., Bodnár, A., Bacsó, Z., Pieri, C., Gáspár, R., Jr., Farkas, T. & Damjanovich, S. (1997) *Proc. Natl. Acad. Sci. USA* 94, 7269–7274.
- Kenworthy, A. K. & Edidin, M. (1998) *J. Cell Biol.* 142, 69–84.
- Vereb, G., Meyer, C. K. & Jovin, T. M. (1997) in *Interacting Protein Domains, Their Role in Signal and Energy Transduction*. NATO ASI Series, ed. Heilmeyer, L. M. G., Jr. (Springer, New York), Vol. H102, pp. 49–52.
- Jacobson, K. & Dietrich, C. (1999) *Trends Cell Biol.* 9, 87–91.
- Horejsi, V., Cebecauer, M., Cerny, J., Brdicka, T., Angelisova, P. & Drbal, K. (1998) *Immunol. Lett.* 63, 63–73.
- Simons, K. & Ikonen, E. (1997) *Nature (London)* 387, 569–572.
- Hwang, J., Gheber, L. A., Margolis, L. & Edidin, M. (1998) *Biophys. J.* 74, 2184–2190.
- Edidin, M. (1997) *Curr. Opin. Struct. Biol.* 7, 528–532.
- Rothberg, K. G., Ying, Y. S., Kamen, B. A. & Anderson, R. G. (1990) *J. Cell Biol.* 111, 2931–2938.
- Bodnár, A., Jenei, A., Bene, L., Damjanovich, S. & Matkó, J. (1996) *Immunol. Lett.* 54, 221–226.
- de Kruijff, B. & Demel, R. A. (1974) *Biochim. Biophys. Acta* 339, 57–63.
- Christian, A. E., Haynes, M. C., Phillips, M. C. & Rothblat, G. H. (1997) *J. Lipid Res.* 38, 2264–2272.
- Liu, P., Ying, Y. & Anderson, R. G. (1997) *Proc. Natl. Acad. Sci. USA* 94, 13666–13670.
- Harder, T. & Simons, K. (1999) *Eur. J. Immunol.* 29, 556–562.
- Nagy, P., Jenei, A., Kirsch, A. K., Szöllösi, J., Damjanovich, S. & Jovin, T. M. (1999) *J. Cell Sci.* 112, 1733–1741.
- Smart, E. J., Ying, Y. S., Mineo, C. & Anderson, R. G. (1995) *Proc. Natl. Acad. Sci. USA* 92, 10104–10108.
- Xavier, R., Brennan, T., Li, Q., McCormack, C. & Seed, B. (1998) *Immunity* 8, 723–732.
- Matkó, J. & Edidin, M. (1997) *Methods Enzymol.* 278, 444–462.
- Sheets, E. D., Lee, G. M., Simson, R. & Jacobson, K. (1997) *Biochemistry* 36, 12449–12458.
- Ciruela, F., Saura, C., Canela, E. I., Mallol, J., Lluís, C. & Franco, R. (1997) *Mol. Pharmacol.* 52, 788–797.
- Craig, A. M., Blackstone, C. D., Haganir, R. L. & Banker, G. (1994) *Proc. Natl. Acad. Sci. USA* 91, 12373–12377.
- Campanelli, J. T., Hoch, W., Rupp, F., Kreiner, T. & Scheller, R. H. (1991) *Cell* 67, 909–916.
- Smith, P. R., Morrison, I. E., Wilson, K. M., Fernandez, N. & Cherry, R. J. (1999) *Biophys. J.* 76, 3331–3344.
- Keller, P. & Simons, K. (1998) *J. Cell Biol.* 140, 1357–1367.
- Wu, C., Butz, S., Ying, Y. & Anderson, R. G. (1997) *J. Biol. Chem.* 272, 3554–3559.
- Ihle, J. N. & Kerr, I. M. (1995) *Trends Genet.* 11, 69–74.
- Ko, Y. G., Liu, P., Pathak, R. K., Craig, L. C. & Anderson, R. G. (1998) *J. Cell. Biochem.* 71, 524–535.
- Huby, R. D., Dearman, R. J. & Kimber, I. (1999) *J. Biol. Chem.* 274, 22591–22596.
- Geppert, T. D. & Lipsky, P. E. (1991) *J. Immunol.* 146, 3298–3305.
- Ramalingam, T. S., Chakrabarti, A. & Edidin, M. (1997) *Mol. Biol. Cell* 8, 2463–2474.
- Marmor, M. D., Bachmann, M. F., Ohashi, P. S., Malek, T. R. & Julius, M. (1999) *Int. Immunol.* 11, 1381–1393.